1101

[redacted]
— 1101

File 8451
2-1.19

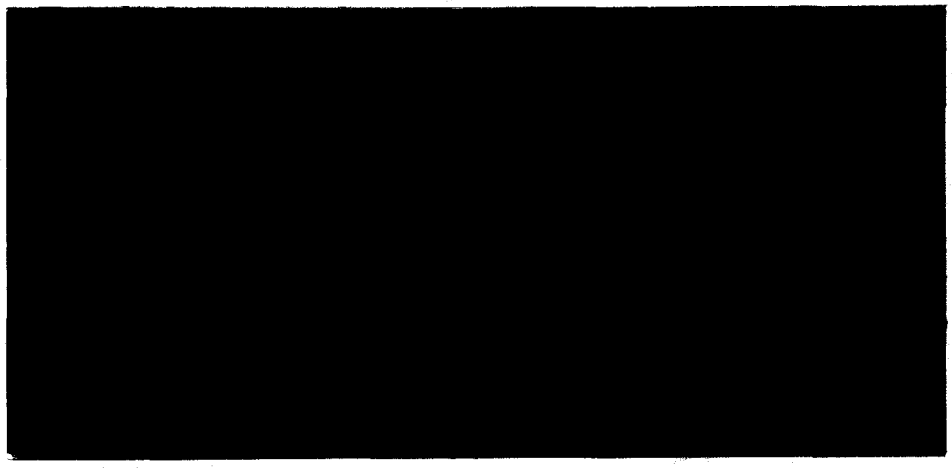

Honeywell

AVIONICS DIVISION
ST. PETERSBURG, FLORIDA

8132 AUG 9

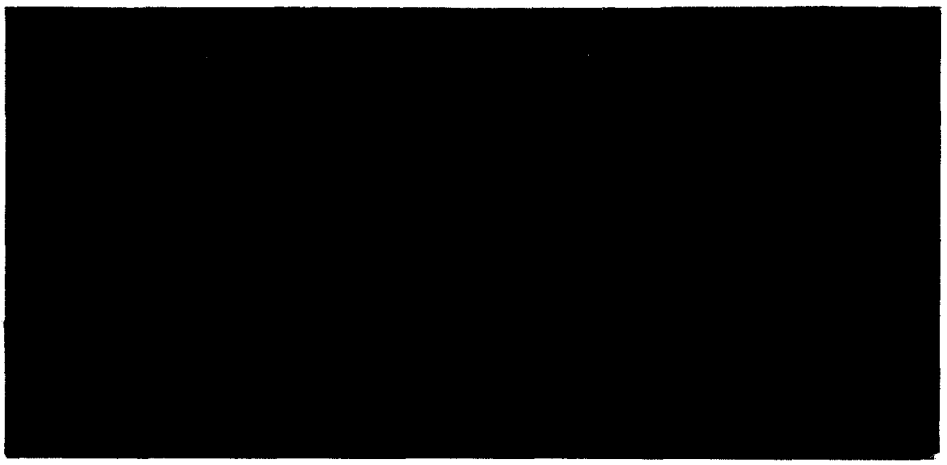

677-14611 30 June 1977

TEST REPORT

WIND TUNNEL TEST OF 1/10 SCALE

HONEYWELL SRE HELIOSTAT MODEL

Prepared by: G L Brown/440

G. L. Brown
Test Engineer

Approved by: L P Ball

L. P. Ball
Program Manager

Contract No. E(04-3)-1109 with

Honeywell, Inc.

Energy Resources Center

ACKNOWLEDGMENTS

I wish to express my sincere appreciation for the assistance given during the conduct of the testing by Professor J. J. Harper and Mr. Harold Meyer of the Georgia Institute of Technology School of Aerospace Engineering. I also wish to thank Pete Peterson and Scott McAfee, Jr., of Omni Tech Associates for their dedication in supporting the build and maintenance of the heliostat models. Honeywell also thanks Kenneth Miller of Sandia Laboratories for the interest shown in the test program and the professional motion pictures taken.

G. L. Brown

TABLE OF CONTENTS

TABLE OF CONTENTS (Continued)

LIST OF ILLUSTRATIONS

LIST OF ILLUSTRATIONS (Continued)

LIST OF TABLES

Section 1

INTRODUCTION

During the period of 4 April through 23 April 1977, Honeywell Inc. performed a series of wind tunnel tests on an instrumented 1/10 scale model of its tilt-tilt, low profile heliostat in the Georgia Institute of Technology 9-foot diameter subsonic wind tunnel. The objective of the test program was to conclusively determine the aerodynamic loading that the heliostat might experience under specified operational and survivability conditions. Using free-stream, flat plate theory analyses, the wind loading was the largest cost driver associated with the heliostat build, primarily due to the induced moments about the inner and outer heliostat axis that had to be withstood to maintain operational tracking accuracies and avoid catastrophic failures under higher wind environments.

Basically, the test involved obtaining, directly, inner and outer axis aerodynamic hinge or axial moments at a number of different wind vectors, wind velocities, and heliostat orientations. Similar heliostat geometries were run again with a second 1/10 scale model up-stream of the instrumented model; pressure distributions were obtained for a few configurations; and comparison runs were made using slotted or vented scaled mirror modules. The tunnel's main 6-degree-of-freedom force balance was used primarily to determine total heliostat drag forces that can be related to moments introduced into the heliostat's two foundations. All tests were run with a 1/10 scaled boundary layer profile to duplicate the specified full scale boundary layer. Ground effects upon moments had always been a large uncertainty. Two hundred and forty separate runs were made.

Test results were excellent. Scaling effects were insignificant; data was consistent; worst-case wind loads were less than a half of previous estimates; and the brief testing of different slotted module configurations gave a good basis for possible future design changes with regard to wind loading.

Section 2

TEST SETUP AND INSTRUMENTATION

2.1 GEORGIA TECH WIND TUNNEL FACILITIES

The Georgia Tech subsonic wind tunnel was selected because of its availability, low operational costs, and location advantages. It is a conventional single-return tunnel powered by a 600 hp slip clutch motor with a maximum test chamber speed of about 160 mph (71 m/s). The test chamber is circular with a 9 foot diameter and 12 foot usable length. Figure 2-1 shows a diagram of the tunnel configuration.

Because the tunnel is circular, a flat floor was installed the full 12 foot length of the test section at such a height to allow the heliostat models to clear the tunnel walls. A 4 foot hole was cut to allow complete freedom to the 4 foot circular turntable connected to the six component electromechanical external wind tunnel balance. These characteristics are clearly shown in Figure 2-2 where the view is looking upstream (from the breather portion of the tunnel towards the front of the test section).

2.1.1 Tunnel Instrumentation and Control

Figure 2-3 shows the wind tunnel's control console. In addition to safety features and fan rpm control, the six force components are presented as a digital readout, i.e., the drag, lift, side force, roll moment, pitch moment, and yaw moment. Subsection 2.4 defines all coordinate systems used. The micromanometer seen on the right of Figure 2-3 was the device used to confirm that the desired tunnel speed was reached for each test run after setting the tunnel fan speed and monitoring the built-in tunnel piezo. The micromanometer was connected to the pitot tube and was set at the following levels and motor adjustments made until the correct fluid height was reached and stability attained.

Velocity (mph)	Q_{oo} (Inches of 0.82 sp.g.alcohol)	Q_{oo} Dynamic Pressure (lb/ft^2)
20	0.240	1.0735
30	0.541	2.303
50	1.5017	6.3971
90	4.865	20.727

The pitot tube was mounted 40 inches (1.02 meters) above the floor level directly over the mounted heliostat model, as can be seen in Figure 2-2.

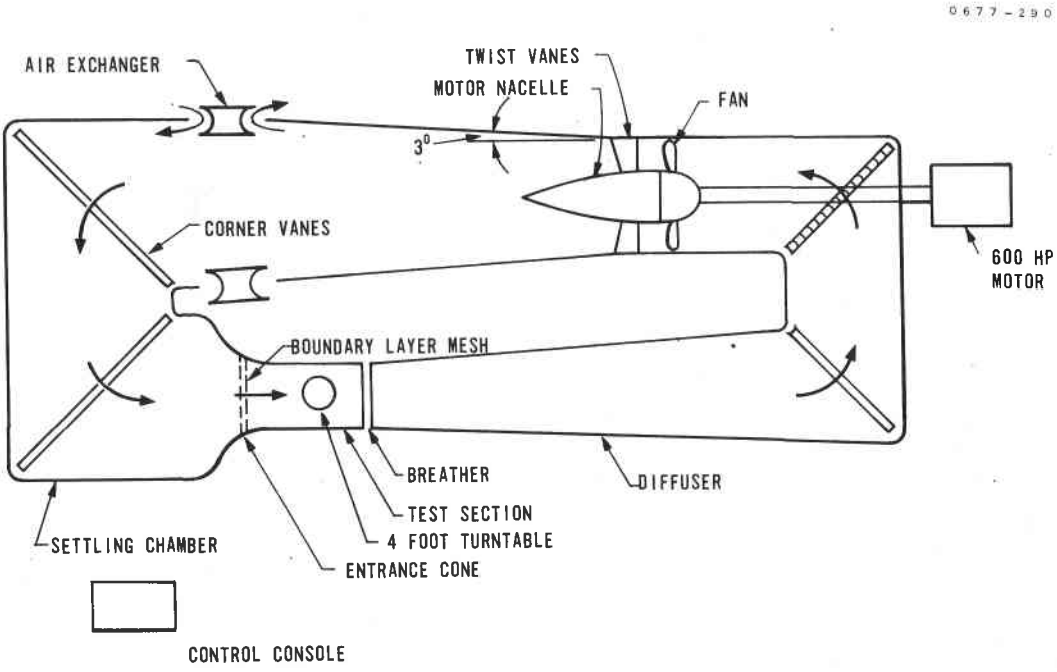

FIGURE 2-1. WIND TUNNEL DIAGRAM
(GA TECH SINGLE RETURN)

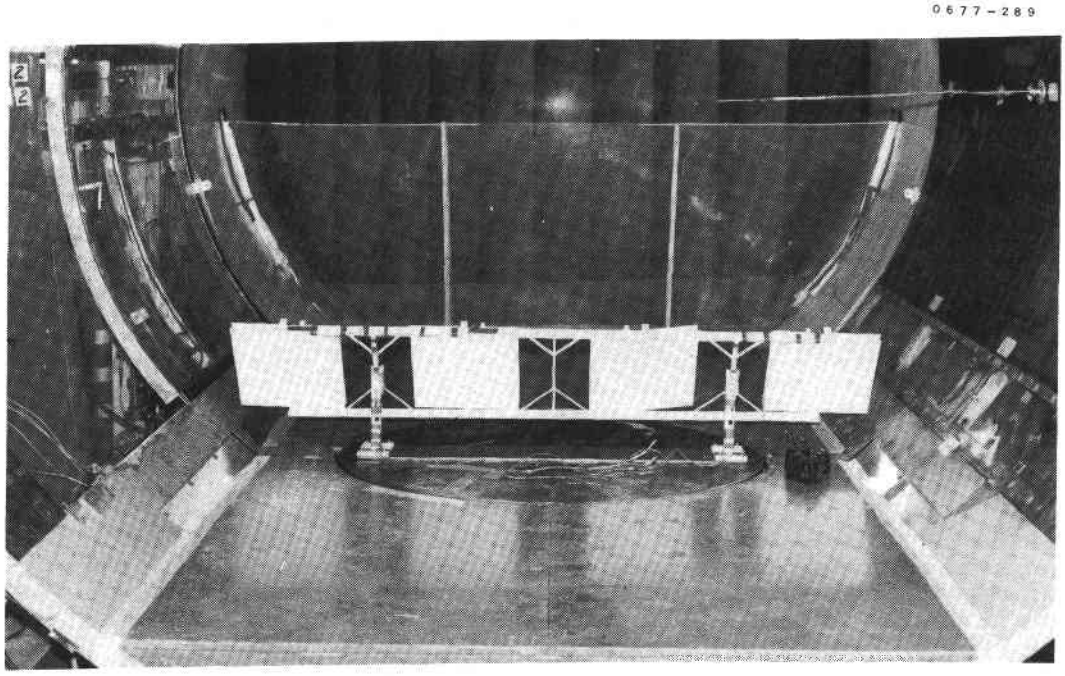

FIGURE 2-2. TEST SECTION CONFIGURATION
(FLAT FLOOR, MODEL MOUNTED ON TURN-TABLE)

0677-288

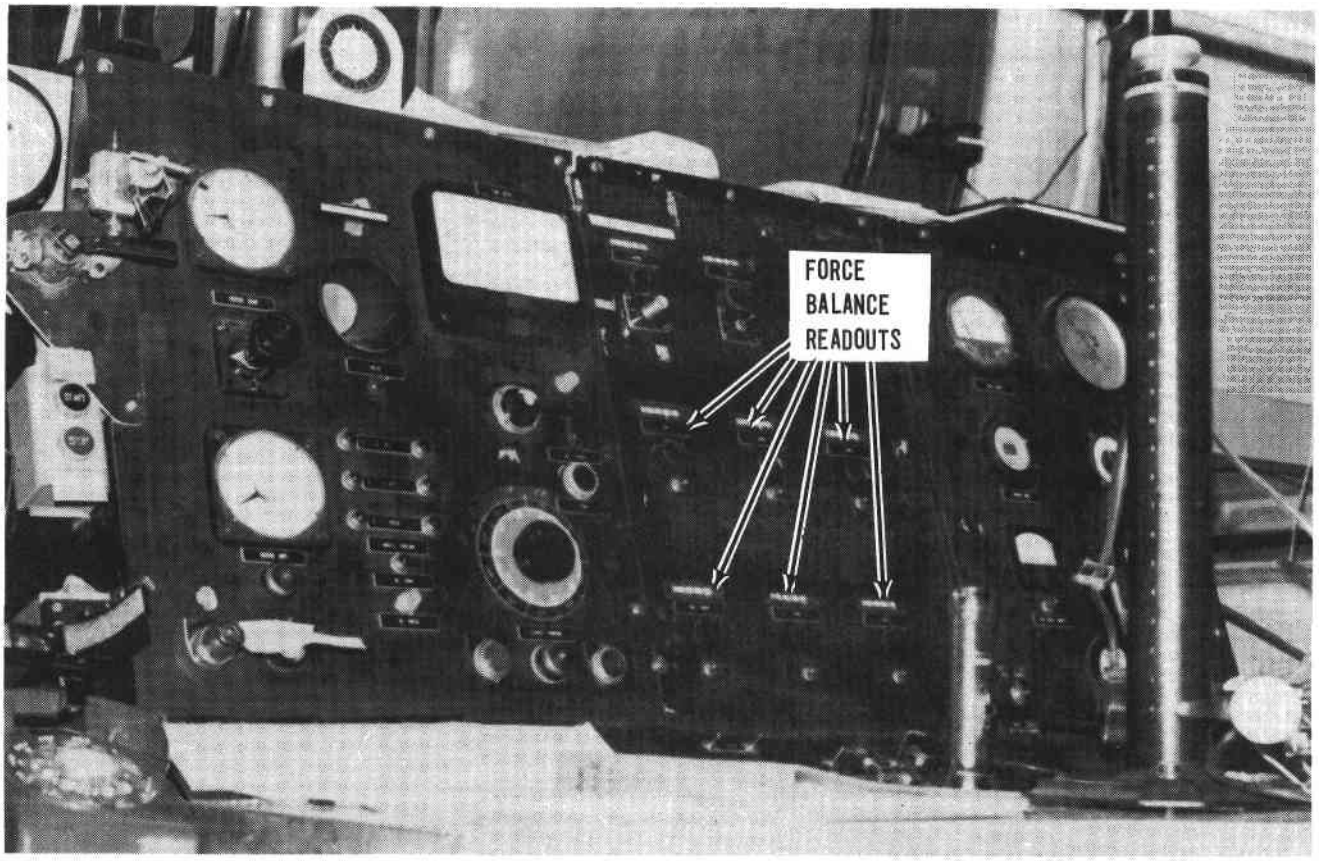

FIGURE 2-3. TUNED CONTROL CONSOLE

With the pitot tube in this location at a 1/10 scaled height of 1.02 meters, free-stream velocities in terms of dynamic pressure ($P-P_{oo}$), where P_{oo} is tunnel static pressure, are directly determinable. Tunnel wind speed variations as a result of differing tunnel blockage ratios at different heliostat orientations and differing ambient conditions (air density, temperature, pressure) are automatically compensated. In other words, the indicated air speed at the pitot tube location is always identical (e.g., 30 mph, 50 mph) when the micromanometer reads the prescribed alcohol level (i.e., measuring tunnel $P-P_{oo}$) from day to day and model orientation-to-orientation. The true ground speed may vary ±2 percent but the indicated air speed, or dynamic pressure, was maintained for each prescribed velocity at the scaled 10 meters height.

When desired, after the tunnel speed stabilized, the force and moment data from the tunnel balance were printed three times (under the operator's control) on the flexowriter connected to the control console. After wind shutdown for each run and before model configuration change, zero balance readings were taken (3 of each component) to insure that the balanced returned back to its prerun values.

Note that under operator control, the model heliostat could be rotated (yawed) to any set angle within a resolution of 0.01 degree with respect to the tunnel downstream wind vector.

2.2 BOUNDARY LAYER SIMULATION

The optical center line of the SRE heliostats, or frame axis, is about 94 inches above ground level. With the frame interference effects and an ERDA specified wind velocity profile at any height, h, of

$$V_h = V_{oo} \left(\frac{h}{100 \text{ meters}} \right)^{0.15}$$

the induced axial moments could not be analytically determined. V_{oo} represents the desired free-stream wind velocity at 10 meter height (33 feet). Therefore, it was necessary to duplicate the boundary layer to the same scale as the heliostats. This was successfully accomplished within the tunnel by fabricating with trial and error a curved 1/4-inch screen mesh of differing densities upstream of the test section. Figure 2-4 is a photograph showing details of the construction.

Figure 2-5 shows velocity data taken with a 36-inch vertical tunnel pressure rake at 20, 30, 50, and 90 mph emphasizing the profile development from zero to 16 inches height. At all heights and speeds, the (V/V_{oo}) magnitudes follow the $((h)/h_{oo})^{0.15}$ constraint except for extra fullness at heights from 6 to 12 inches which would create loads predominately on the larger, or conservative, side. This profile is shown along with the tunnel wind profile with no mesh upstream showing only the normal wall boundary layer effects.

0677-283

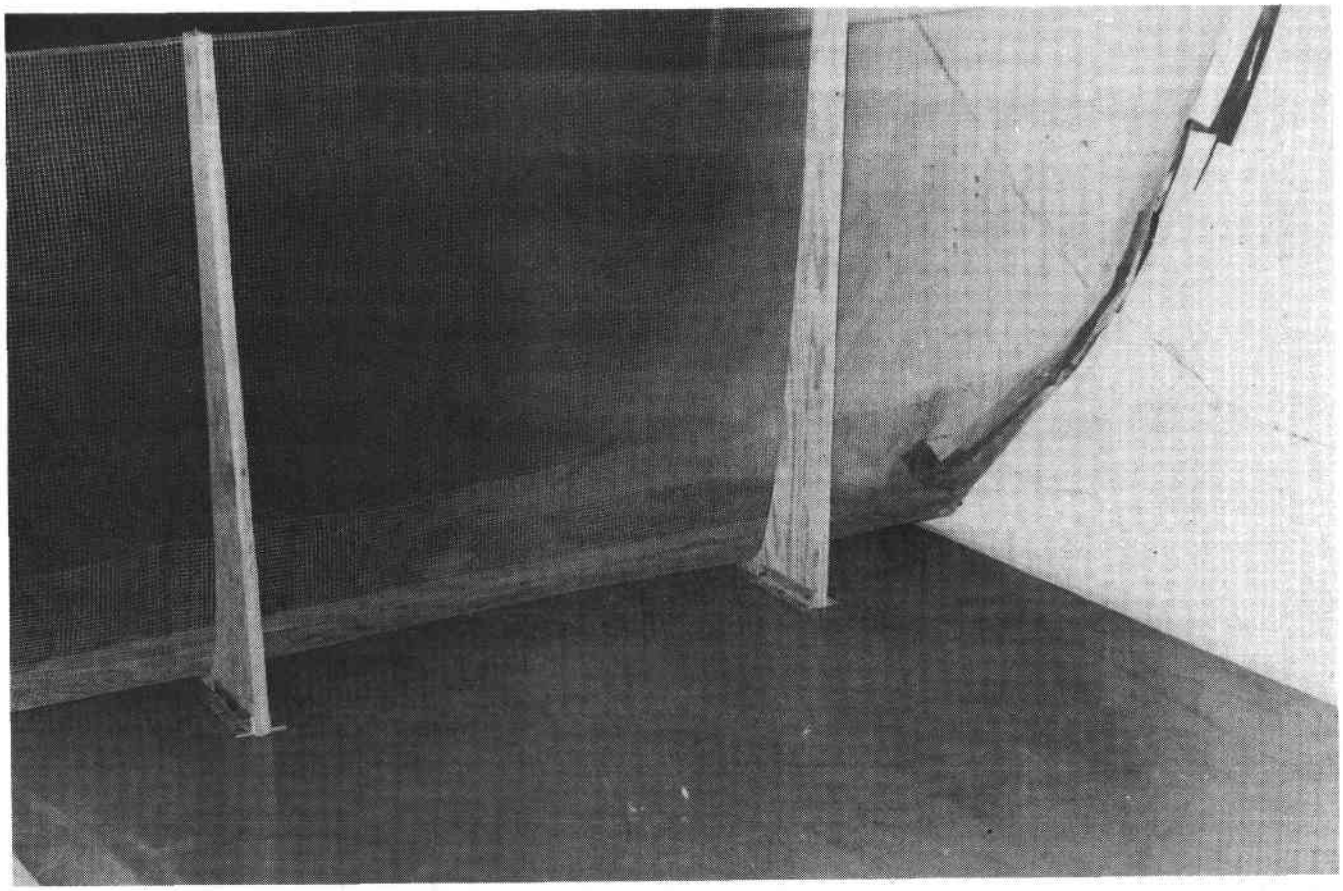

FIGURE 2-4. CONSTRUCTION OF SCALED BOUNDARY LAYER CONTROL SCREENING

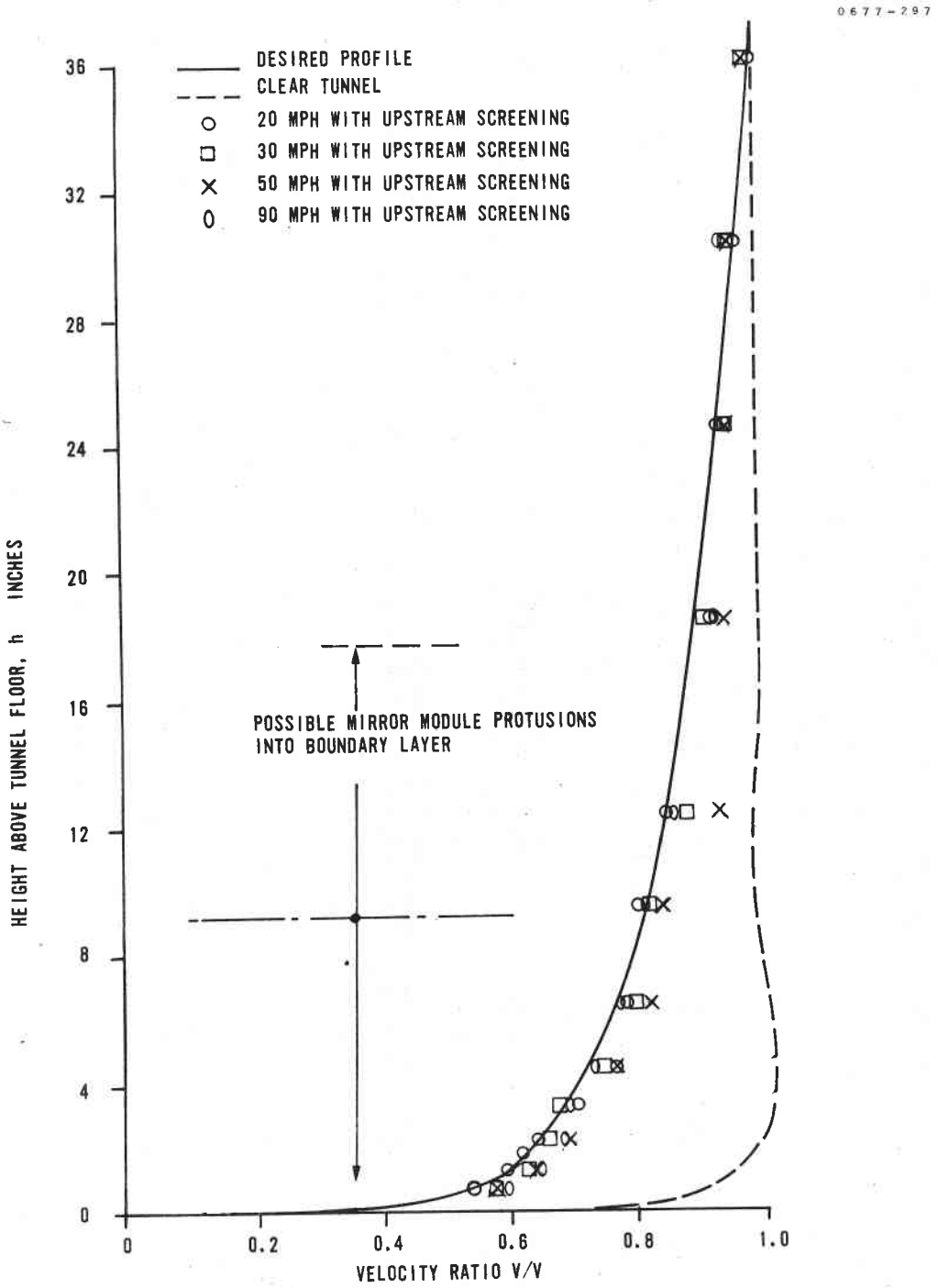

FIGURE 2-5. MEASURED SCALED VELOCITY PROFILE AT DIFFERENT SPEEDS

The rake measurements were taken along a vertical axis up from the location which would be the center of the instrumented model for all subsequent testing as shown in Figure 2-6.

Because of turbulent, periodic gusts caused by attachment and detachment along the top line of the screen mesh hitting the pitot tube at 36-inch height, causing significant vibration, the speed control pitot tube was placed 40 inches above the ground plane which corresponds to the scaled 10-meter reference height.

2.3 HELIOSTAT MODELS

The cornerstone of the test program was the fully instrumented 1/10 scale model heliostat. Each of the four 1-foot square mirror modules were mounted along the frame with precision miniature ball bearings at each shaft. The shafts were centered and aligned such that there was no residual mirror imbalance and no shaft to bearing misalignment to induce rotational friction or binding. The outer axis, or frame, was mounted to the two posts, this time with only one bearing at each gimbal as shown in Figure 2-7. Both "slab foundations" were bolted to a 1/4 inch thick aluminum mounting plate which in turn was centered and mounted on the turntable that was flush with the tunnel floor and interfaced with the external six component force balance system. Clay and tape were used to fair the ground plane up to the 1/4 inch thick plate to prevent an abrupt flow disturbance. The tare drag induced by the mounting plate was determined (ΔC_D=0.0165) and was subtracted from all force balance drag data.

Instrumentation on the 1/10 scale model included strain indicators to determine mirror module and frame rotational moments, 9 pressure taps along each of the 4 mirror modules, and the capability of having the pressure tap mirror modules interchangeable with scaled vented mirror modules.

Each of the mirror modules could be rotated freely ±360 degrees and the outer axis could be rotated between -30 degrees through +73 degrees angular rotation.

2.3.1 Strain Gage Instrumentation

In order to obtain the induced aerodynamic axial moments directly, a hardened steel strain gage block was mounted to one shaft of each mirror module and to both outer axis bearing pins. Figure 2-8 shows how the gage block was affixed to an outer axis shaft. The gage block would remain in place and the outer or inner axis rotated to the desired angular rotation and then the adjustment or clamping bolt torqued down such that no slippage would occur between the shaft and gage block. The gage block arm would then have all residual stresses removed by relaxing the set pins and then retightening. The set pins were rounded such that no inherent side torques would be introduced into the gage block arm. Each gage block was instrumented

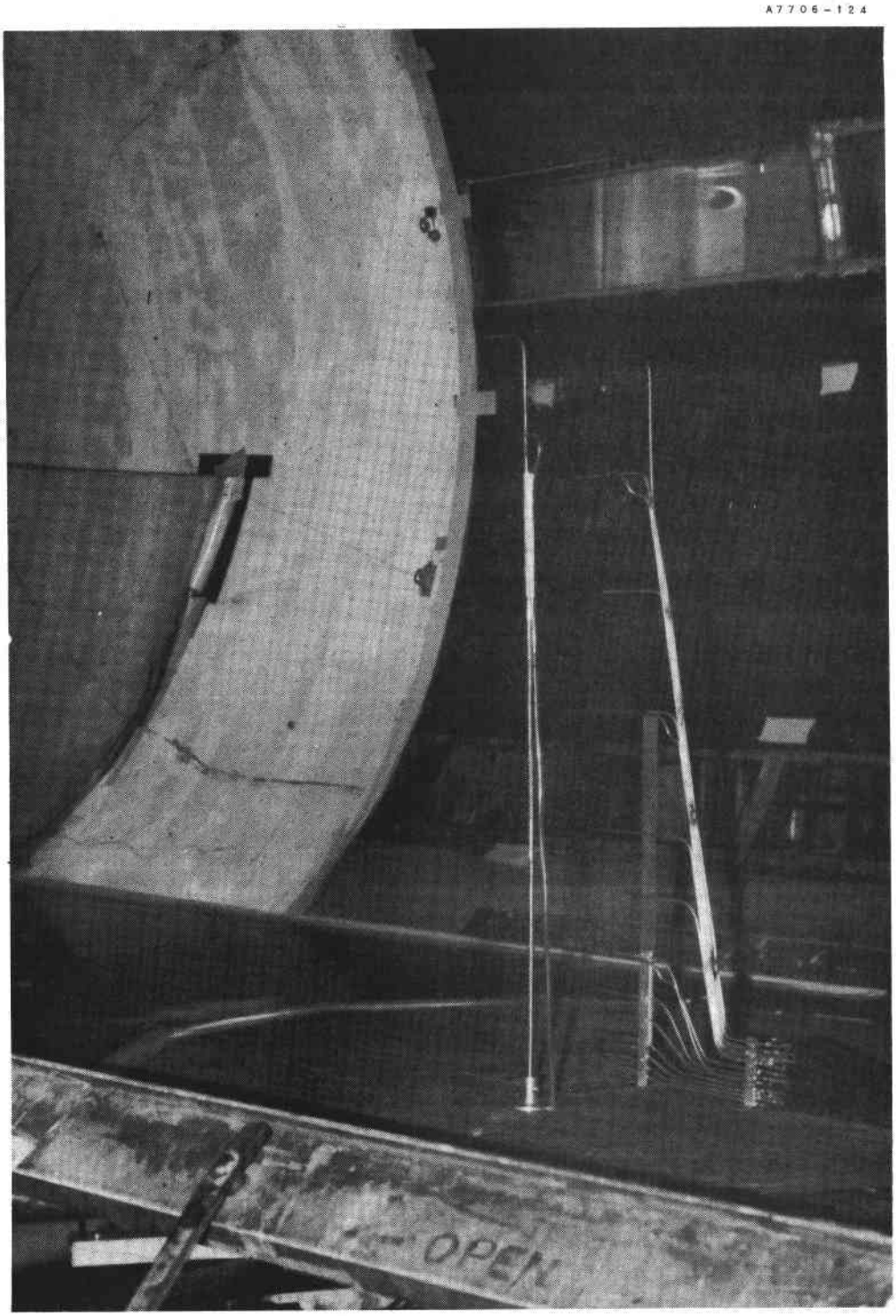

FIGURE 2-6. TESTING THE BOUNDARY LAYER PROFILE

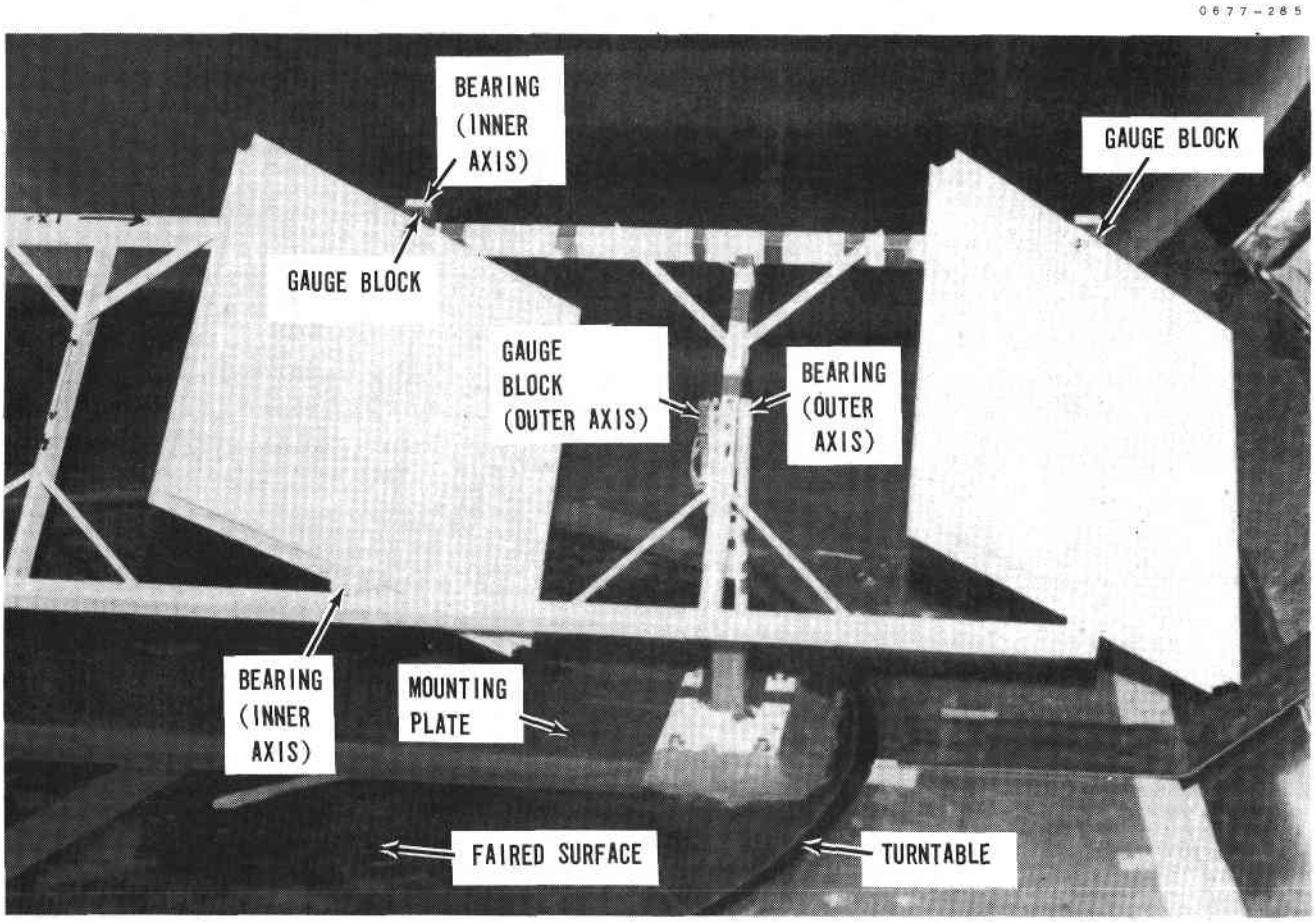

FIGURE 2-7. INSTRUMENTED MODEL MOUNTING DETAIL

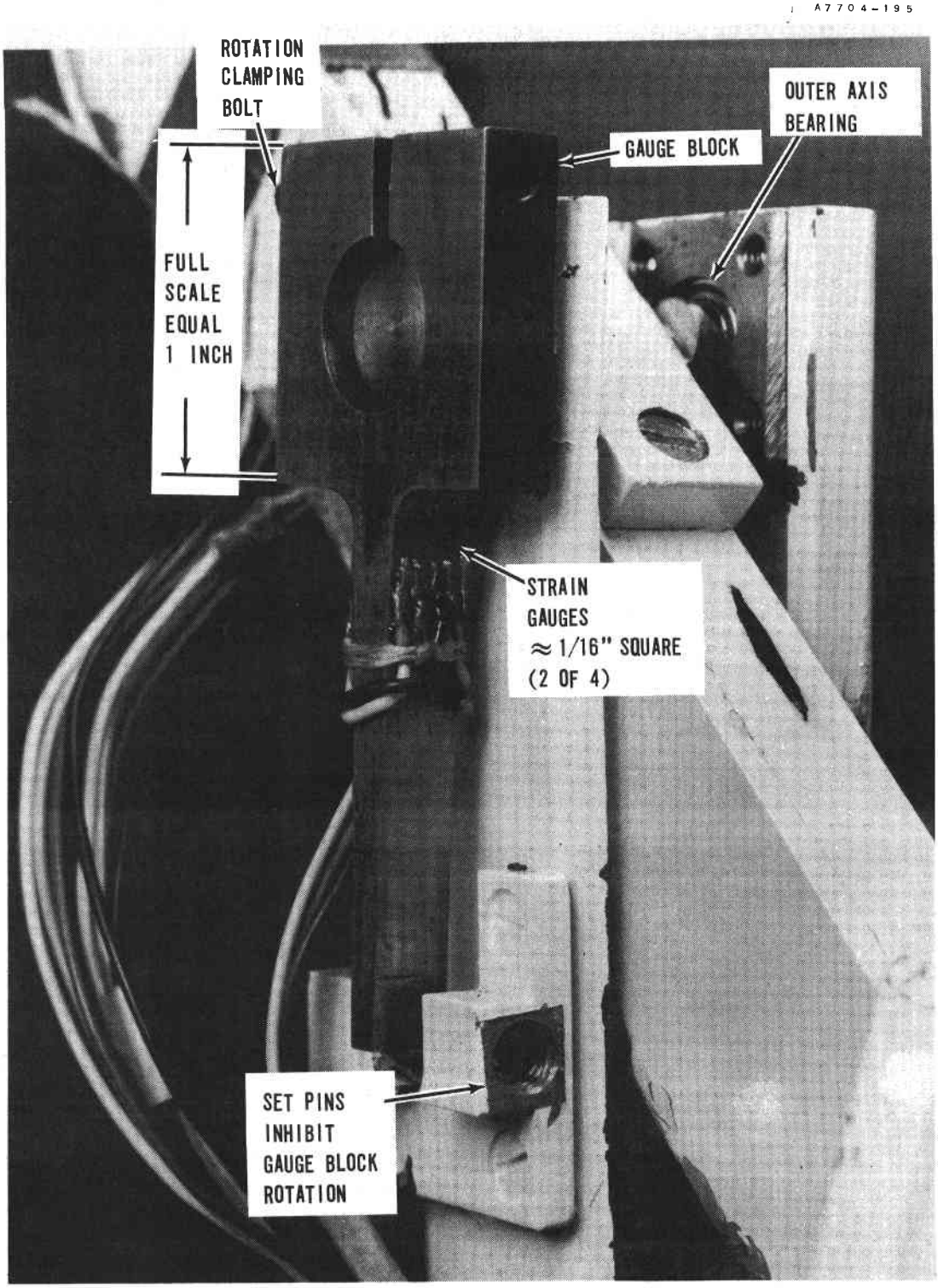

FIGURE 2-8. OUTER AXIS STRAIN GAGE CONFIGURATION

with a full, 4-arm, strain gage bridge using miniature 1/16 inch square gages. A similar arrangement was incorporated for each of the four mirror modules (Figure 2-9). All wires from each set of strain gages (24 total) were taped to the frame with missile tape, routed down the posts and collected near the center of the turntable, routed through a hole and routed underneath the tunnel to the external instrumentation. Each inner axis was designed to cover the range of 0 → ±5 ft-lbs of moment and the outer axis 0 → ±20 ft-lbs of moment.

The axial moments were obtained from the gage outputs that were channeled into a Baldwin-Lima-Hamilton 10-channel switching unit which, in turn, was connected to a Baldwin-Lima-Hamilton type 20 SR-4 strain indicator, shown in Figure 2-10. Resolution of each of the 6 axes was on the order of 0.001 ft-lbs per strain indicator count in either rotational direction. As indicated in Section 3, each 4-arm bridge was checked daily with regard to calibration. The readings were very linear over the full range. During all calibrations, straight line fits of induced moments versus strain reading were accompanied with correlation coefficients of greater than 0.999.

Moment data for a given channel was acquired after steady wind velocities were reached by nulling out the balance needle indicator and recording the strain indicator dial reading counts on a data sheet. To obtain the next mirror module or outer axis axial moment, the channel was switched and the process repeated. Typically, this was done for all 6 channels used, but in some cases only certain selected moments were obtained and not all 6.

2.3.2 Interference Model

A second, less expensive 1/10 scale heliostat model was built with the same degrees of inner and outer axis rotational freedom. However, it was not instrumented, and the shafts were not stiction free. It was used for a few runs by placing it upstream of the instrumented model at two different distances and at the same inner and outer gimbal orientation and yaw (wind vector) angle as the instrumented model. The hinge moments and total drag were recorded from the instrumented balance on the force balance with the interference model upstream as shown in Figure 2-11.

2.3.3 Pressure Distribution Measurements

Each mirror module of the instrumented heliostat had nine pressure taps over one surface which were covered with scotch tape during all testing involving moment determination via the strain gages.

The numbering scheme, 1-36, is shown in Figure 2-12. One tap was in the center of each square panel, and the other eight taps distributed uniformly along each axis per the dimensions of Figure 2-12.

A7704-196

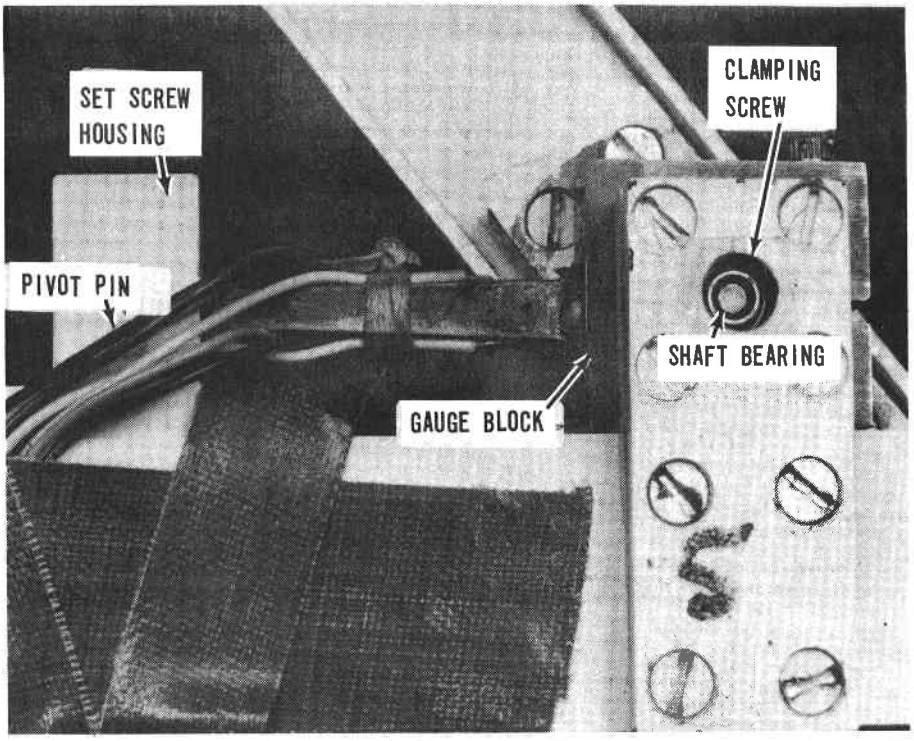

(a)

A7704-197

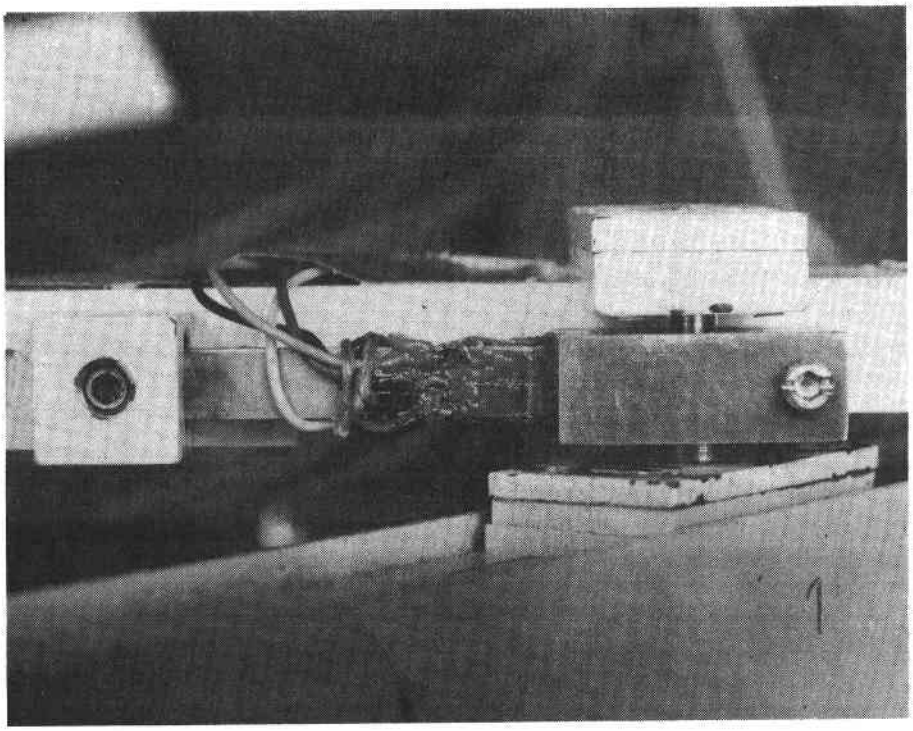

(b)

FIGURE 2-9. INNER AXIS STRAIN GAGE CONFIGURATION

0677-287

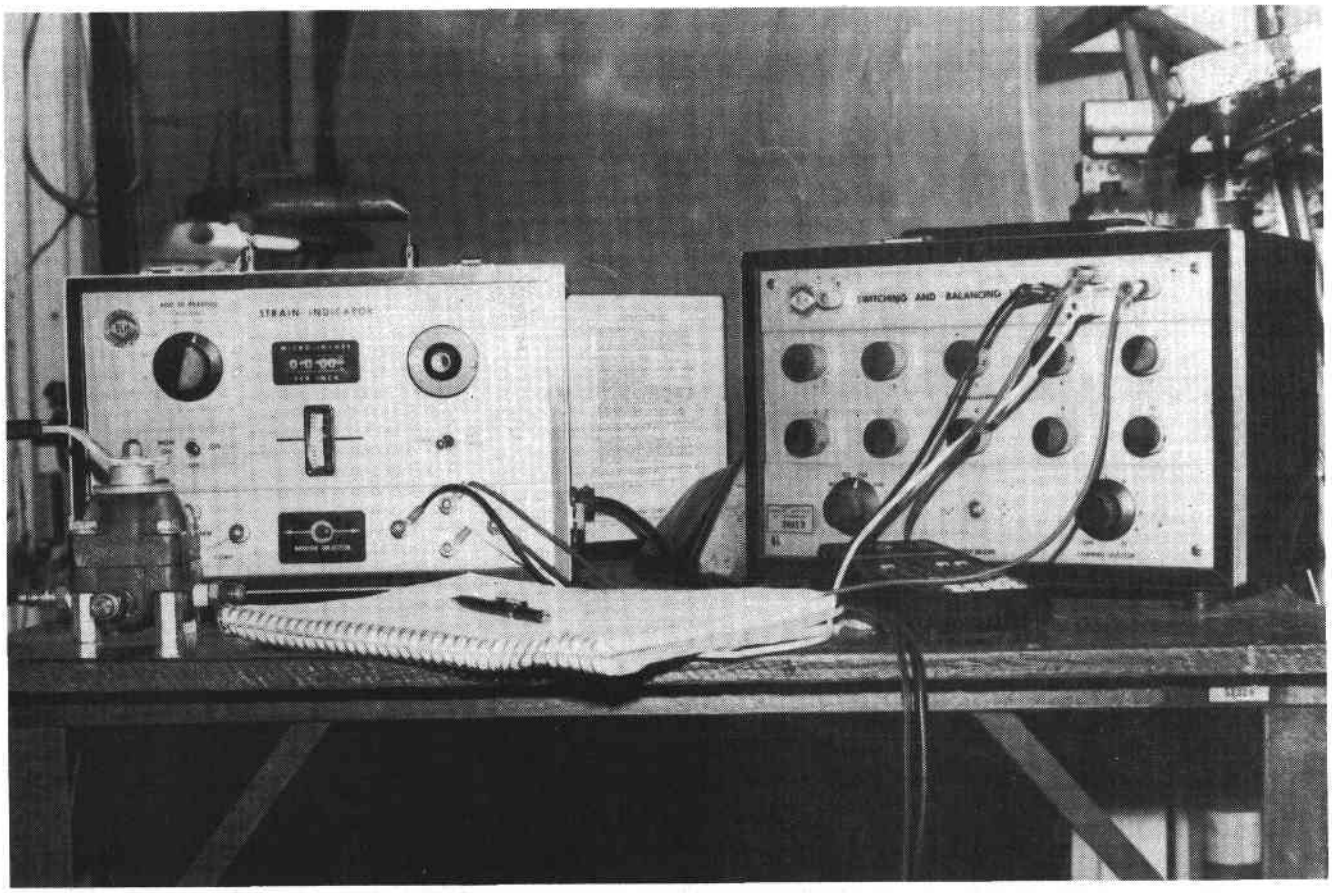

FIGURE 2-10. STRAIN GAGE MAINTAINING INSTRUMENTATION

0677-286

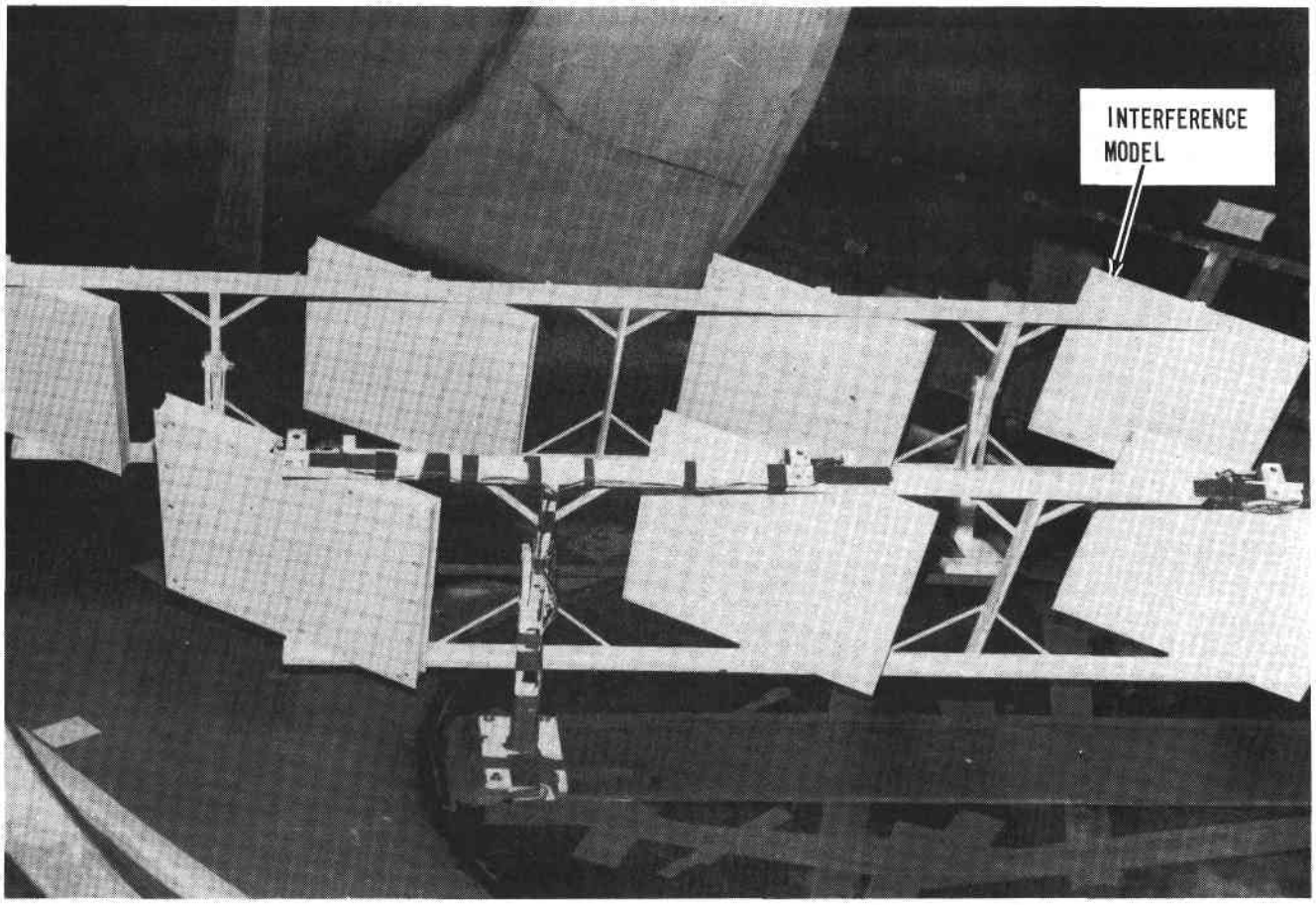

FIGURE 2-11. INTERFERENCE MODEL UPSTREAM OF INSTRUMENTED MODEL

0677-287

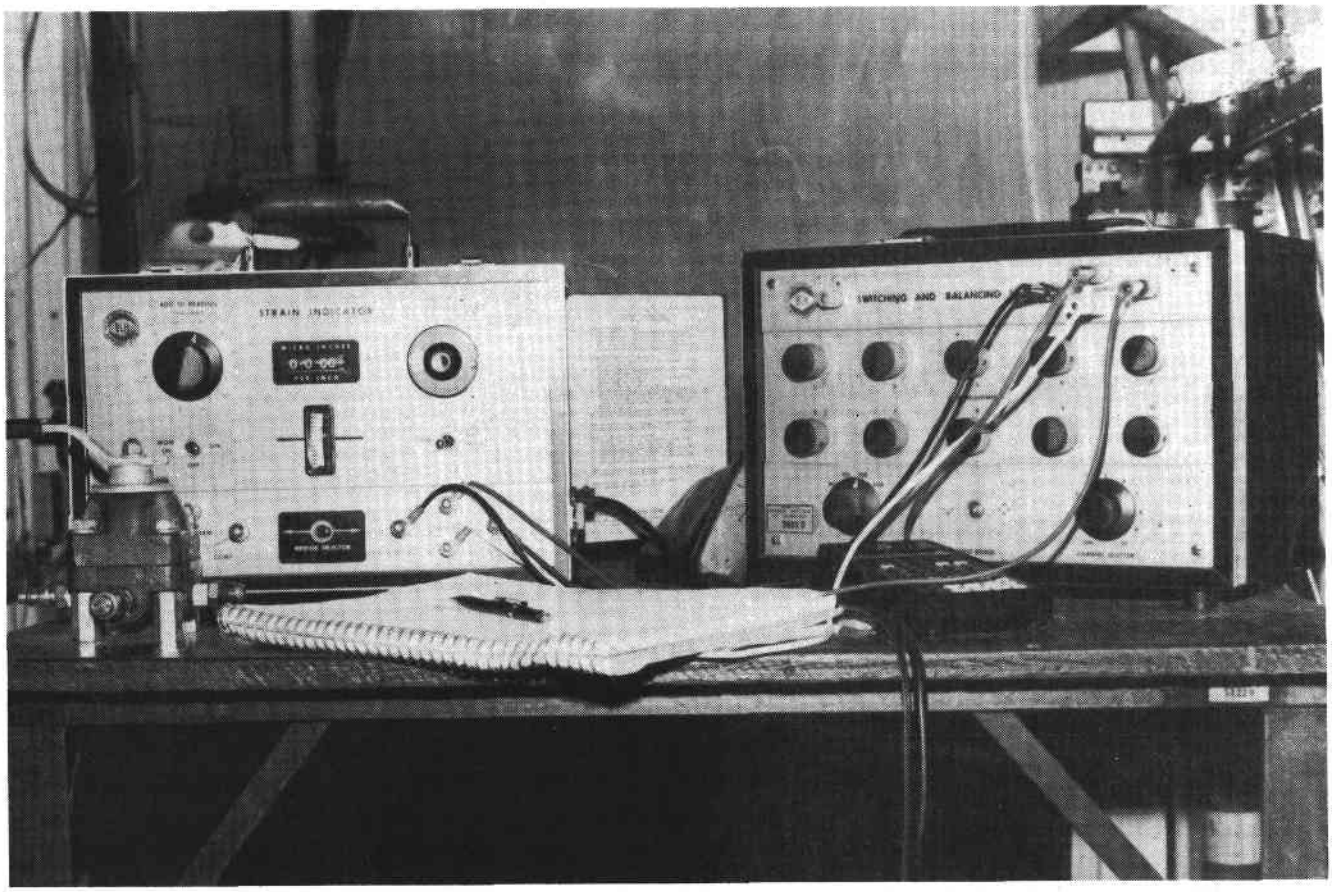

FIGURE 2-10. STRAIN GAGE MAINTAINING INSTRUMENTATION

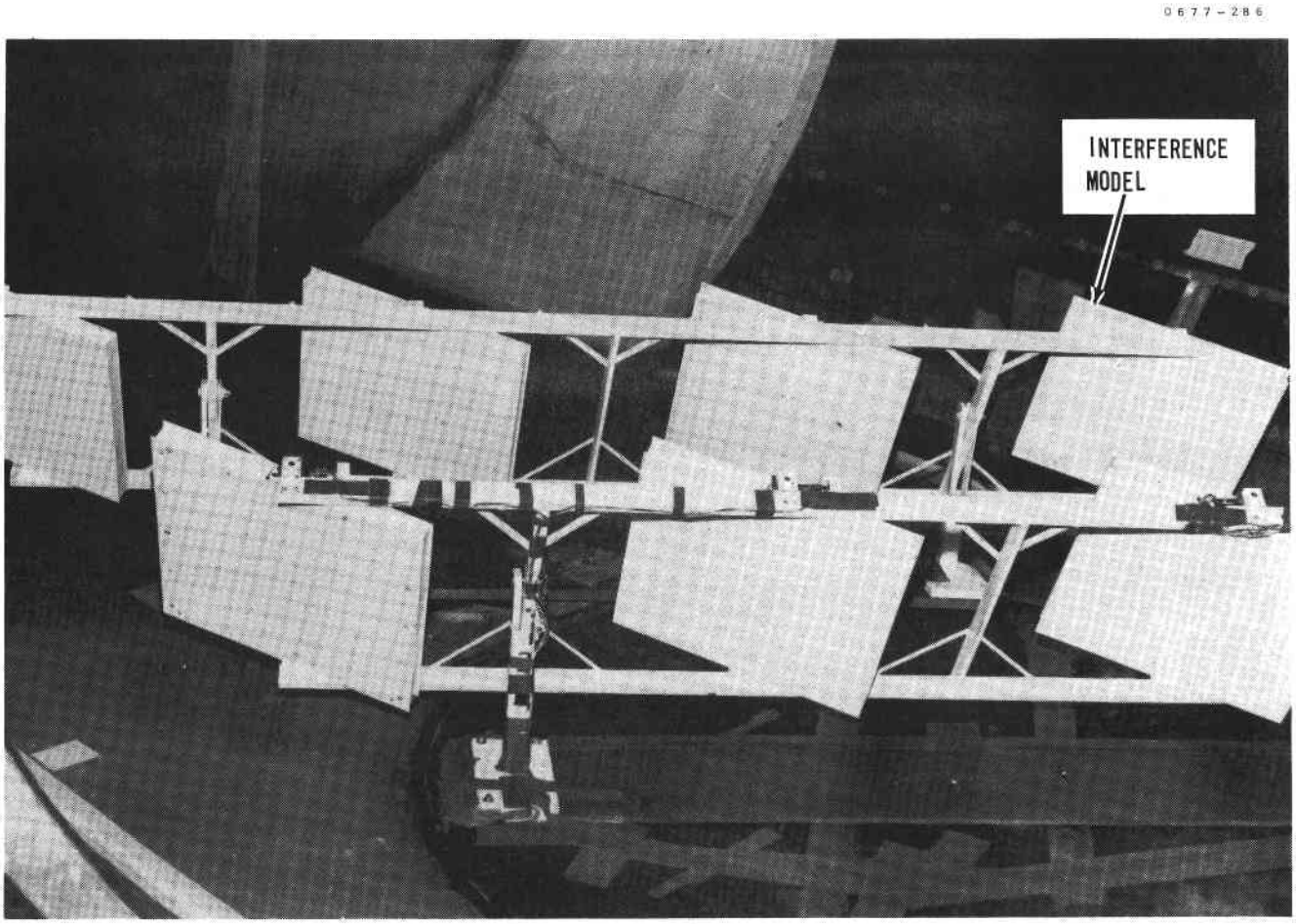

FIGURE 2-11. INTERFERENCE MODEL UPSTREAM OF INSTRUMENTED MODEL

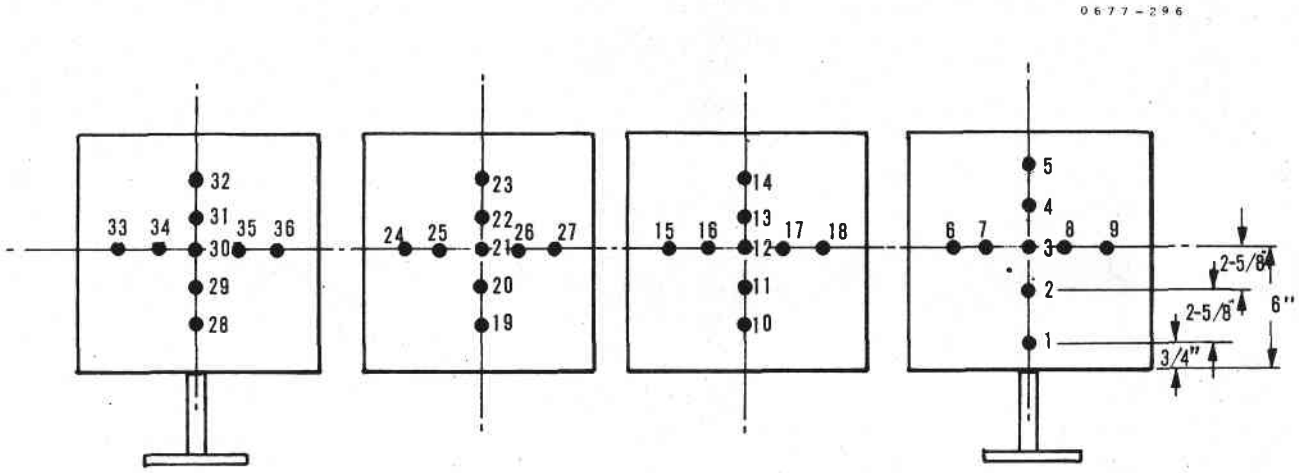

LOOKING DOWNSTREAM AT FORWARD FACE OF MODEL

FIGURE 2-12. MIRROR MODULE PRESSURE TAP CODE

When pressure tap test runs were made, the back skin of each module was removed, 1/16 inch OD Tygon tubing attached to the taps, and routed through a small hole in the back skin in a small bundle. The bundles were routed along the frame and dropped directly vertically through holes drilled in the turntable as shown in Figure 2-13. Note that to obtain a complete pressure distribution, two runs must be made-- one with the taps at one inner axis angle, ϕ, and the other at ϕ +180 degrees such that both up-wind and down-wind mirror module side distributions can be obtained to determine net normal loads.

Pressure data acquisition was automated per the diagram shown as Figure 2-14. The 36 pressure tap lines were routed under the turntable to a 48 part model J Scanivalve which was attached to the underneath side of the turntable (Figure 2-15) and depicted in the flow diagram of Figure 2-14. Except for the Barocell and Scanivalve assemblies, all the other equipment was housed in two racks plus the teletype per the following list and Figure 2-16:

- Teletype with tape punch
- Hewlett Packard 2114B computer
- Monsanto Data Scanner, Model 508A
- Hewlett Packard Tape Reader 2748B
- Hewlett Packard Integrating DVM, Model 2401C
- Scanivalve position indicator
- Scanivalve Corp. 5 channel selenoid controller, Model CTLR2/5XS4
- Datametrics Signal Conditioner, Model 1015-S2
- Datametrics Power Supply, Type 700
- Barocel Pressure Sensor, Type 511-12 (1000 mm Hg range).

Basically, the system worked as follows. A program was written to daily perform an end-to-end calibration of the Barocell and signal conditioners electrical scaled output and bias. This program was run prior to a days testing and applicable calibrated constants were stored into the 2114B memory. The main operational program, which was also developed for this test program, was then loaded. Prior to each test run, the test number and dynamic pressure in terms of millimeters of Hg, were loaded in. Then under computer control, after the desired wind speed was reached and stabilized, the Scanivalve was commanded from port to port once every 5 seconds until all 36 taps were read. For each port, after a 2-second settling time was allowed, the Barocel output was read 10 times from the signal conditioner by the integrating DMV within a period of 1 second. That is, 10 readings were taken, each integrated over a period of 100 ms.

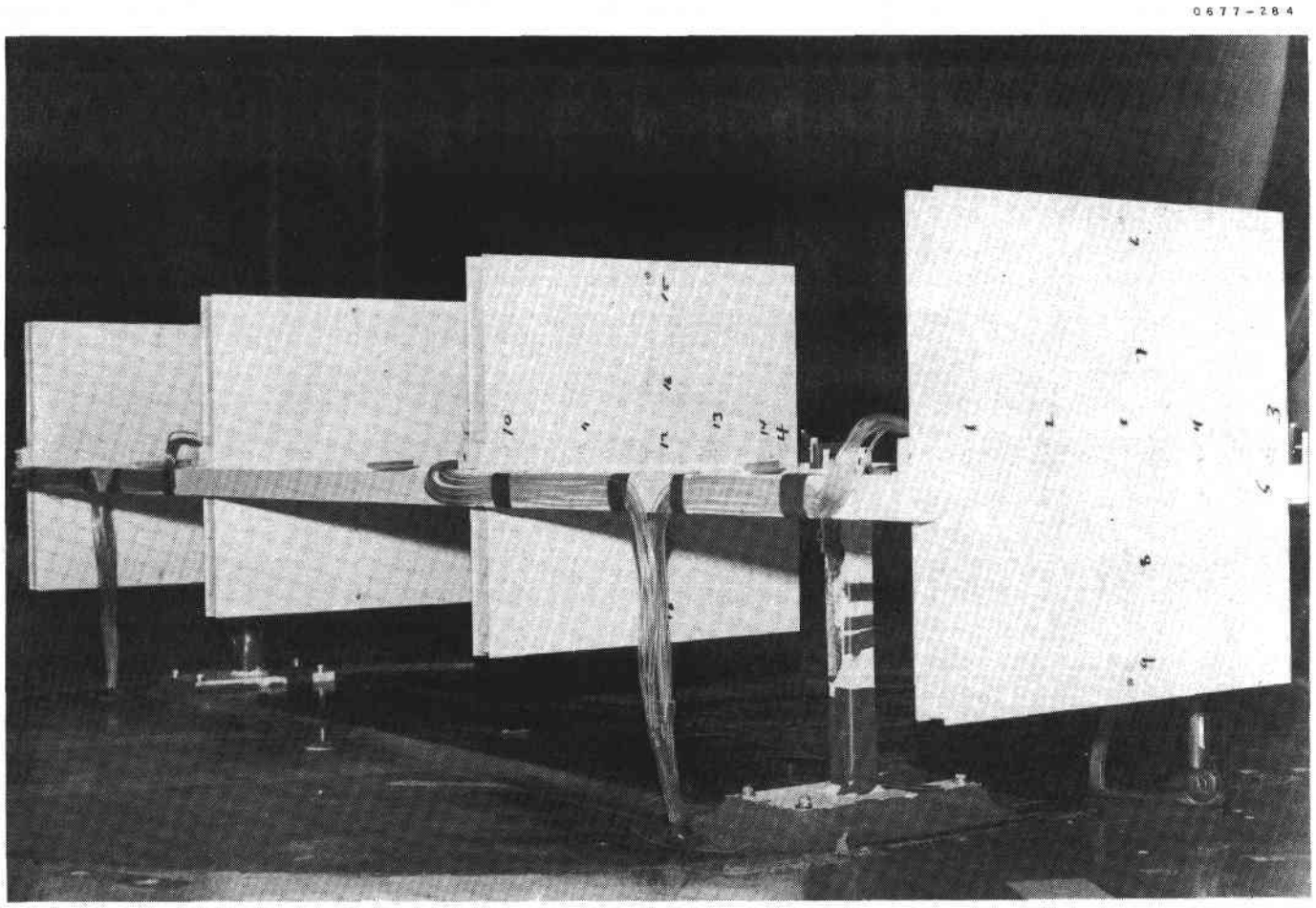

FIGURE 2-13. PRESSURE TUBING DISTRIBUTION

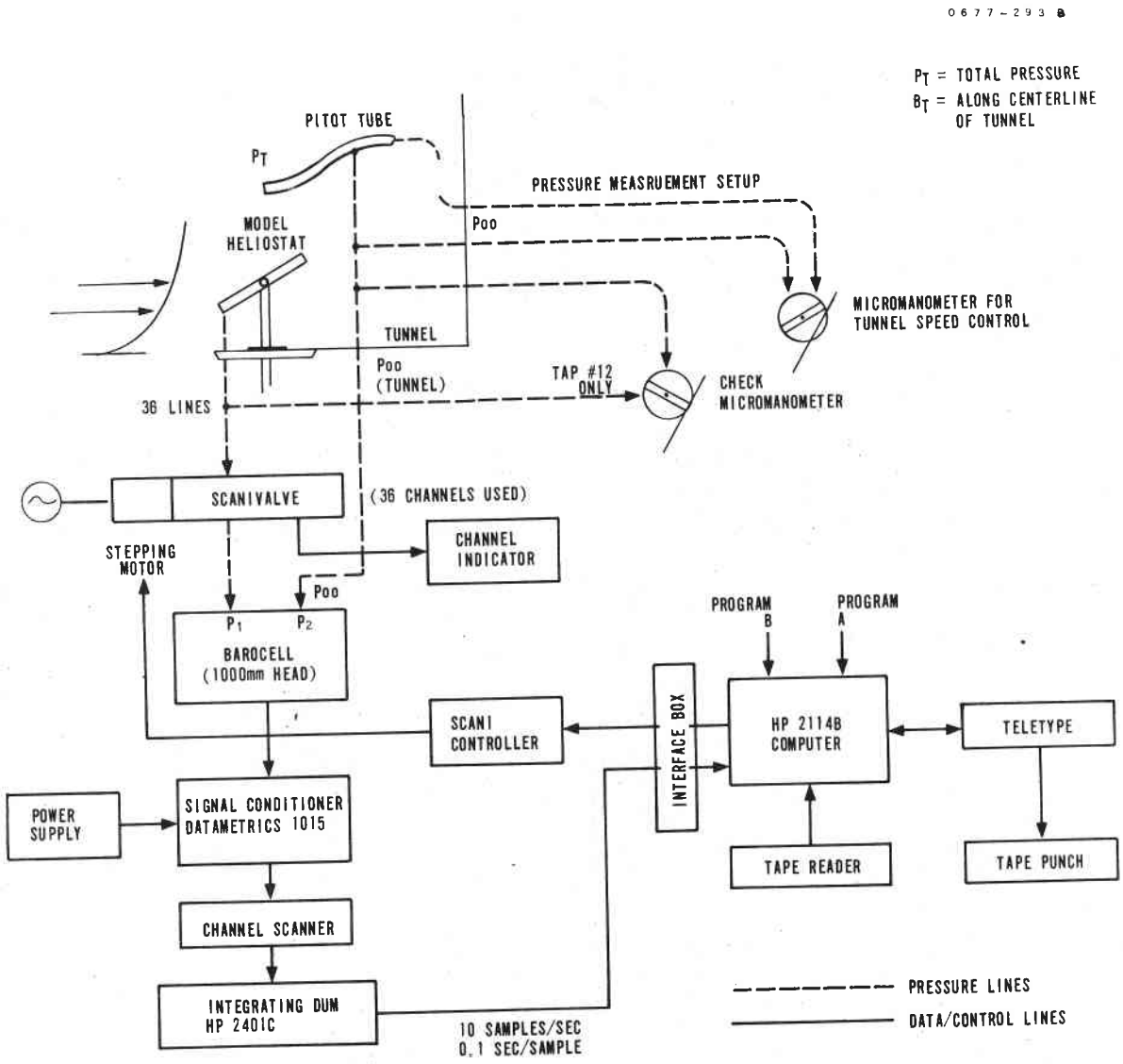

FIGURE 2-14. PRESSURE DATA ACQUISITION SCHEME

0677-282

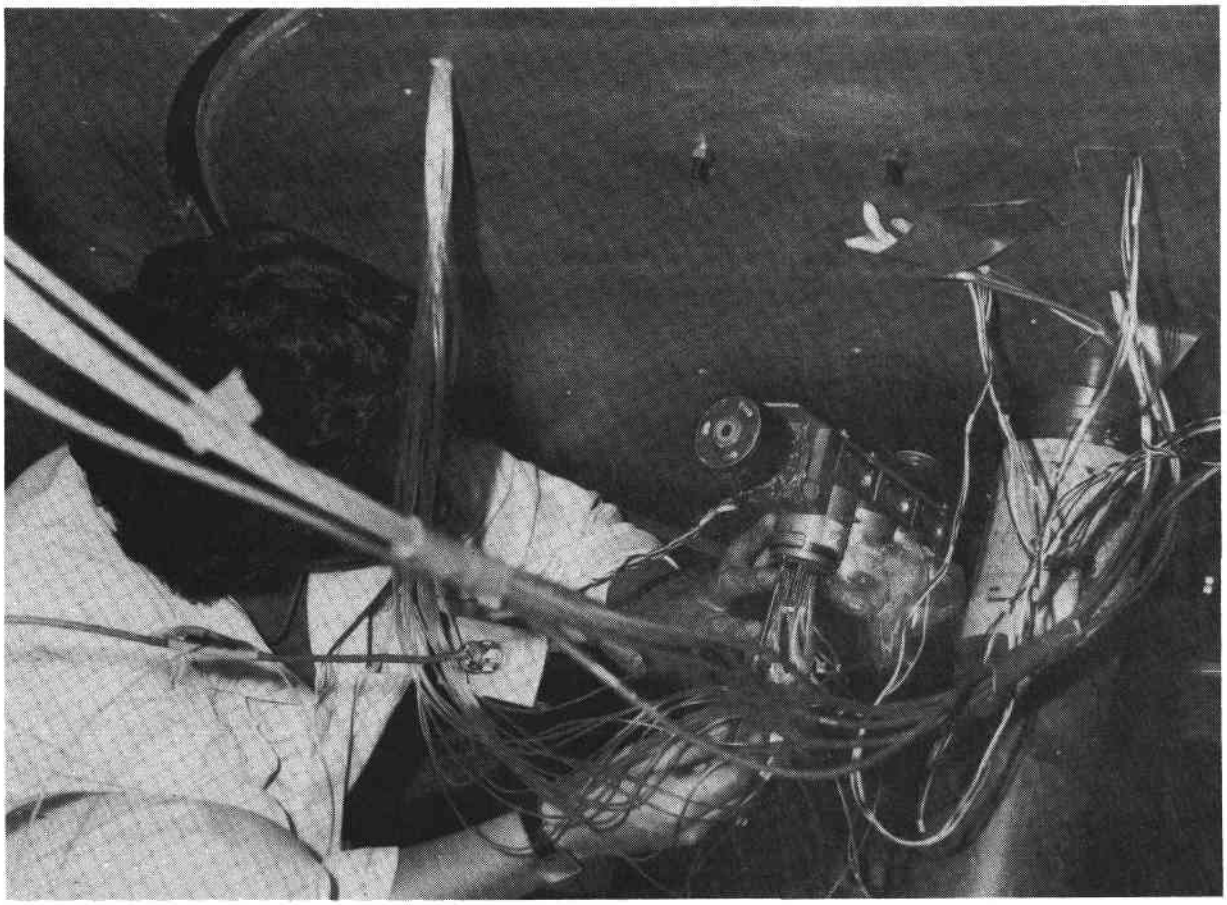

FIGURE 2-15. SCANIVALVE ATTACHMENT TO PRESSURE

0677-292

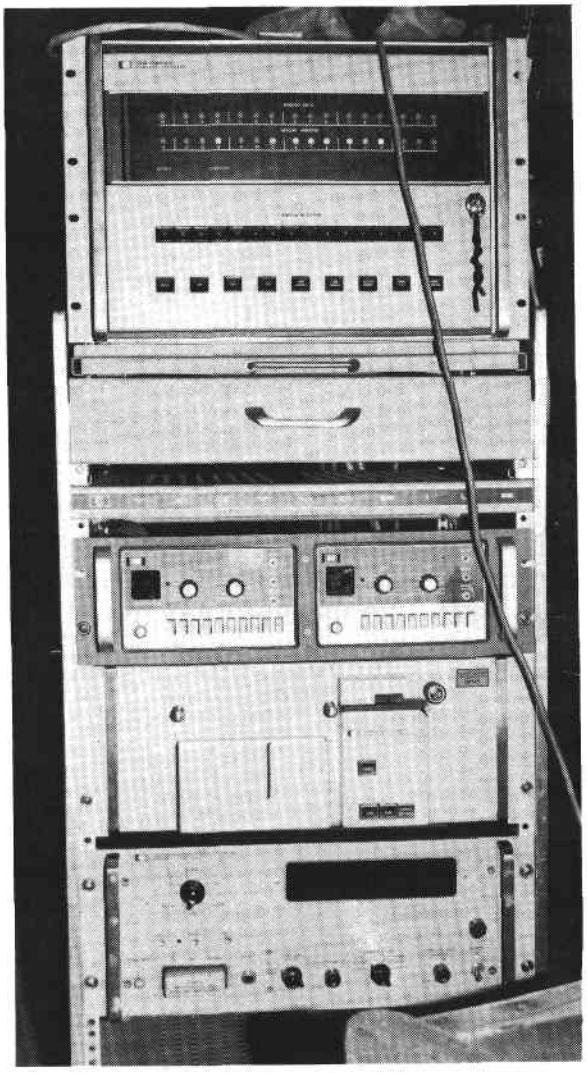

0677-291

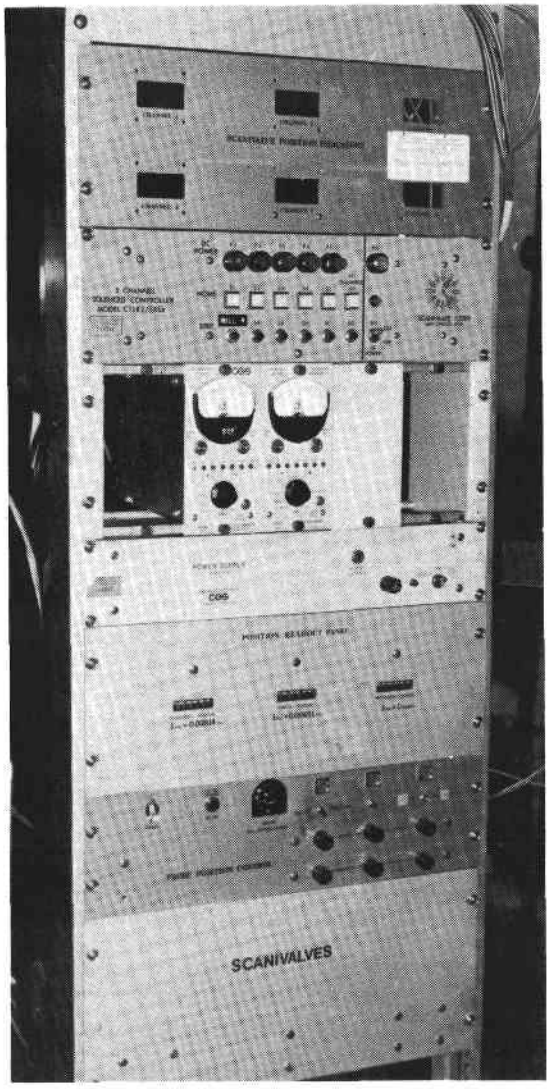

FIGURE 2-16. PRESSURE DATA ACQUISITION HARDWARE

The computer program retained the maximum and minimum reading of the 10 samples, averaged all 10 readings, stored the results in a memory array and then commanded the system to sequence to the next Scanivalve port. After all 36 were obtained, the average reading, maximum and minimum, were dumped onto the teletype as a hardcopy and on paper tape punch. Using the calibrated Barocell constants and the dynamic pressure (indicated air speed), each pressure datum was reduced into its non-dimensional coefficient form:

$$C_p = \frac{P_{indicated} - P_{static}}{q}$$

In addition, to insure the data acquisition complex was producing valid results, one tap (normally No. 12) was picked off and monitored off-line with a second micromanometer. After converting for the specific gravity of alcohol used (0.816), the manometer C_p was compared to the computer printed output.

2.3.4 Vented Mirror Modules

In order to obtain directly comparable data of the influence of slotted mirror modules under specified wind boundary layer conditions, three different configurations (facet aspect ratios) of square mirror modules, each still 0.9 inch thick, were built with a solid balsa wood core and substituted for the 4 solid modules. Figure 2-17 shows the modified instrumented scale heliostat with the tunnel test section. Note that with respect to the mirror module rotational axis, there is in effect three different facet aspect ratio configurations: 1.0, 1.5, and 0.67. The slots were cut 0.25 inch wide. On the 9-facet modules, the solidity ratio was approximately 93.6 percent and on the two different 6-facet modules, the solidity was 95 percent. Testing of these configurations was mainly limited to evaluating each separate module from an upstream, wind end-on wind vector at different inner axis angles (e.g., angle of attacks). Figure 2-18 is a photograph of the instrumented model with the various vented modules taken from the frame side housing the 4 inner axis strain gages. Notice the mirror module number for each aspect ratio/hinge line configuration. The numbers stay with the modules, even though their position on the heliostat may change.

2.4 COORDINATE SYSTEMS AND GEOMETRY

Two coordinate or reference systems are involved: the tunnel frame and the model heliostat frame. Obviously, all inner and outer axis moments obtained from the strain gages read directly within the heliostat coordinate frame. Likewise, so do the normal pressure coefficients.

0677-294

FIGURE 2-17. 1/10 SCALE MODEL WITH VENTED MIRROR MODULES IN WIND TUNNEL

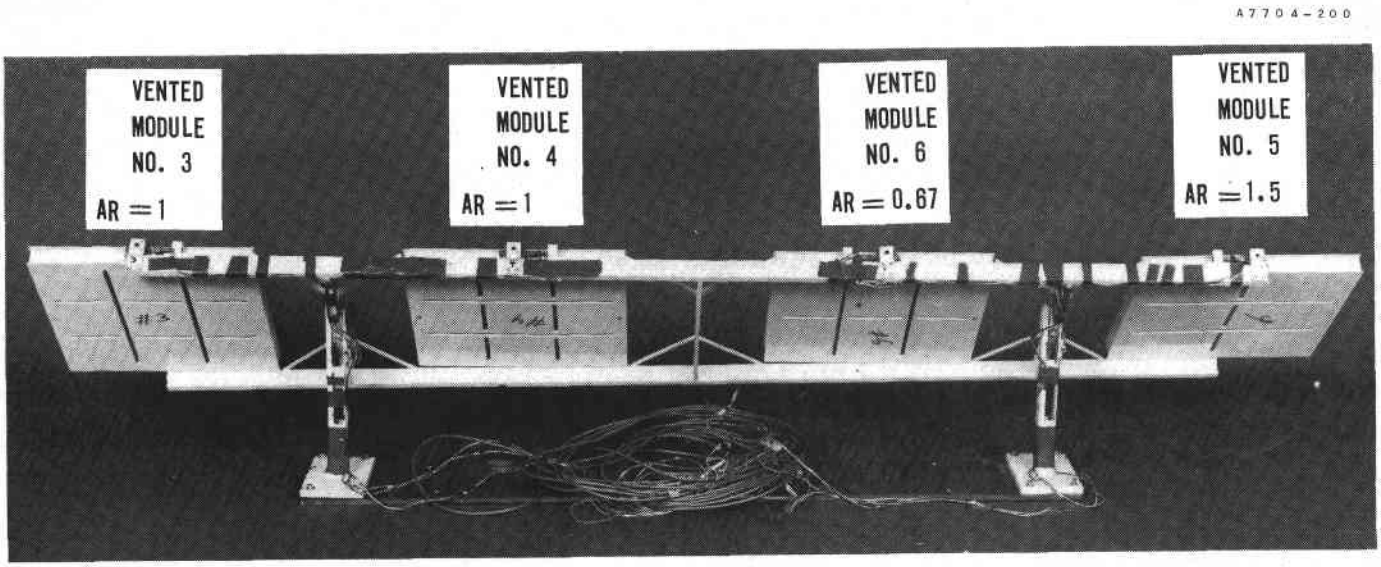

FIGURE 2-18. INSTRUMENTED MODEL WITH VENTED MIRROR MODULES

Figure 2-19 defines the heliostat geometry and zero reference orientations. Throughout all testing, the moment about the outer axis is defined by readings of strain gages No. 1 and No. 2 regardless of the heliostat rotation (γ) with respect to the wind direction. The non-dimensional moment coefficients.

$$C_m = \frac{\text{Moment (ft-lb)}}{q \times 1 \text{ ft}^2 \times 1 \text{ ft}}$$

are always given in terms of strain gages No. 1 or No. 2. Note that for the outer axis readings, C_m is defined with a reference area of 1 foot square and not the total available cross sectional area of the heliostat (4 foot square for the 4 modules + frame area). C_m is always read about heliostat axis X_2, the outer axis.

The induced moments about the 4 mirror modules are also given independently as direct readings. The modules, per Figure 2-19, are numbered identically with their respective strain gages; e.g., mirror module No. 3 given by strain gage No. 3, No. 4 by No. 4, etc. The strain gage locations never changed (No. 1 through No. 6); however, for a few runs with the slotted modules, mirrors No. 5 and No. 6 were interchanged. The strain gages and mirror modules were each marked with ink to insure correct referencing. The module moment coefficient, about axis X_1 at different rotational angles, ϕ, is defined with a reference area X chord of 1 ft^3. Obviously, X_1 and X_2 rotate about X_3.

The wind tunnel 6-component balance is fixed to the tunnel axis as shown in Figure 2-20. Looking from the top down, the drag component is parallel to the tunnel wind vector. Zero reference for the force balance system is 0 degree into the wind vector. Tunnel component terms are always given with respect to tunnel geometry and represent total forces acting upon the heliostat as would be sensed at the foundation. To convert the tunnel force readings into the heliostat model coordinate frame, the following transformations are made:

$$\text{Forces along } +X_1 = [-C_d \cos \gamma - C_y \sin \gamma] \times q \times Z^2$$

$$\text{Forces along } +X_2 = [-C_y \cos \gamma + C_d \sin \gamma] \times q \times Z^2$$

The mounting plate tare values have already been removed from the presented C_d and C_y terms.

q = dynamic pressure in lbs/ft^2

C_d = drag coefficient (tunnel)

C_y = side force coefficient (tunnel)

C = dimension of mirror module (1 ft for model)

$$Z = \frac{\text{Full Scale}}{\text{Model Scale}}$$

Notice that a positive rotation about the heliostat vertical axis, X_3 (i.e., γ positive) is the same as a negative yaw rotation in the tunnel coordinate frame.

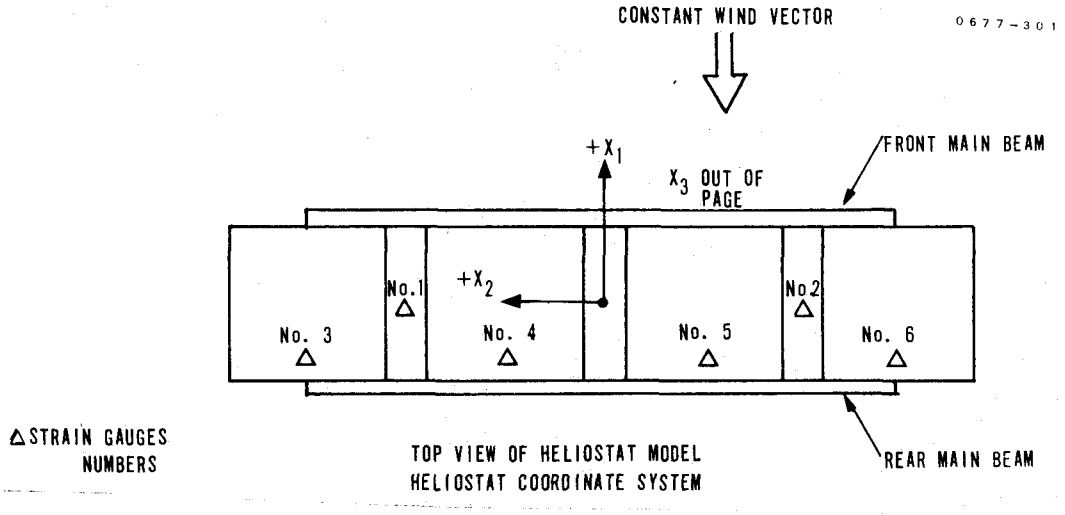

Rotation about $X_1 \simeq \phi \simeq$ mirror module rotation

ϕ_o = mirror module parallel to frame, pressure taps up,
Range = 0 to 360 degrees

X_1 Axis is fixed to frame

Rotation about $X_2 \simeq \theta \simeq$ outer frame rotation about its gimbal axis,
Range = -30 to +73 degrees

θ_o = outer frame horizontal

X_2 Axis is fixed to frame

Rotation about $X_3 \simeq \gamma \simeq$ heliostat assembly

Rotation about beam balance with respect to wind vector

γ_o = frame $\perp$ to wind vector, front main beam upstream
γ Range = ±180 degrees

Notes:

1. All rotations are IAW the RHR.
2. A positive moment about X_1 or X_2 is one that creates a positive rotation.

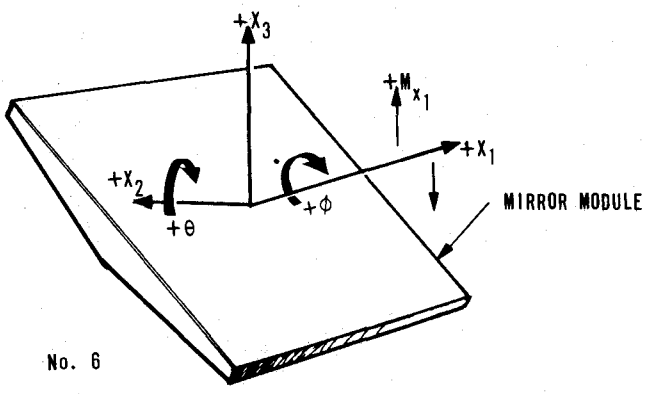

FIGURE 2-19. HELIOSTAT MODEL GEOMETRY

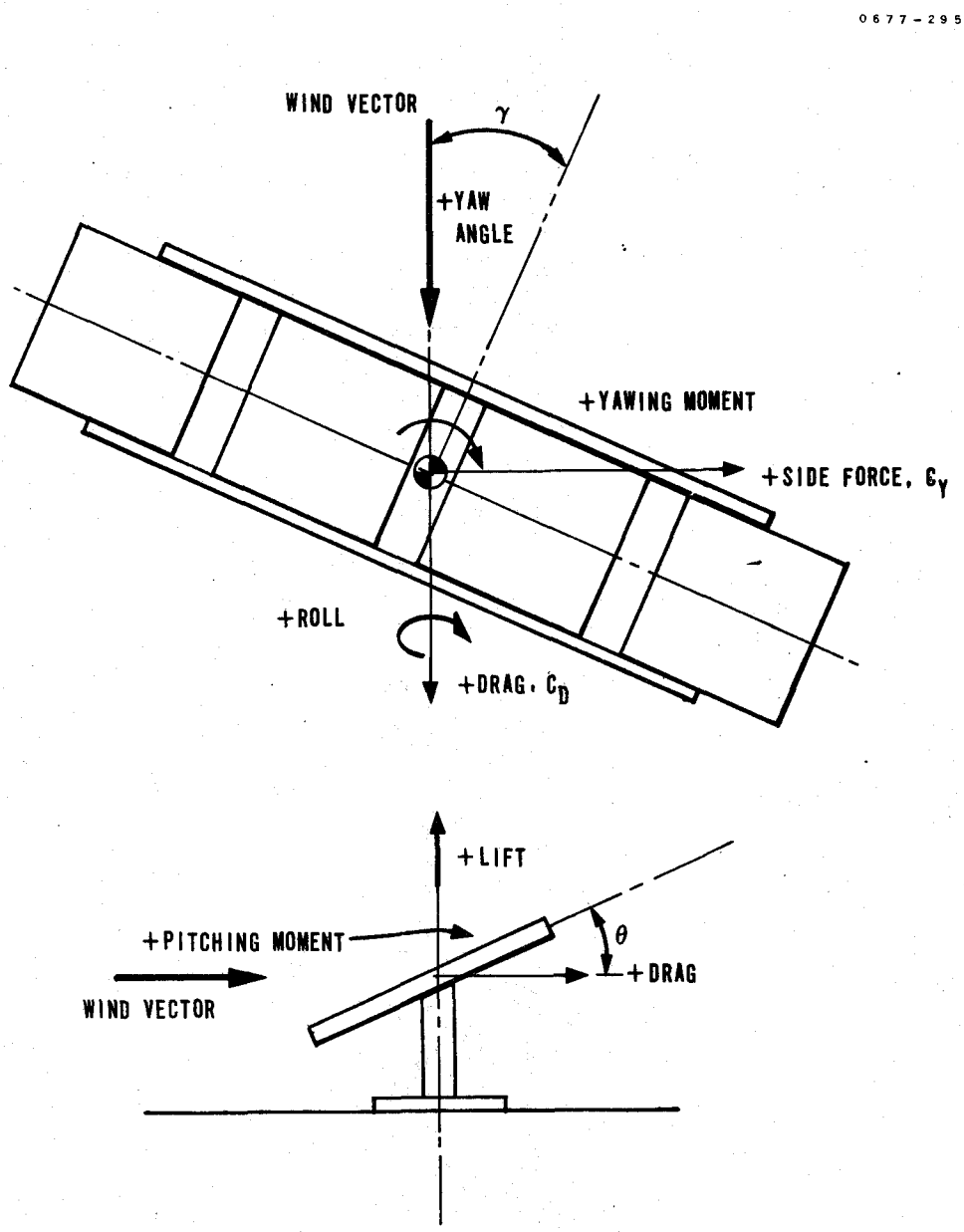

FIGURE 2-20. TUNNEL FORCE BALANCE SIGN CONVENTIONS

Section 3

CONDUCT OF TESTING

This section provides a brief discussion of the chronology of testing performed, data collected, nomenclature and problems encountered.

3.1 TESTING SEQUENCE AND RUN IDENTIFICATION

Table 3-1 identifies the sequence of all heliostat model wind tunnel testing performed along with the run number, heliostat geometry, wind speed and applicable inner and outer reduced moment coefficients, and useful tunnel force balance drag and side force coefficients. Initial testing conformed to the run number sequence of the original test plan (reference 6.1) but the actual sequence and number of tests were soon altered as experience was gained regarding expediting tests and runs needed. For instance, it was found to be unnecessary to run the 20 mph tests because of non-dimensional coefficient consistency. The run numbers are consistent with respect to the following rules:

1. A prefix of 1 - always indicates runs involving the single, instrumented model with solid mirror modules.

2. A prefix of 2 - always indicates runs involving the instrumented model with the interference model upstream.

   a. Where the body of a 2- (xy) number is the same as a 1- (xy) number, the heliostat geometry (γ,θ,ϕ) is the same.

   b. The suffix of a 2-xy-( ) number implies how far upstream the interference model is from the instrumented model:

      2-xy-1 interference model is 1.9 ft upstream.

      2-xy-3 interference model is 3.6 ft upstream,

      where 3.6 feet is the 1/10 scaled distance between heliostat rows associated with the outer perimeter and 1.9 feet is a scaled distance between heliostat rows associated with the rear inner field.

3. A prefix of 3- indicates that pressure tap measurements were taken. Force balance and strain gage measurements were not obtained during these runs due to possible tube effects. Again, where the body of a 3-xy number is the same as a 1-xy or 2-xy number, the heliostat geometry is the same.

TABLE 3-1. DETAILED HELIOSTAT WIND TUNNEL TEST DATA

Item	Run No.	γ degree	θ degree	ϕ degree	Wind Speed (mph)	Reduced Strain Gage Moment Coefficients (Cm)						Applicable Force Balance Data		Remarks
						Outer Axis		Mirror Modules						
						No. 1	No. 2	No. 3	No. 4	No. 5	No. 6	C_D	C_y	
1	00-A	0	45	-45										Shakedown Run
2	00-B	0	45	-45	50	0.137	0.100	0.074	0.068	0.068	0.075			Shakedown Run
3	1-01B	0	10	0	20	0.053	0.061					1.135	0	
4	1-01C	0	10		30	0.046	0.064					1.099	0	
5	1-01D	0	10	0	50	0.046	0.061					1.087	0	
6	1-01E	0	10	0	90	0.050	0.059					1.043	0	
7	1-01F	0	20	0	20	0.104	0.087					1.614	0	
8	1-01G	0	20	0	30	0.120	0.116					1.771	0	
9	1-01H	0	20	0	50	0.118	0.128					1.815	0	
10	1-03	0	30	0	30	0.156	0.174					2.618	0	
11	1-04	0	30	0	50	0.166	0.174					2.625	0	
12	1-06	0	55	0	30	0.145	0.159					4.312	NA	
13	1-07	0	55	0	50	0.159	0.159					4.262	NA	
14	1-09	0	72.5	0	30	0.029	0.081					4.799	NA	
15	1-10	0	72.5	0	50	0.037	0.083					4.869	NA	
16	1-12	0	72.5	22.5	30	0.083	0.090	-0.043	-0.028	-0.028	-0.048	4.740	-1.562	
17	1-13	0	72.5	22.5	50	0.128	0.083	-0.030	-0.028	-0.029	-0.044	4.710	-1.547	
18	1-15	0	72.5	40	30		0.083	-0.043	-0.077	-0.065	-0.069	3.738	-2.452	
19	1-16	0	72.5	40	50		0.078	-0.045	-0.073	-0.067	-0.069	3.673	-2.367	
20	1-18	0	73	60	30	0.003	0.074	-0.073	-0.096	-0.086	-0.083	2.353	-2.235	
21	1-19	0	73	60	50	-0.002	0.051	-0.078	-0.097	-0.089	-0.084	2.403	-2.398	
22	1-21	0	73	70	30	-0.011	0.043	-0.083	-0.083	-0.080	-0.065	1.672	-1.845	
23	1-22	0	73	70	50	-0.015	0.042	-0.088	-0.086	-0.083	-0.069	1.665	-1.836	
24	1-24	0	73	80	30	-0.027	0.009	-0.060	-0.049	-0.046	-0.025	1.177	-0.911	
25	1-25	0	73	80	50	-0.027	0.006	-0.062	-0.047	-0.046	-0.028	1.157	-0.906	
26	1-19A	0	73	65	30	-0.014	0.065	-0.087	-0.100	-0.091	-0.082	2.101	-2.452	
27	1-19B	0	73	65	50	-0.012	0.057	-0.087	-0.095	-0.088	-0.077	2.019	-2.242	
28	1-46A	-75	73	65	30	0.002	-0.036	0.049	0.052	0.054	0.052	1.908	1.194	
29	1-46B	-75	73	65	50	0.007	-0.037	0.050	0.051	0.049	0.054	1.844	1.180	

TABLE 3-1. DETAILED HELIOSTAT WIND TUNNEL TEST DATA
(Continued)

Item	Run No.	γ degree	θ degree	ϕ degree	Wind Speed (mph)	Reduced Strain Gage Moment Coefficients (Cm)						Applicable Force Balance Data		Remarks
						Outer Axis		Mirror Modules						
						No. 1	No. 2	No. 3	No. 4	No. 5	No. 6	C_D	C_y	
30	1-46C	-75	45	65	30		-0.048	0.049	0.049	0.035	0.046	1.832	0.911	
31	1-46D	-75	45	65	50	-0.005	-0.046	0.048	0.045	0.034	0.045	1.782	0.875	
32	1-46E	-90	45	65	30	-0.005	-0.004	0.034	-0.001	0.021	0.024	1.265	0.326	
33	1-46F	-90	45	65	50	-0.000	-0.004	0.035	-0.001	0.022	0.026	1.293	0.320	
34	1-52A	-90	0	65	30	0.010	-0.015	0.036	-0.001	0.032	0.034	1.197	0	
35	1-52B	-90	0	65	50	0.014	-0.019	0.036	-0.001	0.031	0.033	1.189	0	
36	1-48	-90	0	90	30	-0.006	-0.005	0.004	0	0.016	0.003	1.540	0	
37	1-49	-90	0	90	50	-0.005	-0.004	0.008	0.002	0.015	0.011	1.494	0	
38	1-62A	-90	0	10	30	0.006	-0.007	0.044	0.005	-0.030	0.006	0.509	0	
39	1-62B	-90	0	10	50	0.006	-0.006	0.047	0.007	0.012	0.006	0.515	0	
40	1-62C	-90	0	10	20	0.016	0	0.044	0	0.008	0.004	0.472	0	
41	1-62D	-60	0	10	30	-0.057	-0.097	0.053	0.036	0.038	0.034	0.617	0.065	
42	1-62E	-60	0	10	50	-0.065	-0.104	0.054	0.039	0.041	0.036	0.616	0.054	
43	1-62F	-60	0	20	30	-0.287	-0.115	0.071	0.052	0.041	0.051	0.899	0.087	
44	1-62G	-60	0	20	50	-0.272	-0.118	0.073	0.055	0.049	0.054	0.927	0.187	
45	1-62H	-90	0	20	30	0.017	-0.011	0.042	0.025	0.024	0.029	0.759	0	
46	1-62I	-90	0	20	50	0.018	-0.008	0.043	0.031	0.028	0.033	0.789	0	
47	1-57	-90	0	30	30	0.019	-0.023	0.046	0.047	0.043	0.053	1.181	0	
48	1-58	-90	0	30	50	0.021	-0.022	0.050	0.051	0.050	0.053	1.171	0	
49	1-58A	-60	0	30	30	-0.043	-0.039	0.023	0.011	0.009	0.020	1.190	0.174	
50	1-58B	-60	0	30	50	-0.048	-0.043	0.025	0.013	0.013	0.024	1.257	0.172	
51	1-58C	-60	45	30	30	-0.023	-0.040	0.032	0.019	0.023	0.024	0.704	0.152	
52	1-58D	-110	45	30	30	0.047	0.056	0.038	-0.042	-0.014	-0.023	1.077	0.369	After γ slew γ = -110 → -25.5
53	1-58E	-25.5	45	30	30	0.107	0.147	-0.073	-0.074	-0.065	-0.064	1.850	-1.280	Worst case IA moment observed during above slew
54	1-58F	-25.5	45	30	50	0.112	0.155	-0.084	-0.077	-0.067	-0.064	1.908	-1.648	

TABLE 3-1. DETAILED HELIOSTAT WIND TUNNEL TEST DATA
(Continued)

Item	Run No.	γ degree	θ degree	φ degree	Wind Speed (mph)	Reduced Strain Gage Moment Coefficients (Cm)						Applicable Force Balance Data		Remarks
						Outer Axis		Mirror Modules						
						No. 1	No. 2	No. 3	No. 4	No. 5	No. 6	C_D	C_y	
55	1-58G	90	45	30	30	0.024	-0.010	0.052	0.038	0.026	0.045	1.181	0.434	After γ slew γ = -25.5→ γ = 1-3° worse case IA moments
56	1-58H	90	45	30	50	0.029	-0.011	0.050	0.040	0.029	0.048	1.085	0.625	
57	1-58I	128.5	22.5	30	30	-0.060	-0.102	0.049	0.045	0.038	0.052			γ slew γ = +90 → 130°
58	1-58J	-56.5	22.5	30	30	-0.045	-0.096	0.062	0.054	0.054	0.050	0.713	0.803	γ slew γ = 128.5 → -56.5°
59	1-58K	-56.5	22.5	30	50	-0.060	-0.114	0.069	0.061	0.063	0.057	0.880	0.695	
60	1-58L	-90	22.5	30	30	0.030	0.014	0.042	0.047	0.038	0.048	1.138	0.369	γ slew γ = -56.5 → -.30°
61	1-58M	-90	22.5	30	50	0.027	0	0.045	0.050	0.043	0.052	1.142	0.429	
62	1-74A	-50.5	0	25	30	-0.061	-0.096	0.077	0.048	0.028	Error	1.138	0.260	γ slew γ = -56.5 → +120° Back to -50.5°
63	1-74B	-50.5	0	25	50	-0.065	-0.065	-0.103	0.076	0.045	0.031	1.127	0.297	
64	1-75A	50	0	25	30	0.148	0.121	0.046	0.043	0.038	0.062	1.216	-0.217	γ slew γ = -50.5 → +50.0°
65	1-75B	50	0	25	50	0.161	0.121	0.051	0.049	0.043	0.066	1.273	-0.234	
66	1-76A	-112	60	25	30	0.029	0.040	0.042	0.023	0.013	-0.017	1.838	0.890	γ sweep γ = 50 → +120° γ = +120 → -150°
67	1-76B	-36	60	25	30	0.066	0.1377	-0.083	-0.080	-0.066	-0.061	1.954	-2.279	γ sweep γ = -112→ γ = +90°
68	1-76C	-36	60	25	50	0.073	0.135	-0.086	-0.082	-0.071	-0.064	2.024	-2.242	
69	1-77A	0	-45	25	30	-0.098	-0.071	-0.025	-0.024	-0.024	-0.018	2.943	1.389	γ sweep γ = -36 → 0°
70	1-77B	-155	-45	25	30	-0.151	-0.082	-0.078	-0.067	-0.047	-0.059	2.249	1.823	γ sweep γ = 0 → +120° +120 → -167.5°
71	1-77C	-155	-45	25	30	-0.188	-0.098	-0.078	-0.067	-0.062	-0.069	2.251	1.813	
72	1-78A	-90	0	3	50	-0.005	0.004	0.019	-0.017	-0.003	0.013	0.302	0	Outboard module φ = ±3° only inboard, -φ = 0°
73	1-78B	-90	0	3	90	-0.003	0.004	0.020	-0.017	-0.004	-0.014	0.281	0	
74	1-79A	-45	0	3	50	0.008	0.029	0.019	0.001	-0.001	-0.013	0.594	-0.117	
75	1-79B	-45	0	3	90	0.004	0.029	0.019	-0.002	-0.007	-0.014	0.579	-0.125	
76	1-80A	0	0	3	50	0.012	0.006	-0.004	0.002	-0.001	0.001	0.785	0.016	
77	1-80B	0	0	3	90	0.014	0.005	-0.004	0.003	0	0.001	0.748	0	Note: Gage #4 bad from item 78 → 110

TABLE 3-1. DETAILED HELIOSTAT WIND TUNNEL TEST DATA
(Continued)

Item	Run No.	γ degree	θ degree	ϕ degree	Wind Speed (mph)	Reduced Strain Gage Moment Coefficients (Cm)						Applicable Force Balance Data		Remarks
						Outer Axis		Mirror Modules						
						No. 1	No. 2	No. 3	No. 4	No. 5	No. 6	C_D	C_y	
78	2-80A	0	0	3	50	0.022	0.020	0.000	-0.040	0.001	0.003	NA	NA	Assembly was incorrect
79	2-80B	0	0	3	90	0.033	0.029	-0.003	-0.011	0.002	0.005	↓	↓	↓
80	2-19A	0	73	65	30	-0.014	0.029	-0.064	-0.116	-0.041	-0.035			
81	2-19B	0	73	65	50	-0.015	0.034	-0.070	-0.096	-0.045	-0.038			
82	2-06-3	0	55	0	30	0.095	0.087	-0.007	-0.035	0.004	0.008	1.954	-0.130	Assembly corrected
83	2-07-3	0	55	0	50	0.095	0.090	-0.009	-0.031	0.006	0.010	2.032	-0.078	
84	2-09-3	0	73	0	30	0.057	0.073	0.001	-0.032	-0.004	-0.001	1.683	0	
85	2-10-3	0	73	0	50	0.058	0.084	0.005	-0.024	-0.003	0.001	1.775	0	
86	2-58E-3	25.5	45	30	30	0.038	0.076	-0.051	-0.083	-0.028	-0.030	1.008	-0.651	
87	2-58F-3	25.5	45	30	50	0.040	0.085	-0.056	-0.072	-0.030	-0.033	1.087	-0.734	
88	2-76B-3	-36	60	25	30	0.035	0.081	-0.064	-0.036	-0.029	-0.033	1.029	-0.781	
89	2-76C-3	-36	60	25	50	0.032	0.083	-0.061	-0.042	-0.027	-0.032	1.006	-0.781	
90	2-98A	-36	60	25	30	0.024	0.065	0.023	-0.087	-0.029	-0.028	0.708	-0.673	Interference model not same orientation as instrumented model
91	2-98B	-36	60	25	50	0.023	0.075	0.020	-0.056	-0.030	-0.028	0.734	-0.727	
92	2-76B-1	-36	60	25	30	0.045	0.083	-0.049	-0.059	-0.026	-0.029	0.925	-0.738	
93	2-76C-1	-36	60	25	50	0.048	0.088	-0.052	-0.055	-0.027	-0.031	0.969	-0.781	
94	2-58E-1	-25.5	45	30	30	0.035	0.078	-0.050	-0.101	-0.030	-0.031	0.964	-0.651	
95	2-58F-1	-25.5	45	30	50	0.038	0.087	-0.052	-0.072	-0.034	-0.033	1.063	-0.672	
96	2-09-1	0	73	0	30	-0.133	0.101	0.002		-0.019	-0.031	1.876	-0.130	
97	2-10-1	0	73	0	50	0.013	0.093	-0.000	-0.033	-0.018	-0.028	1.810	-0.141	
98	2-06-1	0	55	0	30	0.126	0.128	-0.015	-0.057	-0.010	-0.011	1.880	-0.043	
99	2-07-1	0	55	0	50	0.122	0.140	-0.016	-0.021	-0.006	-0.014	1.891	-0.063	
100	2-81-1	0	20	25	30	0.041	0.077	-0.032	-0.068	-0.024	-0.025	0.999	-0.391	
101	2-82-1	0	20	25	50	0.044	0.081	-0.035	-0.053	-0.027	-0.024	1.058	-0.375	
102	1-81	0	20	25	30	0.093	0.104	-0.013	-0.013	-0.009	-0.025	1.628	-0.760	
103	1-82	0	20	25	50	0.094	0.110	-0.014	-0.022	-0.011	-0.024	1.618	-0.742	
104	1-83	-90	0	-10	50	-0.003	0	-0.036		0.004	0.003	0.337	0	#3 only at -10°
105	1-84	-90	0	-10	90	-0.004	0	-0.037		0	0.002	0.322	0	#3 only at -10°
106	1-85	-90	0	-13	50	-0.002	0	-0.043		0	0.003	0.382	0	#3 only at -13°
107	1-86	-90	0	-13	90	-0.004	0	-0.044		0	0.002	0.359	0	#3 only at -13°

TABLE 3-1. DETAILED HELIOSTAT WIND TUNNEL TEST DATA
(Continued)

Item	Run No.	γ degree	θ degree	ϕ degree	Wind Speed (mph)	Reduced Strain Gage Moment Coefficients (Cm) Outer Axis No. 1	Outer Axis No. 2	Mirror Modules No. 3	Mirror Modules No. 4	Mirror Modules No. 5	Mirror Modules No. 6	Applicable Force Balance Data C_D	Applicable Force Balance Data C_y	Remarks
108	1-87	-45	10	-13	50	0.099	0.138	-0.067	-0.097	-0.040	-0.050	-0.930	-0.266	
109	1-88	-45	10	-13	90	0.092	0.142	-0.067	-0.061	-0.042	-0.049	-0.909	-0.255	
110	1-88A				50									γ slew, worse case on #3 at γ = -45°
111	3-09	0	73	0	30									Pressure data invalid
112	3-10	0	73	0	50									↓
113	3-09-180	0	73	180	30									
114	3-10-180	0	73	180	50									
115	3-03	0	30	0	30									Pressure data invalid - Rerun
116	3-04	0	30	0	50									↓
117	3-03-180	0	30	180	30									
118	3-04-180	0	30	180	50									
119	3-89-180	0	25	180	30									
120	3-90-180	0	25	180	50									
121	3-89	0	25	0	30									
122	3-90	0	25	0	50									
123	3-01G	0	20	0	30									
124	3-01H	0	20	0	50									
125	3-09	0	73	0	30									
126	3-10	0	73	0	50									
127	3-09-180	0	73	180	30									
128	3-10-180		73	180										
129	3-09													
130	3-10													
131	3-06	0	55	0	30									
132	3-07	0	55	0	50									

TABLE 3-1. DETAILED HELIOSTAT WIND TUNNEL TEST DATA
(Continued)

Item	Run No.	γ degree	θ degree	ϕ degree	Wind Speed (mph)	Reduced Strain Gage Moment Coefficients (Cm)						Applicable Force Balance Data		Remarks
						Outer Axis		Mirror Modules						
						No. 1	No. 2	No. 3	No. 4	No. 5	No. 6	C_D	C_y	
133	3-06-180	0	55	180	30									
134	3-07-180	0	55	180	50									
135	3-03-180	0	30	180	30									
136	3-04-180	0	30	180	50									
137	3-03	0	30	0	30									
138	3-04	0	30	0	50									
139	3-89	0	25	0	30									
140	3-90	0	25	0	50									
141	3-89-180	0	25	0	30									
142	3-90-180	0	25	0	50									
143	3-01G-180	0	20	180	30									
144	3-01U-180	0	20	180	50									
145	3-01C-180	0	10	180	30									
146	3-01D-180	0	10	180	50									
147	3-01E-180	0	10	180	90									
148	3-01C	0	10	0	30									
149	3-01D	0	10	0	50									
150	3-01E	0	10	0	90									
151	3-91	0	15	0	30									
151	3-91		15	0	50									
153	3-93	0	-10	0	30									
154	3-94	0	-10	0	50									
155	3-93-180	0	-10	180	30									
156	3-94-180	0	-10	180	50									
157	3-95	0	-20	0	30									
158	3-96	0	-20	0	50									
159	3-95-180	0	-20	180	30									
160	3-96-180	0	-20	180	50									
161	3-48-180	-90	0	-90	30									
162	3-49-180	-90	0	-90	50									

TABLE 3-1. DETAILED HELIOSTAT WIND TUNNEL TEST DATA
(Continued)

Item	Run No.	γ degree	θ degree	φ degree	Wind Speed (mph)	Reduced Strain Gage Moment Coefficients (Cm)						Applicable Force Balance Data		Remarks
						Outer Axis		Mirror Modules						
						No. 1	No. 2	No. 3	No. 4	No. 5	No. 6	C_D	C_y	
163	3-48	-90	0	90	30									
164	3-49	-90	0	90	50									
165	3-97	-60.5	0	-90	50									γ Sweep-while monitoring Tap #16
166	3-99	-57	0	-90	50									Invalid scaling
167	3-99R	-57	0	-90	50									γ Sweep-monitoring Tap #14
168	3-99-180	-57	0	+90	50									
169	1-100	-90	0	25	30	0.013	-0.021	0.046	0.041	0.042	0.048	0.982	-0.022	
170	1-101	-90	0	25	50	0.016	-0.017	0.045	0.042	0.042	0.049	0.984	-0.055	
171	1-102	-90	0	-20	30	-0.021	0.014	-0.045	-0.017	-0.024	-0.023	0.678	0	
172	1-103	-90	0	-20	50	-0.026	0.010	-0.046	-0.017	-0.024	-0.025	0.685	0	
173	1-104	-90	0	-25	30	-0.020	0.011	-0.045	-0.024	-0.037	-0.039	0.838	0	
174	1-105	-90	0	-25	50	-0.022	0.010	-0.046	-0.025	-0.036	-0.042	0.879	0	
175	1-106	-90	0	-22.5	30	-0.021	0.012	-0.047	-0.021	-0.030	-0.033	0.756	0	
176	1-107	-90	0	-22.5	50	-0.024	0.011	-0.047	-0.021	-0.029	-0.034	0.774	0	
177	1-108	-90	0	-30	30	-0.024	0.019	-0.049	-0.027	-0.047	-0.056	1.095	0	
178	1-109	-90	0	-30	50			-0.048	-0.027	-0.045	-0.057	1.080	0	
179	1-110	-90	0	-35	30			-0.047	-0.025	-0.049	-0.063	1.264	0	
180	1-111	-90	0	-35	50			-0.048	-0.025	-0.049	-0.063	1.296	0	
181	1-112	-90	0	-40	30			-0.047	-0.023	-0.053	-0.062	1.468	0	
182	1-113	-90	0	-40	50			-0.046	-0.022	-0.049	-0.061	1.433	0	
183	1-114	-90	45	-25	50			-0.052	-0.024	-0.030	-0.039	NA		
184	1-115		45	-25	50									γ sweep from γ = -90 to γ = 0° γ = -90° worse case IA moments
185														
186	4-48	-90	0	90	30			0.005	-0.014	0.007	0.014	1.330	0	
187	4-49	-90	0	90	50			0.005	-0.015	0.008	0.014	1.228	-0.03	
188	4-52A	-90	0	65	30			0.043	0.003	0.030	0.034	1.251	0	
189	4-52B	-90	0	65	50			0.044	0.002	0.030	0.033	1.190	0	

TABLE 3-1. DETAILED HELIOSTAT WIND TUNNEL TEST DATA
(Continued)

Item	Run No.	γ degree	θ degree	ϕ degree	Wind Speed (mph)	Reduced Strain Gage Moment Coefficients (Cm)						Applicable Force Balance Data		Remarks
						Outer Axis		Mirror Modules						
						No. 1	No. 2	No. 3	No. 4	No. 5	No. 6	C_D	C_y	
190	4-57	-90	0	30	30			0.045	0.029	0.035	0.023	1.082	0	
191	4-58	-90	0	30	50			0.045	0.031	0.035	0.025	1.080	0	
192	4-62H	-90	0	20	30			0.025	0.025	0.025	0.014	0.747	0	
193	4-62I	-90	0	20	50			0.024	0.026	0.025	0.015	0.735	0	
194	4-62A	-90	0	10	30			0.002	0.009	0.010	0.008	0.496	0	
195	4-62B	-90	0	10	50			0.003	0.011	0.011	0.008	0.477	0	
196	4-83	-90	0	-10	50			-0.002	-0.007	-0.002	0.001	0.413	0	
197	4-84	-90	0	-10	90			-0.004	-0.007	-0.004	0.000	0.390	0	
198	4-102	-90	0	-20	30			-0.021	-0.016	-0.013	-0.015	0.674	0	
199	4-103	-90	0	-20	50			-0.023	-0.014	-0.014	-0.015	0.679	0	
200	4-108	-90	0	-30	30			-0.035	-0.014	-0.030	-0.023	0.990	0	
201	4-109	-90	0	-30	50			-0.038	-0.015	-0.029	-0.024	1.021	0	
202	4-112	-90	0	-40	30			-0.041	-0.007	-0.032	-0.027	1.181	0	
203	4-113	-90	0	-40	50			-0.045	-0.008	-0.033	-0.031	1.258	0	
204	4-116	-90	0	-50	30			-0.037	-0.009	-0.028	-0.033	1.307	0	
205	4-117	-90	0	-50	50			-0.035	-0.008	-0.028	-0.034	1.386	0	
206	4-118	90	0	-50	30			-0.036	-0.035	-0.011	-0.045	1.038	0.022	
207	4-119	90	0	-50	50			-0.035	-0.034	-0.013	-0.047	1.156	0.023	
208	4-120	90	0	-30	30			-0.018	-0.028	-0.035	-0.044	0.908	0	
209	4-121	90	0	-30	50			-0.018	-0.029	-0.036	-0.046	0.920	0.031	
210	4-122	90	0	-20	30			-0.009	-0.016	-0.025	-0.026	0.652	0	
211	4-123	90	0	-20	50			-0.008	-0.016	-0.026	-0.027	0.655	0	
212	4-124	90	0	10	50			0.000	0.007	0.011	0.008	0.226	0	
213	4-125	90	0	10	90			0.001	0.006	0.010	0.010	0.346	0	
214	4-126	90	0	20	30			0.012	0.015	0.019	0.025	0.465	0	
215	4-127	90	0	20	50			0.012	0.015	0.019	0.024	0.538	0	
216	4-128	90	0	30	30			0.024	0.026	0.019	0.033	0.695	0	
217	4-129	90	0	30	50			0.028	0.028	0.021	0.035	0.791	0	
218	4-130	90	0	40	30			0.031	0.032	0.010	0.043	0.886	0	
219	4-130	90	0	40	50			0.033	0.032	0.011	0.044	1.022	0	

TABLE 3-1. DETAILED HELIOSTAT WIND TUNNEL TEST DATA
(Continued)

Item	Run No.	γ degree	θ degree	ϕ degree	Wind Speed (mph)	Reduced Strain Gage Moment Coefficients (Cm)						Applicable Force Balance Data		Remarks
						Outer Axis		Mirror Modules						
						No. 1	No. 2	No. 3	No. 4	No. 5	No. 6	C_D	C_y	
220	4-132	90	0	50	30			0.033	0.029	0.009	0.034	0.743	0	
221	4-133	90	0	50	50			0.036	0.032	0.012	0.037	1.106	0	
222	4-132(5)	90	0	50	30			0.033	0.028	0.010	0.035	0.956	0	Module #5 and #6 interchanged
223	4-133-5	90	0	50	50			0.037	0.032	0.012	0.038	1.142	0	
224	4-130(5)	90	0	40	30			0.033	0.032	0.009	0.044	1.134	-0.195	
225	4-131-5	90	0	40	50			0.033	0.035	0.010	0.037	1.218	-0.070	
226	4-128-5	90	0	30	30			0.025	0.024	0.010	0.037	0.834	-0.087	
227	4-129-5	90	0	30	50			0.027	0.028	0.013	0.043	0.955	-0.047	
228	4-126-5	90	0	20	30			0.013	0.014	0.017	0.031	0.409	-0.130	
229	4-127-5	90	0	20	50			0.014	0.016	0.020	0.034	0.559	-0.047	
230	4-124-5	90	0	10	50			0.002	0.007	0.011	0.022	0.230	0.023	
231	4-125	90	0	10	90			0.001	0.005	0.009	0.020	0.329	0.012	
232	4-122-5	90	0	-20	30			-0.009	-0.014	-0.027	-0.033	0.591	0.043	
233	4-123-5	90	0	-20	50			-0.008	-0.015	-0.029	-0.035	0.615	0.015	
234	4-120-5	90	0	-30	30			-0.017	-0.026	-0.023	-0.045	0.864	0	
235	4-121-5	90	0	-30	50			-0.017	-0.027	-0.029	-0.046	0.872	0	
236	4-118-5	90	0	-50	30			-0.036	-0.035	-0.011	-0.058	1.077	0.043	
237	4-119-5	90	0	-50	50			-0.035	-0.033	-0.010	-0.054	1.071	0.063	
238	4-134-5	90	0	90	30			-0.011	-0.011	-0.013	-0.005	0.695	0.043	Module #5 and 6 interchanged
239	4-135-5	90	0	90	50			-0.011	-0.009	-0.016	-0.005	1.012	0.046	
240	4-136-5	0	60	-50	50	0.074	0.022	0.053	0.055	-0.062	0.067			γ Sweep γ = +90° → -90°, γ = 0° = largest reading at γ = 0°

a. A 3-xy number with a (-180) suffix designates a run which is identical to a 3-xy run except that all four minor modules were rotated (that is, ϕ) 180 degrees from the basic inner axis angle. To obtain the total pressure distributions across a module (both sides), two separate runs were necessary, 3-xy-180 and 3-xy.

4. A prefix of four indicates that the instrumented model was tested with 1 ft^2 vented mirror modules. Modules 3, 4, 5, and 6 are as shown in Figure 2-18.

   a. With no suffix, a 4-xy run number is with the standard configuration of module No. 3 attached to strain gage No. 3, No. 4 to No. 4 gage, etc. A run number suffix of -5 (e.g., 4-xy-5) designates the following configuration where positions of modules 5 and 6 are interchanged:

Module	Attached to Strain Gage No.
3	No. 3
4	No. 4
5	No. 6
6	No. 5

   As in previous cases, where the body of a 4-xy number is the same as a 1-xy, 2-xy, or 3-xy run number, the heliostat angular geometry (γ, θ and ϕ) is identical.

3.2 TEST CHRONOLOGY

The item column of Table 3-1 identifies the order in which the different tests were run. To put the testing in perspective, the following summarizes the sequence of events on a daily basis:

Prior to April 4	Boundary layer generated and tunnel change over.
April 4, 5, 6	Model and tunnel checked out and calibrated. Strain gages No. 5 replaced. Placed model in tunnel.
April 7	Recalibration of model, Sandia movies, shakedown runs.
April 8	Ran items 3 through 19. Tunnel down after 1430.
April 11	Ran items 20 through 42. Tunnel down 5 hours.
April 12	Ran items 43 through 65. Interference model completed.

April 13	Ran items 66 through 81. Installed interference model in tunnel.
April 14	Modified model mounting run items 82 through 110. Removed interference model. Strain gage No. 4 drift is too large.
April 15	Started conversion to pressure measurements. Strain gage No. 4 returned for rework.
April 18	Assembly of pressure monitoring test equipment and software checkout. Replaced strain gages No. 4.
April 19	Ran pressure tests; items 111 through 122. Determined that data was invalid due to signal condition error.
April 20	Ran pressure tests, items 123 through 156.
April 21	Ran items 157 through 184. Retrofitted vented mirror modules axial supports.
April 22	Completed mounting vented mirror modules. Ran items 185 through 223.
April 23	Ran items 224 through 241. Determined mounting plate fare values.

3.3 TEST METHODOLOGY

3.3.1 Zero Settings and Data Reading

Initially, it was planned to run each defined heliostat orientation geometry at three speeds, 20, 30, and 50 mph. However, the goodness and repeatability of the non-dimensional moment coefficient about each respective axis allowed a reduction in the number of speeds such that additional orientations could be tested. In most cases an orientation was tested at only two speeds, 30 and 50 or 50 and 90 mph. In all cases, after a model configuration change, all six strain gage balances were adjusted to the same reference level at zero velocity in order to compensate for residual strains within the gage block arms. After stabilizing at each desired speed by reaching a constant dynamic pressure, q_{oo}, the torsional load was sequencially read for each gage. After values were obtained for the highest wind speeds, each gage reading was again checked with wind off to insure the gage returned to the zero stress condition. All return to zero values were recorded on the data sheets.

To insure that no residual strain or cross coupling rotation induced strain existed within the gage blocks after each inner or outer axis rotation, the following sequence was followed on each gage block:

1. Loosened threaded clamping bolts in the gage block.
2. Relaxed each set screw to relieve tension.
3. Rotated axis.
4. Tightened clamping screw.
5. Tightened set screw.

As would be expected, the tunnel turbulence and downstream vortex shedding caused rapid oscillations in the induced hinge moments about some average value. This phenomena was much more evident with the introduction of the interference model and downstream mirror modules when blocked by upstream mirror modules ($|\gamma| > |5.5°|$). The tunnel turbulence factor has been estimated to be 1.2. Under some orientations, individual modules were buffetted at rates of at least 4 to 5 Hz. The magnitudes of the buffetting reached ±45 counts (microinches per inch) which represents, based upon an average scale factor of 0.0011 ft-lb/count, oscillating moment loads of ±0.05 ft-lb at frequencies of up to 3 Hz. Since the frequency response of the sensitive strain gage bridges/gage blocks has not been determined, these values are relatively qualitative in nature. When these conditions were observed, they were noted on the data sheets then the oscillation was studied and a mid point reading was found and set on the SR-4 strain indicator dial readout, such that the meter needle oscillated about the meter centerline. The dial indication was then recorded on the data sheets, thereby giving the average moment load.

A wind-off force balance reading was also taken after a model configuration change and then again immediately at shutdown after completion of the highest velocity run. The only force balance data collected was lift, drag, side force and yawing moment of which the drag and side force are the only two meaningful data that is of interest to the heliostat foundation and post/frame bearing loads. Three readings of each wind-off condition and each steady state wind velocity condition were taken from the force balance readout and the values were averaged. At the higher velocities, drag and side force values nominally varied ±0.03 pounds between the three readings; however, during a few runs, because of the turbulence and interference effects, differences of 0.45 pounds of drag load were observed between the three samples (e.g., Run Nos. 2-10-1, 1-88 and 4-119-5).

3.3.2 Atmospheric Variations and Dynamic Pressure

Ambient conditions were recorded 2 or 3 times each day. Barometric pressure ranged from 29.22 inches Hg to 29.62 inches and the tunnel air temperature ranged from 76°F to 83°F over the 3 week period.

However, all tunnel wind velocities were stabilized to a constant dynamic pressure for each speed to compensate for the varying conditions and simplify data reduction task. Values of q that may be used by the reader to convert the non-dimensional load coefficients to actual loads or relate to other conditions are:

Wind Velocity (mph)/(m/s)	q (lbs/ft^2)	q_{oo} (inches of 0.82 sp.g. alcohol) (used to set tunnel speed)	q_{oo} mm Hg
20/8.9	1.024	0.240	0.368
30/13.4	2.303	0.541	0.827
50/22.4	6.397	1.5017	2.298
90/40.2	20.727	4.867	7.444

3.3.3 Instrumentation Calibration

The wind tunnel calibration was checked once prior to the start of tests. Known lateral loads and known moments were induced into the force balance system and the readouts recorded. All readouts were very linear with respect to the inputs. The only other calibration check was to insure that each usable balance component returned to its previous "wind-off" value after the sequence of wind velocities were stepped through and the tunnel's wind speed was reduced to zero again. A copy of the raw force balance data is being retained at Honeywell.

Because of the sensitive nature of strain gages and their susceptability to drift and sudden malfunction during the course of three weeks, 4 or 5 calibrations were made on each bridge by edge loading in both rotational directions the axial with increments of weights. For the inner axis modules, 0 → 10 pounds (0 → ±5 ft-lb) range was used for calibration and for the outer, 0 → 40 pounds (0 → ±10.84 ft-lb per bearing) was used. Each day before the beginning of test, each axis was spot checked in both orientations to insure readings between consecutive days were the same. One additional check for goodness of data was the recording of the wind-off return to zero value for each gage after each test run. The linearity over the calibrated range was very good. Correlation coefficients for the outer axis least squares (first order) ranged from 0.994 for the outer axis to 0.9999 or better for the inner axis mirror modules.

One of the four strain gages within the No. 4 strain gage bridge suffered fatigue failure after run No. 1-80B (Item 77), on 13 April. After run No. 2-80B (Item 79) it failed to return to zero reading and exhibited excessive drift. Because of time limitations, testing continued before it could be repaired. Therefore, moment coefficients

for gage No. 4 (mirror module No. 4) are invalid for test items 78 through 110. Otherwise, the instrumented model worked flawlessly during all testing. Table 3-2 provides the actual calibrated scale factors used to reduce the raw recorded data.

Return-to-zero offsets for the inner axis reached ±4 counts (≃±0.005 ft-lb) as a nominal. The outer axis return-to-zero offsets were normally less than ±0.012 ft-lb moment even though the shaft about gage No. 1 on occasion exhibited higher residual loads due to stiction from side loading.

Except for the electronic calibration discussed in Paragraph 2.3.3, there were no calibrations on the pressure tap measurements. However, two checks confirmed proper operation. Each model configuration was run at two different wind velocities. The computer averaged non-dimensional pressure coefficients for each tap for the different speeds are very close, indicating good end-to-end calibration. In addition, an independent micromanometer was tapped off one of the 36 heliostat pressure taps in parallel to the Scanivalve path and spot checks with the computer printout were made. After compensating for the specific gravity of alcohol used with this manometer (0.816) and calculating the pressure differential, the following spot checks were made:

Run Number	Speed (mph)	Average Computer C_p (Tap No. 12)	Manometer C_p (Tap No. 12)
3-03-180	30	-0.589	-0.600
3-04-180	50	-0.587	-0.599
3-04	50	0.196	0.206
3-94-180	50	0.228	0.235
3-97	30	0.339	0.342
3-96	50	-0.478	-0.482
3-95-180	30	0.255	0.256
3-96-180	50	0.259	0.259
3-49-180	50	-0.134	-0.129
3-48	30	-0.123	-0.120
3-49	50	-0.111	-0.106

As can be seen, the two methods checked closely, verifying correct end-to-end calibration of the pressure data acquisition system.

3.3.4 Model Configuration Changes

After each velocity sweep and after the zero wind readings were obtained, the inner and outer angular orientations were set with a precision inclinometer with an 0.1 degree resolution. With the frame level, all four mirror modules were set (discussed in Paragraph 3.3.1), the outer axis was then set, and finally the model was rotated to the proper yaw (γ) orientation via the tunnel control console, which gives the angular position to the nearest 0.01 degree.

TABLE 3-2. CALIBRATED SCALE FACTOR USED FOR STRAIN GAGE READINGS (Ft/lb Indicator Count)

Strain Gage Channel	Positive Moments	Negative Moments	Use On and After
No. 1	0.001199	0.001233	07 April
	0.001221	0.001217	11 April
No. 2	0.001333	0.001268	07 April
	0.001310	0.001265	11 April
No. 3	-0.001159	-0.001164	07 April
	-0.001197	-0.001153	11 April
No. 4	-0.001241	-0.001247	07 April
	-0.001340	-0.001321	22 April
No. 5	-0.001252	-0.001273	07 April
	-0.001263	-0.001262	22 April
No. 6	-0.001296	-0.001323	07 April

Some of the 241 test runs involved slewing the turntable over large increments of ± yaw angles while at a sustained tunnel wind speed of either 30 or 50 mph. The strain indicator was monitored to observe the point of maximum mirror module moment loading. The turntable was reversed and the position that gave the peak loading was hunted and found. The hinge moments and yaw angle was then recorded. The remarks column of Table 3-1 states which cases were a result of a γ slew. So in essence, a very huge number of wind vector orientations with respect to the heliostat were investigated at various heliostat inner and outer axis angles, with only the worst case observations documented.

Section 4

TEST RESULTS

4.1 OVERVIEW OF AVAILABLE DATA

Table 3-1 presents all of the applicable, axial moment data and total heliostat loading data obtained. It is in non-dimensional coefficient form, which merits a brief discussion on how to use it. The run number designators are explained in Subsection 3.1 and coordinate system in Subsection 2.4.

a. Mirror Module Moments - are based upon an actual 1/10 scaled, square module. Therefore, to relate to full scale total moments, the reader needs to perform only the following calculations:

$$\text{Moment (ft-lb)} = Cm \times q \times s \times c$$

where

Cm = individual strain gage (Nos. 3, 4, 5, 6) non-dimensional coefficient, Table 3-1

q = dynamic pressure, $1/2\ pV^2$ in pounds per square foot and given in Paragraph 3.3.2 for 4 wind velocities in mph

s = total surface area in square feet (full scale) square, non-parabolic, mirror module

c = length of one side of mirror module

Obviously, the non-dimensional coefficients can be used with a consistent set of metric units if desired.

b. Outer Axis Moments - are non-dimensionalized to a 1 square foot reference area. Since the moments include a coupling of side forces, total heliostat torsional response along with the frames and post-influences, no single reference area is actually applicable. Therefore, to extend these values to a full scale heliostat similar to the wind tunnel model tested, simply use:

$$\text{Moment (ft-lb)} = Cm \times q \times \left[\frac{\text{full scale}}{\text{model scale}}\right]^3$$

where

Cm = non-dimensional coefficient (Nos. 1 and 2)

and

$$\left[\frac{\text{full scale}}{\text{model scale}}\right]$$

is the ratio of the full scale heliostat dimensions to the 1/10 scale model used with 1 square foot modules and a frame 5 feet long, etc. As an example,

$$\left[\frac{FS}{MS}\right]^3 = 1000$$

for the Honeywell SRE configuration heliostat. The moment about each outer axis bearing must be calculated individually.

c. Drag and Side Force Components - These forces are computed in the same manner as the outer axis moments:

$$\text{Drag Force (\#)} = Cd \times q \times \left[\frac{\text{full scale}}{\text{model scale}}\right]^2$$

along the wind vector

$$\text{Side Force (\#)} = Cy \times q \times \left[\frac{\text{full scale}}{\text{model scale}}\right]^2$$

perpendicular to the wind vector direction.

Subsection 2.4 defines how to resolve the tunnel forces into the heliostat coordinate frame. Again, it should be noted that strain gage No. 4 values are invalid for items 78 through 110, which are predominantly runs made with the interference model.

Appendix A provides all of the raw pressure tap data for each run. Figure 4-1 demonstrates the location of each datum for each tap for each of the four mirror modules. Notice that in each grouping of three data points, the first is the average pressure coefficient

$$\left[Cp = \frac{P_{TAP} - P_{oo}}{q}\right]$$

over 10 samples within one second, the second value is the maximum of the 10 samples and the third is the minimum of the 10 samples. Note that taps 1 through 5, 10 through 14, etc., are along the module inner axis line and 6 through 9, 15 through 18, etc., are across the centerline of the mirror module as described in Paragraph 2.3.3.

677-14611

Run No. 3-10

MIRROR MODULE

Tap No.	No. 3	Tap No.	No. 4	Tap No.	No. 5	Tap No.	No. 6
1	0.541942←Avg Cp→	10	0.593009	19	0.571146	28	0.587115
	0.583059←Max Cp→		0.601928		0.609423		0.599459
	0.45829 ←Min Cp→		0.579708		0.531079		0.566438
2	0.627896	11	0.65956	20	0.664242	29	0.650447
	0.664886		0.666341		0.678509		0.661535
	0.558061		0.653335		0.637331		0.636273
3	0.620137	12	0.627777	21	0.62287	30	0.646682
	0.659419		0.641387		0.634465		0.681022
	0.563396		0.613435		0.612245		0.62481
4	0.550151	13	0.566645	22	0.544711	31	0.549561
	0.558899		0.613744		0.564013		0.593566
	0.531079		0.537825		0.533857		0.519969
5	0.279046	14	0.286594	23	0.25769	32	0.310035
	0.310639		0.338724		0.277794		0.342691
	0.236043		0.265008		0.242391		0.276604
6	0.460389	15	0.447943	24	0.421468	33	0.265749
	0.480466		0.460979		0.430911		0.288022
	0.41795		0.430074		0.410366		0.248916
7	0.622738	16	0.614348	25	0.599548	34	0.561645
	0.638036		0.629792		0.611011		0.573095
	0.606249		0.603472		0.581692		0.552109
8	0.568109	17	0.589623	26	0.623404	35	0.62667
	0.610129		0.607439		0.661623		0.694425
	0.522262		0.574462		0.605632		0.581516
9	0.318849	18	0.410344	27	0.46168	36	0.459979
	0.328627		0.431969		0.471604		0.477556
	0.305658		0.392467		0.450178		0.436334

Note: Data is in terms of Cp

$$Cp = \frac{\Delta P}{q}$$

FIGURE 4-1. SAMPLE PRESSURE DATA PRINTOUT

Note also that to correctly integrate total net forces across a module, the 3-xy run must be coupled with the 3-xy-180 run. After the 180-degree inner axis rotation, taps 1 through 5, 10 through 14, etc., are in the same relative location (except being to the rear) for normal force applications, but tap 9 is now behind where tap 6 was and tap 8 is now behind where tap 7 was. Likewise, tap 18 is now behind where tap 15 was and 17 behind 16, etc. Taps 3, 12, 21, and 30 are the center taps of each mirror module, respectively. Since there are numerous manners in which the reader may want to investigate or explore the data, all of the data has been presented, reduced only to non-dimensional form. Several observations can be made. The difference between the maximum and minimum value gives a clue to the flow instability and turbulence at any location for a given orientation. Note also that the Cp values for 30 mph and 50 mph runs at the same heliostat orientation configuration are nearly identical. The edge loads are, of course, zero and are not shown within the data tables.

4.2 BOUNDARY LAYER, SCALING AND TUNNEL EFFECTS

The validity of the test results must be addressed, since in any scaled model wind tunnel test, scaling influences could possibly make final results questionable.

Based on a scaled mirror module length of one foot, and a tunnel turbulence factor of 1.2, the effective Reynolds numbers (Rn) for the wind speeds used are:

Speed (mph)	Rn
20	2.08×10^5
30	3.12×10^5
50	5.20×10^5
90	9.36×10^5

A turbulence factor of 1.1 - 1.2 is often attributed to normal atmospheric ground winds.

For flat plates in a normal wind flow, this Rn range is well within the linear drag versus Reynolds number region (above 10^3) as is documented in references 6.3 and 6.4. The transition for smooth circular cylinders is about 5×10^5, and for a rough surface is 1.05×10^5.

The air flow pattern around sharp edged bodies is relatively independent of the Reynolds number because the sharp edges fix the flow separation characteristics. This in turn makes, for sharp bodies, the moment and pressure distributions independent of Rn above about 10^4. These conclusions are well supported by observing the excellent consistency of the moment coefficients and pressure coefficients across the total range of speeds for any single heliostat orientation. As would be expected, the interference of another heliostat upstream will cause some variations of center of pressures on the downstream heliostats due to the introduction of vortex shedding and localized eddy currents. Reference 6.5 discusses some of these effects.

On a few test runs between two velocities, the drag and side force coefficients varied as much as 10 percent. Some of these heliostat level variations may be associated with changes in vortex shedding off the mirror modules, unsteady air speed due to screen turbulence and model buffet, and the fact that the balance tended to chase the air speed. These factors are relatively small but do provide typical tunnel contributing unknowns.

The tunnel walls did affect individual runs in which the heliostat outer axis was normal to the wind vector. The two outboard mirror modules were close to the tunnel walls (approximately 6 inches, depending on the outer axis angle, θ). Observe run numbers 1-12 and 1-13 (items 16 and 17 of Table 3-1) and 1-24 and 1-25 (items 24 and 25). Notice that outboard modules (Nos. 3 and 6) are very different in moment loading for the inboard modules and are also different from

each other. Here $\gamma = 0$ and the outer axis is down at a maximum angle of $\theta = 73$ with the mirrors at various rotational angles (ϕ). For these types of runs, the moments indicated on the inner axis are the actual loads that would be experienced by all 4 mirror modules, not just the two inner modules. Where the yaw angle, $|\gamma| > \pm 30$ degrees, no wall boundary layer/interference effects will exist upon the two outboard mirror modules.

Total, worst case tunnel blockage by the heliostat at the worst case orientation ($\gamma = 0$, $\theta = 73$ deg, $\phi = 0$ deg) is only 9.5 percent of available cross sectional working test section area. Most runs were at blockage percentages of <5 percent at which point no wake blockage corrections should be necessary. Because of the extraneous suction effects introduced into the model's wake by the walls, the static pressure within the wake or base pressure will be less than a full scale unconfined air stream. Therefore, wind forces, mainly pressure drag, will be slightly higher on the model heliostat in the tunnel than the full scale heliostat. This effect will be more pronounced on the heliostat orientations presenting a blunt body to the wind vector than on the more streamline orientations. The net result is that the non-moment loads determined from this wind tunnel test are probably slightly conservative because of two effects:

1. The boundary layer was fuller than the 0.15 ($\approx$0.14) power defined, and

2. The wake blockage pressure effects.

No correction was applied to the presented load coefficients to compensate for the wake blockage.

The boundary layer profile exponent of $(h/10 \text{ meters})^{0.15}$ is probably more severe than that which would be experienced in a slightly built-up area such as the heliostat field with a surrounding perimeter fence. The total load on a low wall, or heliostat panel, is reduced by a small percentage (10 percent) when subjected to a boundary layer profile as opposed to a uniform freestream flow field, based upon available literature. However, the turning moment is increased due to the non-uniform pressure across the upstream module face. Our results show this same phenomena, as shown by the moments on a mirror module perpendicular to the boundary layer (module No. 3 on run Nos. 1-48, 1-49, 4-48, 4-49, etc.). The higher a module sticks into the boundary layer, the greater adverse influence the profile has on turning moments.

4.3 HELIOSTAT TORSIONAL AND DRAG LOADS

4.3.1 Single Heliostat Moment Loads

The worst case with respect to total, combined loading on the inner drive was observed to be case 1-19A and 1-19B (items 26 and 27 of Table 3-1) where the outer axis is normal to the wind vector, tilted a maximum $\theta = 73$ and inner axis rotated $\phi = +65$. The inboard mirror modules recorded a moment corresponding to a Cm = -0.100. This, made applicable to each of the 4 modules, gives a maximum moment load on a full scale SRE heliostat of

-230 ft-lbs	(2,760 in-lbs)	at 30 mph per mirror module
-640 ft-lbs	(7,680 in-lbs)	at 50 mph per mirror module

Other large inner axis moments occur at orientations defined by the following items in Table 3-1:

2
20,21
22,23
53,54
67,68
70,71
108,109
240

As can be seen, consistence of moment coefficient is good at the same heliostat orientations for significantly differing wind speeds. Loads are directly proportional to the wind speed squared and, therefore, between the most common two speeds

$$\left(\frac{50}{30}\right)^2 = 2.78 \text{ times as great}$$

$$\left(\frac{90}{50}\right)^2 = 3.24 \text{ times as great}$$

The worse case of 2,760 in-lbs at operational wind speeds to maintain a 2 mr tracking accuracy is only 37 percent of the design load of 7,500 in-lbs used in the preliminary design analysis. This value was based upon a theoretical worst case moment coefficient using a 30 mph uniform freestream velocity and flat plate theory. The 50 mph load is within hardware stress yield points.

Items 106 through 109 (cases 1-85, 86, 87, and 88) are of great interest. If the pilot plant freestream approaches a heliostat at an angle of attack of 10 degrees, the combined angle experienced by the first mirror module with the largest set toe-in angle of 3 degrees could be ϕ = -13 degrees with the heliostats in a stowed condition. Cases 1-85 and 86 have survivability level winds approaching end on to the heliostat (γ = -90 degrees) and module No. 3 experiences a load of Cm = -0.044; at 90 mph, this would result in a torsional load of 912 ft-lbs (10,944 in-lbs). All 4 modules could receive this load simultaneously. Cases 1-87 and 88 have the same ϕ = -13 degrees but also θ = +10 degrees and a wind vector coming in at γ = 45 degrees. Here the Cm = -0.067 on the first module at 50 mph and 90 mph. At 90 mph this would correspond to a torsional load of 1,389 ft-lbs (16,665 in-lbs). A full yaw slew was made with θ = 10 deg, ϕ = -13 deg, and the γ = 45 deg wind vector was the absolute worst case.

With regard to the outer axis cases 1-62F and 62G (items 43 and 44) produced an uniquely large combination of torsional loads equivalent to Cm = -0.280 on one bearing and -0.118 on the other. This corresponds to a worst-case-full-scale load of an estimated

661 ft-lbs	(7,932 in-lbs)	at 30 mph
1,836 ft-lbs	(22,032 in-lbs)	at 50 mph

on the leading bearing and 41 percent of those loads on the rear outer axis bearing. On the SRE heliostat, these loads will directly create a column load on the outer axis drive actuators.

Many different plots and analyses could be made from the data. For instance, for the end-on condition (γ = ±90 deg), the plots of each inner module versus angle of attacks (ϕ) could be made. Observe cases 1-102 through 1-113 (items 171 through 182) in the following tabulations with θ = 0, and γ = -90 deg. For negative ϕ, we have the existing orientation.

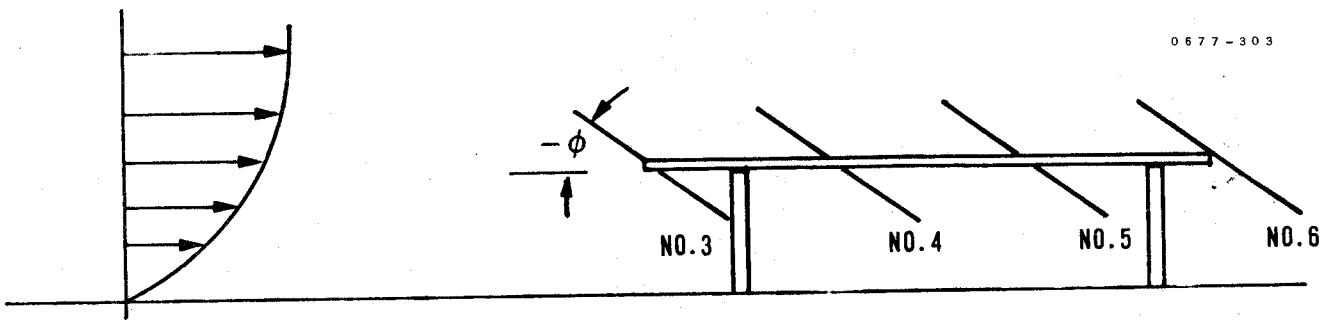

For smaller $|-\phi|$, the leading mirror module (No. 3) experiences the largest load but as $|-\phi|$ increases (increasing the angle of attack), the most downstream module axial moment becomes greater than the leading mirror module. Observe the following trend for the solid mirror modules.

MOMENT COEFFICIENT AT 50 MPH
(Solid Mirror Modules)

Case	Deg	No. 3	No. 4	No. 5	No. 6
1-103	-20	-0.046	-0.017	-0.024	-0.025
1-107	-22.5	-0.047	-0.021	-0.029	-0.034
1-105	-25	-0.046	-0.025	-0.036	-0.042
1-109	-30	-0.048	-0.027	-0.045	-0.057
1-111	-35	-0.048	-0.025	-0.049	-0.063
1-113	-40	-0.046	-0.022	-0.049	-0.061

However, when the slotted mirror modules were mounted under identical orientations, the following trends were recorded. Remember that each of the slotted modules had a different aspect ratio. More of this testing is discussed later in paragraph 4.3.4.

MOMENT COEFFICIENT AT 50 MPH
(Slotted Mirror Modules)

Case	Deg	No. 3	No. 4	No. 5	No. 6
4-83	-10	-0.002	-0.007	-0.002	-0.001
4-103	-20	-0.023	-0.014	-0.014	-0.015
4-109	-30	-0.038	-0.015	-0.029	-0.024
4-113	-40	-0.045	-0.008	-0.033	-0.031
4-117	-50	-0.035	-0.008	-0.028	-0.034

In both heliostat mirror module configurations, as the angle of attack increased, the module directly behind (that is, No. 4) the leading module (No. 3) was significantly shadowed. But the last module (No. 6) downstream suffered a larger load as the angle increased. In fact, for the solid modules, module No. 6 experienced a moment 43 percent greater than the leading mirror module at $\phi = -40$ deg. The main contributor to reduction in downstream module torsional loading is the relatively uniform pressure relief offered across the surface of the modules by the grooves. The aspect ratio of the downstream module facets has little influence as can be seen by cases 4-126 through 4-133 (items 214 through 221). Here, at the same relative angles, the most downstream module (No. 3) which has 9 square facets shows almost identically the same moment coefficients as No. 6 in the above tabulation.

4.3.2 Single Heliostat Drag Loads

As would be expected, the largest lateral force upon the heliostat (which would be directly translated to the foundation as a rocking moment and to the two outer axis bearings as direct normal loads) results from the bluntest profile offered against the wind vector. Cases 1-09 and 1-10 (items 14 and 15) depict this case where

$$C_D \text{ max} = 4.869$$

At 50 mph this would result in a total load of 3,115 pounds.

Case 1-80A (item 76) gave a drag coefficient of $C_D = 0.78$. With the heliostat in a stowed condition, and a 90 mph wind approaching directly from the side ($\gamma = 0$), the total normal load would be 1,617 pounds. This would induce a torsional moment at the slab foundations of 12,128 ft-lbs or 6,064 ft-lbs per foundation.

To further evaluate cases 1-80A and 1-80B, where a known, flat plate cross sectional area was normal to the wind, the actual total exposed surface was:

$$S = \underbrace{4 \text{ x } 12 \text{ in. x } 0.9 \text{ in.}}_{\text{modules sides}} + \underbrace{61 \text{ in. x } 1 \text{ in.}}_{\text{frame}} = 104.2 \text{ in}^2 = 0.724 \text{ ft}^2$$

neglecting the mostly open post area.

Removing the mounting plate tare value, the drag forces were

5.02 lbs at 50 mph

15.60 lbs at 90 mph

Computing the actual drag coefficients, we get

$$C_D \text{ 50 mph} = \frac{5.02}{6.397 \text{ x } (0.724)} = 1.08$$

$$C_D \text{ 90 mph} = \frac{15.60}{20.727 \text{ x } (0.724)} = 1.04$$

As expected, the values are significantly less than theoretical free-stream drag coefficients of rectangular plates normal to the flow. For a 0.9 in./12 in. height to length ratio (mirror module sides), the theoretical drag is $C_D = 1.5$, and for the frame, a 1 in./60 in. ratio gives a theoretical value of $C_D = 1.96$ due to the 2 dimensional-no pressure relief effect. The reduced drag of the heliostat is due to the fact it lies lower in the boundary layer-- the outer axis center-line at about a (V/V_{OO}) of 0.81. In a gross sense, neglecting all interference effects, we would anticipate a drag pressure reduction of about $1 - (0.81)^2 = 34$ percent for this particular case.

4.3.3 Influence of an Interference Heliostat

A few worst-case orientations were run with a second 1/10 scale heliostat mounted upstream at two different scaled distances. Table 4-1 summarizes these results, and discussion in the following paragraphs will be related to this table.

At those heliostat orientations that induced large moments about the inner axis, such as cases 58E, F, 76B, C, 19A, B, the average moment across 30 mirror module samples is reduced to 54 percent of the moment experienced by the exposed heliostat with no interference model. This 46 percent torsional load decrease is a combination of the 1.9 foot and 3.6 foot upstream interference effects at two different velocities. The leading mirror module (No. 3) for $-\gamma$'s exhibited the smallest load decrease. Note that in cases 98A, B the heliostat geometry is the same as 76B, C. However, the interference model is at $\gamma = 0$, therefore, providing more frontal blocking 3.6 feet upstream. The induced moments upon the most upstream module (No. 3) on the instrumented model is reduced further from a Cm = -0.064 (case 2-76B-3) to Cm = +0.023, changing even the rotational direction. This type of effect would be seen by the influence of wind fences.

The outer axis moments are also often reduced at some orientations--up to a factor of 1/3 as large. However, significant increases in the outer axis torsional loads are seen in cases 80A, B, 9, 10. These are orientations where the loading is predominately about the outer axis and the vortex shedding and flow attachment-detachment off the heliostat fluctuates randomly. In addition to the normal tunnel turbulence influence upon the heliostat, large individual gusts (vortex) struck the downstream, instrumented heliostat at random intervals 2-5 seconds apart. This phenomena was more pronounced with the interference model upstream 3.6 feet than at 1.9 feet and with the heliostats nearer $\gamma = 0$ deg.

One fully expected result was the reduction in total drag and side loads with the interference model. Cases 6, 7, 9 and 10, which are blunt, frontal orientations with respect to the wind, show that the drag is reduced by a factor of >2. This reduction could safely and conservatively be applied to the design of lateral and torsional foundation loadings and post supports throughout the entire field. With numerous heliostats and a wind fence, the net drag, or pressure loads, will be significantly reduced. All total drag loads are not reduced by a factor of 1/2; however, the worst-case loads are in the cases investigated and all other orientations demonstrated significant reductions in drag and side loads. These reduced, largest pressure force drag loadings should probably be used as the driving design criteria regarding wind loading effects upon foundations rather than the noninterference drag magnitudes.

Because of the limited number of runs made, a good envelope of influence effects cannot be made. It is recommended that a larger number of various heliostat geometries be wind tunnel tested with one interference model at various distances upstream and also with a vertical wall placed upstream.

TABLE 4-1. COMPARISON OF LOADS
WITH AND WITHOUT INTERFERENCE MODEL

Case	Strain Gage	Aerodynamic Coefficients					
		Without I/F Model		3.6 ft Upstream		1.9 ft Upstream	
		C_M	$\frac{C_D}{C_Y}$	C_M	$\frac{C_D}{C_Y}$	C_M	$\frac{C_D}{C_Y}$
58E							
γ = -25.5	1	0.107		0.038		0.035	
θ = 45	2	0.147		0.076		0.078	
ϕ = 30	3	-0.073		-0.051		-0.050	
V = 30 mph	4	-0.074					
	5	-0.065		-0.028		-0.030	
	6	-0.064		-0.030		-0.031	
	Total Drag		$\frac{1.850}{-1.280}$		$\frac{1.008}{-0.651}$		$\frac{0.964}{-0.651}$
58F							
	1	0.112		0.040		0.038	
V = 50 mph	2	0.155		0.085		0.087	
	3	-0.084		-0.056		-0.052	
	4	-0.077					
	5	-0.067		-0.030		-0.034	
	6	-0.064		-0.033		-0.033	
	Total Drag		$\frac{1.908}{-1.648}$		$\frac{1.087}{-0.734}$		$\frac{1.063}{-0.672}$

TABLE 4-1. COMPARISON OF LOADS
WITH AND WITHOUT INTERFERENCE MODEL
(Continued)

Case	Strain Gage	Aerodynamic Coefficients					
		Without I/F Model		3.6 ft Upstream		1.9 ft Upstream	
		C_M	$\frac{C_D}{C_Y}$	C_M	$\frac{C_D}{C_Y}$	C_M	$\frac{C_D}{C_Y}$
76B							
γ = -36	1	0.066		0.035		0.045	
θ = 60	2	0.138		0.081		0.083	
ϕ = 25	3	-0.083		-0.064		-0.049	
V = 30 mph	4	-0.080					
	5	-0.066		-0.029		-0.026	
	6	-0.061		-0.033		-0.029	
	Total Drag		$\frac{1.954}{-2.279}$		$\frac{1.029}{-0.781}$		$\frac{0.925}{-0.738}$
76C							
	1	0.073		0.032		0.048	
V = 50 mph	2	0.135		0.083		0.088	
	3	-0.086		-0.061		-0.052	
	4	-0.082					
	5	-0.071		-0.027		-0.027	
	6	-0.064		-0.032		-0.031	
	Total Drag		$\frac{2.024}{-2.242}$		$\frac{1.006}{-0.781}$		$\frac{0.969}{-0.781}$

TABLE 4-1. COMPARISON OF LOADS
WITH AND WITHOUT INTERFERENCE MODEL
(Continued)

Case	Strain Gage	Aerodynamic Coefficients					
		Without I/F Model		3.6 ft Upstream		1.9 ft Upstream	
		C_M	$\frac{C_D}{C_Y}$	C_M	$\frac{C_D}{C_Y}$	C_M	$\frac{C_D}{C_Y}$
98A							
γ = -36	1	0.066		0.024			
θ = 60	2	0.138		0.065			
ϕ = 25	3	-0.083		0.023			
V = 30 mph	4	-0.080					
Note: I/F Model at γ = 0 (more blocking)	5	-0.066		-0.029			
	6	-0.061		-0.038			
	Total Drag		$\frac{1.954}{-2.279}$		$\frac{0.708}{-0.673}$		
98B							
	1	0.073		0.023			
V = 50 mph	2	0.135		0.075			
Note: I/F Model at γ = 0	3	-0.086		0.020			
	4	-0.082					
	5	-0.071		-0.030			
	6	-0.064		-0.028			
	Total Drag		$\frac{2.024}{-2.242}$		$\frac{0.734}{-0.727}$		

TABLE 4-1. COMPARISON OF LOADS
WITH AND WITHOUT INTERFERENCE MODEL
(Continued)

Case	Strain Gage	Aerodynamic Coefficients					
		Without I/F Model		3.6 ft Upstream		1.9 ft Upstream	
		C_M	$\frac{C_D}{C_Y}$	C_M	$\frac{C_D}{C_Y}$	C_M	$\frac{C_D}{C_Y}$
81							
γ = 0	1	0.093				0.041	
θ = 20	2	0.104				0.077	
ϕ = 25	3	-0.013				-0.032	
V = 30 mph	4						
	5	-0.009				-0.024	
	6	-0.025				-0.025	
	Total Drag		$\frac{1.628}{-0.760}$				$\frac{0.999}{-0.391}$
82							
	1	0.094				0.044	
V = 50 mph	2	0.110				0.081	
	3	-0.014				-0.035	
	4						
	5	-0.011				-0.027	
	6	-0.024				-0.024	
	Total Drag		$\frac{1.618}{-0.742}$				$\frac{1.058}{-0.375}$

TABLE 4-1. COMPARISON OF LOADS
WITH AND WITHOUT INTERFERENCE MODEL
(Continued)

Case	Strain Gage	Aerodynamic Coefficients					
		Without I/F Model		3.6 ft Upstream		1.9 ft Upstream	
		C_M	$\frac{C_D}{C_Y}$	C_M	$\frac{C_D}{C_Y}$	C_M	$\frac{C_D}{C_Y}$
81							
γ = 0	1	0.093				0.041	
θ = 20	2	0.104				0.077	
ϕ = 25	3	-0.013				-0.032	
V = 30 mph	4						
	5	-0.009				-0.024	
	6	-0.025				-0.025	
	Total Drag		$\frac{1.628}{-0.760}$				$\frac{0.999}{-0.391}$
82							
	1	0.094				0.044	
V = 50 mph	2	0.110				0.081	
	3	-0.014				-0.035	
	4						
	5	-0.011				-0.027	
	6	-0.024				-0.024	
	Total Drag		$\frac{1.618}{-0.742}$				$\frac{1.058}{-0.375}$

TABLE 4-1. COMPARISON OF LOADS
WITH AND WITHOUT INTERFERENCE MODEL
(Continued)

Case	Strain Gage	Aerodynamic Coefficients					
		Without I/F Model		3.6 ft Upstream		1.9 ft Upstream	
		C_M	$\frac{C_D}{C_Y}$	C_M	$\frac{C_D}{C_Y}$	C_M	$\frac{C_D}{C_Y}$
80A							
$\gamma = 0$	1	0.012		0.022			
$\theta = 0$	2	0.006		0.020			
$\phi = \pm 3$	3	-0.004					
V = 50 mph	4	0.002					
	5	-0.001		0.001			
	6	0.001		0.003			
	Total Drag		$\frac{0.785}{0.016}$		Not Obtained		
80B							
	1	0.014		0.033			
V = 90 mph	2	0.005		0.029			
	3	-0.004		-0.003			
	4	0.003					
	5			0.002			
	6	0.001		0.005			
	Total Drag		$\frac{0.740}{0.0}$		Not Obtained		

TABLE 4-1. COMPARISON OF LOADS
WITH AND WITHOUT INTERFERENCE MODEL
(Continued)

Case	Strain Gage	Aerodynamic Coefficients					
		Without I/F Model		3.6 ft Upstream		1.9 ft Upstream	
		C_M	$\frac{C_D}{C_Y}$	C_M	$\frac{C_D}{C_Y}$	C_M	$\frac{C_D}{C_Y}$
19A							
γ = 0	1	-0.014		-0.014			
θ = 73	2	0.065		0.029			
ϕ = 65	3	-0.087		-0.064			
V = 30 mph	4	-0.100					
	5	-0.091		-0.041			
	6	-0.082		-0.035			
	Total Drag		$\frac{2.101}{-2.452}$		N/A		
19B							
	1	-0.012		-0.015			
V = 50 mph	2	0.057		0.034			
	3	-0.087		-0.070			
	4	-0.095					
	5	-0.088		-0.045			
	6	-0.077		-0.038			
	Total Drag		$\frac{2.019}{-2.242}$		N/A		

TABLE 4-1. COMPARISON OF LOADS
WITH AND WITHOUT INTERFERENCE MODEL
(Continued)

Case	Strain Gage	Aerodynamic Coefficients					
		Without I/F Model		3.6 ft Upstream		1.9 ft Upstream	
		C_M	$\frac{C_D}{C_Y}$	C_M	$\frac{C_D}{C_Y}$	C_M	$\frac{C_D}{C_Y}$
06							
γ = 0	1	0.145		0.095		0.126	
θ = 55	2	0.159		0.087		0.128	
ϕ = 0	3	-0.005		-0.007		-0.015	
V = 30 mph	4	0.003					
	5	-0.002		0.004		-0.010	
	6	-0.017		0.008		-0.011	
	Total Drag		$\frac{4.312}{N/A}$		$\frac{1.954}{-0.130}$		$\frac{1.880}{-0.043}$
07							
	1	0.159		0.095		0.122	
V = 50 mph	2	0.159		0.090		0.140	
	3			-0.009		-0.016	
	4	0.003					
	5	-0.003		0.006		-0.006	
	6	-0.013		0.010		-0.014	
	Total Drag		$\frac{4.262}{N/A}$		$\frac{2.032}{-0.078}$		$\frac{1.891}{-0.063}$

TABLE 4-1. COMPARISON OF LOADS
WITH AND WITHOUT INTERFERENCE MODEL
(Continued)

Case	Strain Gage	Aerodynamic Coefficients					
		Without I/F Model		3.6 ft Upstream		1.9 ft Upstream	
		C_M	$\frac{C_D}{C_Y}$	C_M	$\frac{C_D}{C_Y}$	C_M	$\frac{C_D}{C_Y}$
09							
$\gamma = 0$	1	0.029		0.057		0.099	
$\theta = 73$	2	0.081		0.073		0.101	
$\phi = 0$	3			0.001		0.002	
V = 30 mph	4						
	5			-0.004		-0.019	
	6			-0.001		-0.031	
	Total Drag		$\frac{4.799}{N/A}$		$\frac{1.683}{0.0}$		$\frac{1.876}{-0.130}$
10							
	1	0.037		0.058		0.097	
V = 50 mph	2	0.083		0.084		0.093	
	3			0.005			
	4					-0.033	
	5			-0.003		-0.018	
	6			0.001		-0.028	
	Total Drag		$\frac{4.869}{N/A}$		$\frac{1.775}{0.0}$		$\frac{1.810}{-0.141}$

4.3.4 Vented Mirror Module Investigation

Paragraph 4.3.1 has already addressed the reduction in the individual downstream mirror module moment coefficients when vented modules are used as compared to single, large facets. Paragraph 2.3.4 describes the construction and facet aspect ratios of the vented one square foot slotted modules.

One additional investigation was made comparing the influence of various square module configurations. Run numbers of the 4-XY series (items 186 through 241) as shown in Table 3-1 represent this portion of the testing. With the heliostat at a yaw angle of -90 deg and +90 deg and θ = 0 deg, different module configurations were stepped through various inner axis angles (ϕ). The hinge moments (of the leading mirror module) have all been reduced to a common angle of attack relationship and the moments plotted as Figure 4-2. The influence of the facet aspect ratios is very apparent in a predictable manner between angles of attacks between -30 deg and +30 deg.

Even more dramatic is the factor of 10 reduction in the moment of the 9-facet module compared to the solid module at the ±10 deg angle of attack (α). At α = +10 deg, Cm of the solid module = 0.045 (run 1-62A, B, C) and Cm of the 9 facet module = 0.0025 (run 4-62A, B). At α = -10 deg, the 9 facet module Cm = -0.003 (4-83, 84) and the solid module, -0.0365 (run 1-83, 84). Other aspect ratio modules show significant load decreases, but not the magnitude of the 9-facet module.

Presently, large stress conditions within the heliostat inner drive network caused by the 90 mph, 10 deg angle of attack survivability environmental condition is a large cost driver. The significantly reduced moment loads exhibited by the slotted modules as compared to solid mirror panels, when mounted on Honeywell's low profile heliostat, may well eliminate this particular problem.

At the larger α's, the vented modules appear not to offer much advantage. Notice also that as an average, the positive angles of attack result in larger moments than negative. This is due to the boundary layer profile. The effective center of pressure moves more towards the mirror module leading edge at positive angles because of a relatively larger aerodynamic load compared to the negative angle case. Note also that at α = 90 deg, a positive Cm = 0.005 to 0.006 exists for all module configurations due to the boundary layer profile and ground effects. Run 4-136-5 shows one orientation in which the moment coefficient for each module avarages a fairly large Cm = 0.060.

The end on drag was reduced from approximately C_D = 1.52 to 1.28 using the slotted modules at α = 90 deg. Five percent of this 16 percent decrease can be directly attributed to a reduction in total cross sectional due to the slots. The remaining 11 percent is caused by the vents preventing a large negative pressure to build up behind the module.

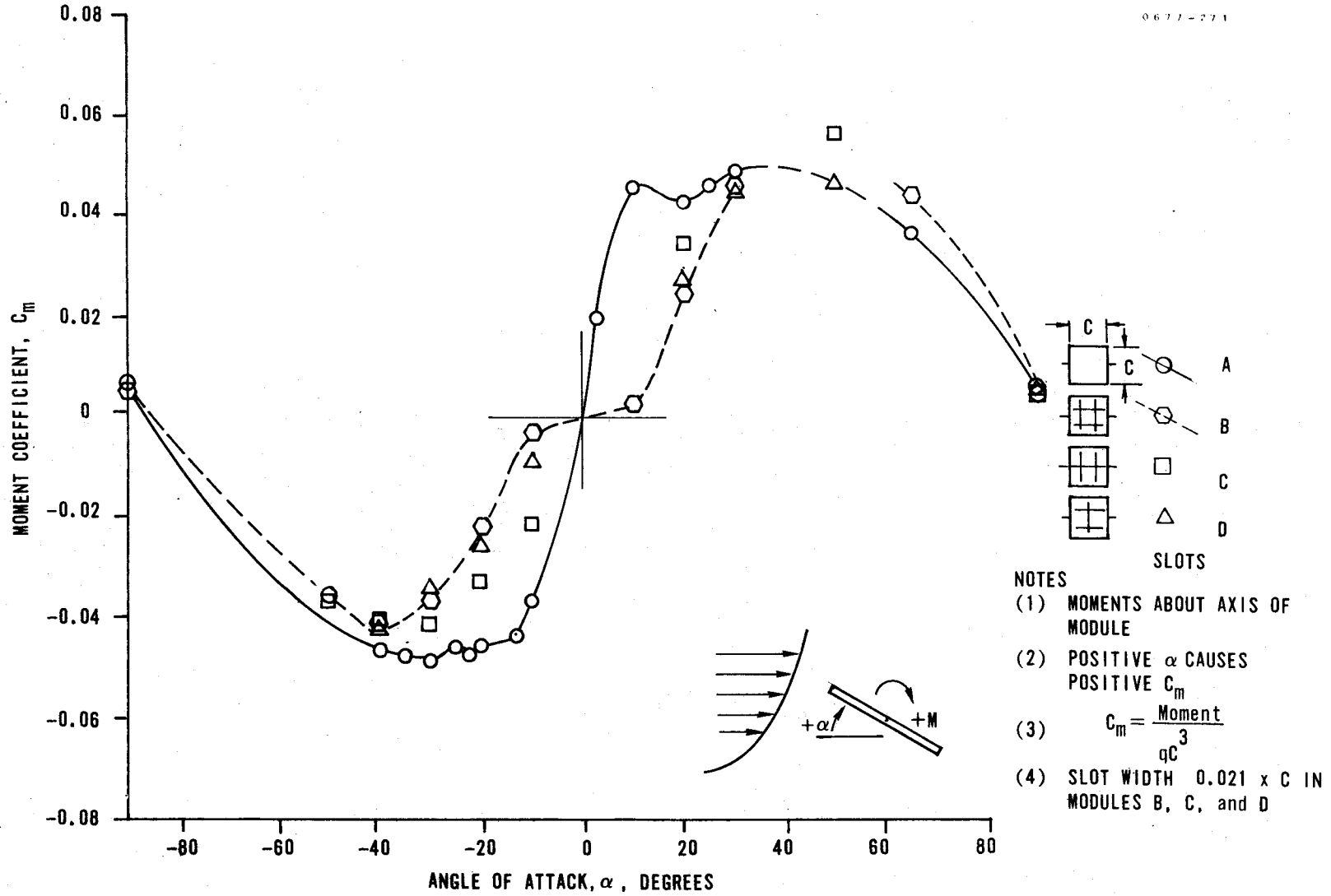

FIGURE 4-2. MOMENT COEFFICIENT AS FUNCTION OF ANGLE OF ATTACK FOR DIFFERENT SQUARE MIRROR MODULE CONFIGURATIONS

4.4 MIRROR MODULE PRESSURE PROFILES AND LOADS

4.4.1 Method of Handling Pressure Data

Paragraph 2.3.3 describes the pressure distribution test mechanization and the mirror module tap orientation. Subsection 4.1 addresses the data format in which the reduced pressure coefficient data is presented in Appendix A for each run made. This section gives a brief summary of some of the results obtained from the data reduction efforts.

With the orientation of the 9 taps per module, 18 average C_p data points are obtained for each combination of the ϕ and $\phi + 180$ deg runs. Different methods can be used to integrate this data over the entire front and back surfaces. Because most of our orientations were at $\gamma = 0$ and $\phi = 0$, 180 deg for varying θ, an off line program was developed to distribute the load in a logical manner and then derive the net normal force and moments. Run Nos. 3-04 and 3-04-180 along module No. 3 are an example. The pressure distribution profile along the inner axis (taps 1-5 along with zero pressure at the edges) was assumed to extend across the width of the module (taps 6-7-3-8-9) decreased or increased in magnitude only by the ratio of tap 6 compared to 3, 7 compared to 3, etc. Figure 4-3A shows the reduced C_p data for the 4 mirror modules' front face-- taken from Page 14 of Appendix A. The remainder of the pressure distribution matrix was filled out as described above. For example, Point A on mirror module No. 3 was assumed to be

$$C_{p_{\text{Point A}}} = \underset{\substack{\uparrow \\ \text{Tap 5}}}{-0.0931} \times \left[\frac{0.1757 \text{ Tap 7}}{0.1908 \text{ Tap 3}}\right] = -0.0857$$

After a 7x7 matrix was filled out for each module, a function was defined by this matrix and the module broken into 24 x 24 = 576 small areas and interpolation made from the 7x7 matrix to acquire a derived pressure for each area as shown in Figure 4-3B for module No. 3 only. Note that for presentation purposes the scaling was multiplied by 1000 with no decimal shown.

The same procedure was performed on the back side (3-04-180 run) of each module shown in Figures 4-3C and 4-3D.

The back side pressures were then subtracted from the front side pressures to obtain the net resultant pressures at each relative module location. For instance, for tap No. 3, module No. 3.

$$C_p \text{ Total No. 3} = 0.1908 - (-0.6178) = 0.8086$$

which is shown in Figure 4-3E. Note that the -180 cases are reversed about the inner axis. That is, tap No. 9 from the 3-04-180 case must be subtracted from tap No. 6. A net 24x24 matrix was then formed (Figure 4-3F) by interpolating between values of the 7x7 matrix.

CONFIGURATION = 3-04 OPTION = 3

M = +3

0.0000	0.0000	0.0000	0.0000	0.0000	0.0000	0.0000
0.0000	-0.0314	-0.0857	-0.0931	-0.0907	-0.0145	0.0000
0.0000	0.0223	0.0608	0.0660	0.0643	0.0103	0.0000
0.0000	0.0643	0.1757	0.1908	0.1859	0.0297	0.0000
0.0000	0.1014	0.2769	0.3008	0.2930	0.0468	0.0000
0.0000	0.1534	0.4190	0.4551	0.4434	0.0708	0.0000
0.0000	0.0000	0.0000	0.0000	0.0000	0.0000	0.0000

M = +4

0.0000	0.0000	0.0000	0.0000	0.0000	0.0000	0.0000
0.0000	-0.0289	-0.0836	-0.0905	-0.0886	-0.0142	0.0000
0.0000	0.0227	0.0657	0.0704	0.0697	0.0196	0.0000
0.0000	0.0634	0.1834	0.1963	0.1944	0.0546	0.0000
0.0000	0.0962	0.2783	0.2979	0.2950	0.0829	0.0000
0.0000	0.1314	0.3802	0.4070	0.4030	0.1133	0.0000
0.0000	0.0000	0.0000	0.0000	0.0000	0.0000	0.0000

M = +5

0.0000	0.0000	0.0000	0.0000	0.0000	0.0000	0.0000
0.0000	-0.0224	-0.0810	-0.0907	-0.0807	-0.0268	0.0000
0.0000	0.0188	0.0681	0.0763	0.0679	0.0225	0.0000
0.0000	0.0462	0.1676	0.1876	0.1670	0.0554	0.0000
0.0000	0.0634	0.2297	0.2572	0.2289	0.0760	0.0000
0.0000	0.0962	0.3487	0.3903	0.3474	0.1153	0.0000
0.0000	0.0000	0.0000	0.0000	0.0000	0.0000	0.0000

M = +6

0.0000	0.0000	0.0000	0.0000	0.0000	0.0000	0.0000
0.0000	-0.0007	-0.0626	-0.0750	-0.0789	-0.0336	0.0000
0.0000	0.0009	0.0775	0.0928	0.0977	0.0416	0.0000
0.0000	0.0018	0.1608	0.1928	0.2102	0.0895	0.0000
0.0000	0.0017	0.1556	0.1863	0.1960	0.0834	0.0000
0.0000	0.0039	0.3531	0.4227	0.4449	0.1894	0.0000
0.0000	0.0000	0.0000	0.0000	0.0000	0.0000	0.0000

TAP #5

TAP #6

TAP #9

TAP #1

FIGURE 4-3A. OFF-LINE COMPUTER REDUCED PRESSURE DATA, RUN NO. 3-04

*** INTERPOLATED PRESSURE DISTRIBUTION ***
FOR MODULE NUMBER = 3

-3	-10	-13	-17	-20	-24	-27	-28	-29	-29	-30	-30	-30	-30	-30	-30	-30	-29	-24	-19	-14	-9	-4	-1
-10	-31	-41	-52	-62	-72	-83	-86	-88	-89	-90	-92	-92	-92	-91	-91	-90	-87	-72	-58	-43	-28	-14	-4
-7	-21	-28	-35	-42	-49	-56	-58	-59	-60	-61	-62	-62	-62	-61	-61	-61	-58	-48	-39	-29	-19	-9	-3
-3	-10	-14	-18	-21	-25	-28	-30	-30	-31	-31	-32	-32	-32	-32	-31	-31	-30	-25	-20	-15	-10	-5	-1
0	0	0	-1	-1	-1	-1	-1	-2	-2	-2	-2	-2	-2	-2	-2	-2	-2	-1	-1	-1	0	0	0
3	9	12	15	18	22	25	26	26	27	27	27	28	27	27	27	27	26	21	17	13	8	4	1
6	19	26	32	39	45	52	54	55	56	57	58	58	58	57	57	57	54	45	36	27	18	9	3
9	28	37	46	56	65	74	78	79	80	81	83	83	83	82	82	82	78	65	52	39	26	13	4
12	36	48	60	72	84	96	100	101	103	105	106	107	106	106	105	105	100	83	67	50	33	16	5
14	44	58	73	88	102	117	122	124	126	128	130	131	130	129	129	128	122	102	81	61	40	20	6
17	52	69	86	104	121	138	144	146	149	151	154	154	154	153	152	151	145	120	96	72	48	24	8
20	60	80	100	119	139	159	166	169	172	174	177	178	177	176	175	174	167	139	111	83	55	27	9
22	67	90	112	134	157	179	187	190	193	196	199	200	199	198	197	196	188	156	125	94	62	31	10
24	74	99	124	149	173	198	207	210	213	217	220	221	220	219	218	217	207	173	138	103	69	34	11
27	81	109	136	163	190	217	226	230	234	237	241	242	241	240	239	237	227	189	151	113	75	37	12
29	89	118	147	177	206	235	246	250	254	258	262	263	262	260	259	258	247	205	164	123	82	41	13
32	96	127	159	191	222	254	265	270	274	278	282	284	282	281	280	278	266	222	177	133	88	44	14
34	103	138	172	206	240	275	287	291	296	301	305	307	305	304	302	301	288	240	192	144	95	47	15
37	113	151	188	226	263	301	314	319	324	329	335	336	335	333	331	330	315	263	210	157	105	52	17
41	123	164	205	246	286	327	341	347	353	358	364	366	364	362	360	358	343	285	228	171	114	57	19
44	133	177	221	265	309	353	369	375	381	387	393	395	393	391	389	387	370	308	247	185	123	61	20
47	143	190	238	285	332	380	396	403	409	416	422	424	422	420	418	416	398	331	265	198	132	66	22
51	153	204	254	305	355	406	424	431	437	444	451	454	451	449	447	445	425	354	283	212	141	70	23
17	51	68	84	101	118	135	141	143	145	148	150	151	150	149	149	148	141	118	94	70	47	23	7

FIGURE 4-3B. INTERPOLATED PRESSURE DISTRIBUTION FOR MODULE NO. 3

CONFIGURATION = 3-04-180 OPTION = 3

M = +3

0.0000	0.0000	0.0000	0.0000	0.0000	0.0000	0.0000
0.0000	-0.3777	-0.4147	-0.3725	-0.4190	-0.4044	0.0000
0.0000	-0.4891	-0.5369	-0.4823	-0.5424	-0.5236	0.0000
0.0000	-0.6264	-0.6876	-0.6178	-0.6947	-0.6706	0.0000
0.0000	-0.7186	-0.7889	-0.7088	-0.7971	-0.7694	0.0000
0.0000	-0.7007	-0.7692	-0.6911	-0.7772	-0.7502	0.0000
0.0000	0.0000	0.0000	0.0000	0.0000	0.0000	0.0000

M = +4

0.0000	0.0000	0.0000	0.0000	0.0000	0.0000	0.0000
0.0000	-0.3995	-0.4123	-0.4115	-0.4205	-0.4143	0.0000
0.0000	-0.5031	-0.5192	-0.5181	-0.5296	-0.5217	0.0000
0.0000	-0.5698	-0.5880	-0.5868	-0.5997	-0.5908	0.0000
0.0000	-0.5780	-0.5965	-0.5953	-0.6084	-0.5993	0.0000
0.0000	-0.5513	-0.5689	-0.5677	-0.5802	-0.5716	0.0000
0.0000	0.0000	0.0000	0.0000	0.0000	0.0000	0.0000

M = +5

0.0000	0.0000	0.0000	0.0000	0.0000	0.0000	0.0000
0.0000	-0.3977	-0.4053	-0.3967	-0.4055	-0.3858	0.0000
0.0000	-0.5144	-0.5242	-0.5130	-0.5243	-0.4990	0.0000
0.0000	-0.5818	-0.5929	-0.5803	-0.5931	-0.5644	0.0000
0.0000	-0.5958	-0.6072	-0.5942	-0.6073	-0.5779	0.0000
0.0000	-0.5677	-0.5785	-0.5662	-0.5787	-0.5507	0.0000
0.0000	0.0000	0.0000	0.0000	0.0000	0.0000	0.0000

M = +6

0.0000	0.0000	0.0000	0.0000	0.0000	0.0000	0.0000
0.0000	-0.3706	-0.3949	-0.3805	-0.3803	-0.3220	0.0000
0.0000	-0.4974	-0.5300	-0.4436	-0.4836	-0.4322	0.0000
0.0000	-0.6512	-0.6939	-0.5807	-0.6331	-0.5659	0.0000
0.0000	-0.7492	-0.7982	-0.6681	-0.7284	-0.6510	0.0000
0.0000	-0.7601	-0.8099	-0.6778	-0.7390	-0.6604	0.0000
0.0000	0.0000	0.0000	0.0000	0.0000	0.0000	0.0000

FIGURE 4-3C. OFF-LINE COMPUTER REDUCED PRESSURE DATA, RUN NO. 3-04-180

*** INTERPOLATED PRESSURE DISTRIBUTION ***
FOR MODULE NUMBER = 3

-41	-125	-128	-130	-132	-135	-137	-136	-133	-130	-128	-125	-125	-128	-131	-134	-137	-139	-138	-137	-136	-135	-134	-44
-125	-377	-384	-391	-398	-405	-412	-408	-400	-392	-384	-376	-376	-385	-394	-403	-412	-418	-415	-412	-409	-407	-404	-134
-132	-398	-406	-413	-421	-428	-436	-431	-423	-414	-406	-397	-398	-407	-416	-426	-435	-441	-438	-435	-432	-430	-427	-142
-140	-420	-427	-435	-443	-451	-459	-454	-445	-436	-427	-418	-419	-429	-438	-448	-458	-465	-462	-459	-455	-452	-449	-149
-147	-441	-449	-457	-466	-474	-482	-477	-468	-458	-449	-439	-440	-450	-461	-471	-481	-488	-485	-482	-479	-475	-472	-157
-154	-462	-471	-479	-488	-497	-505	-500	-490	-480	-470	-461	-461	-472	-483	-494	-504	-512	-508	-505	-502	-498	-495	-165
-161	-483	-492	-501	-510	-519	-528	-523	-513	-502	-492	-482	-482	-494	-505	-516	-528	-535	-532	-528	-525	-521	-517	-172
-169	-508	-518	-527	-537	-546	-556	-550	-539	-528	-517	-507	-507	-519	-531	-543	-555	-563	-559	-555	-552	-548	-544	-181
-178	-534	-544	-554	-564	-574	-584	-578	-567	-555	-544	-533	-533	-546	-558	-571	-583	-592	-588	-584	-580	-576	-572	-190
-186	-560	-571	-581	-592	-602	-613	-606	-594	-583	-571	-559	-559	-572	-586	-599	-612	-621	-617	-612	-608	-604	-600	-200
-195	-587	-598	-609	-619	-630	-641	-635	-622	-610	-597	-585	-585	-599	-613	-627	-640	-650	-645	-641	-637	-632	-628	-209
-204	-613	-624	-636	-647	-658	-670	-663	-650	-637	-624	-611	-612	-626	-640	-655	-669	-679	-674	-670	-665	-661	-656	-218
-211	-635	-646	-658	-670	-682	-694	-687	-673	-660	-646	-633	-633	-648	-663	-678	-693	-703	-698	-693	-689	-684	-680	-226
-217	-652	-664	-677	-689	-701	-713	-706	-692	-678	-664	-650	-651	-666	-681	-697	-712	-722	-717	-713	-708	-703	-698	-232
-223	-670	-682	-695	-707	-720	-732	-725	-710	-696	-682	-668	-668	-684	-700	-716	-731	-742	-737	-732	-727	-722	-717	-239
-229	-687	-700	-713	-726	-739	-751	-744	-729	-714	-700	-685	-686	-702	-718	-734	-750	-761	-756	-751	-746	-741	-736	-245
-235	-705	-718	-731	-744	-757	-771	-763	-748	-733	-718	-703	-704	-720	-737	-753	-770	-781	-775	-770	-765	-760	-755	-251
-239	-717	-731	-744	-757	-771	-784	-776	-761	-746	-730	-715	-716	-733	-749	-766	-783	-794	-789	-784	-779	-773	-768	-256
-238	-714	-727	-740	-754	-767	-780	-772	-757	-742	-727	-712	-712	-729	-746	-763	-779	-791	-785	-780	-775	-770	-764	-254
-236	-710	-724	-737	-750	-763	-777	-769	-754	-738	-723	-708	-709	-726	-742	-759	-776	-787	-782	-776	-771	-766	-761	-253
-235	-707	-720	-733	-747	-760	-773	-765	-750	-735	-720	-705	-706	-722	-739	-755	-772	-783	-778	-773	-767	-762	-757	-252
-234	-704	-717	-730	-743	-756	-769	-761	-746	-731	-716	-701	-702	-719	-735	-752	-768	-779	-774	-769	-764	-759	-753	-251
-233	-700	-713	-726	-739	-752	-765	-758	-743	-728	-713	-698	-699	-715	-732	-748	-764	-775	-770	-765	-760	-755	-750	-250
-77	-233	-237	-242	-246	-250	-255	-252	-247	-242	-237	-232	-233	-238	-244	-249	-254	-258	-256	-255	-253	-251	-250	-83

FIGURE 4-3D. INTERPOLATED PRESSURE DISTRIBUTION FOR MODULE NO. 3

CONFIGURATION = 3-04-180 OPTION = -2

M = 23

0.0000	0.0000	0.0000	0.0000	0.0000	0.0000	0.0000	0.0000	0.0000	0.0000	0.0000	0.0000	0.0000	0.0000
0.0000	0.2540	0.3008	0.2795	0.3019	0.2268	0.0000	0.0000	0.2690	0.3220	0.3220	0.3217	0.2567	0.0000
0.0000	0.4985	0.5903	0.5484	0.5924	0.4449	0.0000	0.0000	0.4916	0.5885	0.5885	0.5879	0.4692	0.0000
0.0000	0.7350	0.8704	0.8086	0.8735	0.6561	0.0000	0.0000	0.6542	0.7831	0.7831	0.7823	0.6244	0.0000
0.0000	0.9176	1.0867	1.0096	1.0906	0.8191	0.0000	0.0000	0.7461	0.8932	0.8932	0.8923	0.7122	0.0000
0.0000	1.0418	1.2338	1.1462	1.2382	0.9300	0.0000	0.0000	0.8142	0.9747	0.9748	0.9738	0.7772	0.0000
0.0000	0.0000	0.0000	0.0000	0.0000	0.0000	0.0000	0.0000	0.0000	0.0000	0.0000	0.0000	0.0000	0.0000

M = 24

0.0000	0.0000	0.0000	0.0000	0.0000	0.0000	0.0000	0.0000	0.0000	0.0000	0.0000	0.0000	0.0000	0.0000
0.0000	0.2433	0.3031	0.3060	0.3028	0.2539	0.0000	0.0000	0.1859	0.2619	0.2555	0.2960	0.2425	0.0000
0.0000	0.4686	0.5838	0.5893	0.5831	0.4890	0.0000	0.0000	0.3901	0.5498	0.5364	0.6213	0.5090	0.0000
0.0000	0.6106	0.7607	0.7680	0.7599	0.6372	0.0000	0.0000	0.5677	0.8000	0.7805	0.9041	0.7407	0.0000
0.0000	0.6770	0.8434	0.8514	0.8425	0.7065	0.0000	0.0000	0.6214	0.8757	0.8544	0.9896	0.8108	0.0000
0.0000	0.7606	0.9476	0.9566	0.9465	0.7938	0.0000	0.0000	0.8005	1.1280	1.1006	1.2748	1.0444	0.0000
0.0000	0.0000	0.0000	0.0000	0.0000	0.0000	0.0000	0.0000	0.0000	0.0000	0.0000	0.0000	0.0000	0.0000

M = 25

0.0000	0.0000	0.0000	0.0000	0.0000	0.0000	0.0000	0.0000	0.0000	0.0000	0.0000	0.0000	0.0000	0.0000
0.0000	0.2433	0.3031	0.3060	0.3028	0.2539	0.0000	0.0000	0.1859	0.2619	0.2555	0.2960	0.2425	0.0000
0.0000	0.4686	0.5838	0.5893	0.5831	0.4890	0.0000	0.0000	0.3901	0.5498	0.5364	0.6213	0.5090	0.0000
0.0000	0.6106	0.7607	0.7680	0.7599	0.6372	0.0000	0.0000	0.5677	0.8000	0.7805	0.9041	0.7407	0.0000
0.0000	0.6770	0.8434	0.8514	0.8425	0.7065	0.0000	0.0000	0.6214	0.8757	0.8544	0.9896	0.8108	0.0000
0.0000	0.7606	0.9476	0.9566	0.9465	0.7938	0.0000	0.0000	0.8005	1.1280	1.1006	1.2748	1.0444	0.0000
0.0000	0.0000	0.0000	0.0000	0.0000	0.0000	0.0000	0.0000	0.0000	0.0000	0.0000	0.0000	0.0000	0.0000

M = 26

0.0000	0.0000	0.0000	0.0000	0.0000	0.0000	0.0000	0.0000	0.0000	0.0000	0.0000	0.0000	0.0000	0.0000
0.0000	0.1859	0.2619	0.2555	0.2960	0.2425	0.0000	0.0000	0.1859	0.2619	0.2555	0.2960	0.2425	0.0000
0.0000	0.3901	0.5498	0.5364	0.6213	0.5090	0.0000	0.0000	0.3901	0.5498	0.5364	0.6213	0.5090	0.0000
0.0000	0.5677	0.8000	0.7805	0.9041	0.7407	0.0000	0.0000	0.5677	0.8000	0.7805	0.9041	0.7407	0.0000
0.0000	0.6214	0.8757	0.8544	0.9896	0.8108	0.0000	0.0000	0.6214	0.8757	0.8544	0.9896	0.8108	0.0000
0.0000	0.8005	1.1280	1.1006	1.2748	1.0444	0.0000	0.0000	0.8005	1.1280	1.1006	1.2748	1.0444	0.0000
0.0000	0.0000	0.0000	0.0000	0.0000	0.0000	0.0000	0.0000	0.0000	0.0000	0.0000	0.0000	0.0000	0.0000

FIGURE 4-3E. NET PRESSURE DISTRIBUTION MATRIX

*** INTERPOLATED PRESSURE DISTRIBUTION ***
FOR MODULE NUMBER = 3

28	84	87	90	93	96	99	99	97	96	95	93	93	95	96	98	99	99	94	89	85	80	75	25
84	254	262	271	280	289	298	297	293	289	285	281	281	285	290	294	298	298	284	269	255	241	226	75
100	300	311	321	332	342	353	352	347	342	337	333	333	338	343	348	353	353	336	319	302	285	268	89
115	347	359	371	383	395	408	406	401	395	390	384	384	390	396	402	408	407	388	368	348	329	309	103
131	393	407	421	435	448	462	461	455	448	442	436	436	443	449	456	462	462	440	417	395	373	351	117
146	440	455	471	486	502	517	516	509	501	494	487	488	495	502	510	517	517	492	467	442	417	392	130
162	486	503	520	538	555	572	570	562	555	547	539	539	547	556	564	572	571	544	516	489	461	434	144
177	532	550	569	588	606	625	623	615	606	598	589	590	598	607	616	625	625	595	565	535	505	475	158
192	577	597	617	638	658	678	676	667	658	648	639	639	649	659	669	678	677	645	612	580	547	515	171
207	622	644	666	687	709	731	729	719	709	699	689	689	700	710	721	731	730	695	660	625	590	555	185
222	667	690	714	737	761	784	782	771	760	750	739	739	751	762	773	784	783	746	708	670	633	595	198
237	712	737	762	787	812	837	835	823	812	800	789	789	801	813	825	837	836	796	756	716	676	635	211
250	752	778	805	831	857	884	881	869	857	845	833	834	846	859	872	884	883	841	798	756	713	671	223
262	787	814	842	870	897	925	922	910	897	884	872	872	885	899	912	925	924	881	835	791	747	702	234
273	821	850	879	908	937	966	963	950	937	924	910	911	925	938	952	966	965	918	872	826	780	733	244
285	856	886	916	946	977	1007	1004	990	976	963	949	949	964	978	993	1007	1006	957	909	861	813	764	254
297	891	922	954	985	1016	1048	1045	1030	1016	1002	988	988	1003	1018	1033	1048	1047	996	946	896	846	795	265
307	923	955	988	1020	1053	1085	1082	1067	1053	1038	1023	1023	1039	1054	1070	1085	1084	1032	980	928	876	824	274
315	947	980	1013	1046	1080	1113	1110	1095	1080	1064	1049	1050	1066	1081	1097	1113	1112	1059	1005	952	898	845	281
323	970	1004	1039	1073	1107	1141	1138	1122	1107	1091	1075	1076	1092	1108	1125	1141	1140	1085	1030	976	921	866	288
331	994	1029	1064	1099	1134	1169	1165	1149	1133	1118	1102	1102	1119	1135	1152	1169	1167	1111	1055	999	943	887	295
339	1018	1053	1089	1125	1161	1196	1193	1177	1160	1144	1128	1128	1145	1163	1180	1197	1195	1138	1081	1023	966	908	302
347	1041	1078	1114	1151	1188	1224	1221	1204	1187	1171	1154	1154	1172	1190	1207	1225	1223	1164	1106	1047	988	930	310
115	347	359	371	383	396	408	407	401	395	390	384	384	390	396	402	408	407	388	368	349	329	310	103

FIGURE 4-3F. INTERPOLATED PRESSURE DISTRIBUTION FOR MODULE NO. 3

Each module's net pressure distribution matrix was then integrated across the entire surface (576 points) to obtain the total normal force and subsequent moments and center of pressures.

Figure 4-3G shows a typical printout of the resultant nondimensional normal force coefficients,

$$C_n = \frac{\text{Pounds Force}}{q}$$

and the derived moments about the mirror module's center lines along with the effective center of pressure. It is recognized that no procedure will be absolutely accurate using only the 18 pressure data points per module that were used. However, it is felt that the approach used will give a good approximation to the actual forces experienced on the modules for the cases run.

4.4.2 Discussion of Results

Table 4-2 summarizes the results obtained from each case. Notice that there is normally close agreement between values of the normal force coefficient for the different wind speeds at the same heliostat geometries. Therefore, it is felt that the assumptions made in generating the total module profiles were good. The moment coefficients about the outer axis, when added up, normally are slightly smaller than summing the two outer axis strain gage readings. This is probably due to not compensating for the frame effects. The directions confirm where like cases can be compared.

In reviewing the pressure data from Appendix A, it is noted that the negative pressures on the back sides are often larger and more significant than the front side positive pressures. However, the back side distributions are normally more uniform, showing that the smaller but less uniform front side positive pressures are actually more influential in causing net torsional moments about the inner and outer axis.

The largest normal loads are seen in cases 3-09 and 3-10 and reach $C_n = 0.96$. At 50 mph on a full scale SRE heliostat with 100 square foot mirror modules, this value represents 614 pounds of normal force to be applied against the combination of the mirror module bearings. For $\theta = 10$ deg, a 90 mph wind could result in a load of 425 pounds normal to the module as determined from case 3-01D. Even though a larger load would result from $\theta = -10$ deg as shown in runs 3-93 and 94, a negative angle of attack at 90 mph (that is, wind vector rising up from the ground) does not appear physically possible.

There are many different plots that could be made of the various distributions. Figures 4-4 through 4-6 show a few interesting ones. Figure 4-4 shows the top and bottom side (with reference to wind vector) pressure distributions for all four modules for $\phi = 0$ and a typical positive outer axis angle, $\theta = +20$ deg. Notice the small positive pressures on the "top" surface which go negative near the trailing edge, indicating flow separation. The diagram view is as if looking at the heliostat from one end.

```
NORMAL FORCES (LBF/3) =
 0.67827       0.60778       0.58896       0.62844
   #3            #4            #5            #6
 X/Y MOMENTS (FT-LBF/3) =
-0.38262E-02 -0.14858E-02  0.12582E-02  0.12584E-01  <-- ABOUT THE I/A
 0.66175E-01  0.45529E-01  0.43359E-01  0.58610E-01      ABOUT THE O/A

X/Y COORININATES OF THE CENTER OF PRESSURE (INCHES)=
-0.67693E-01 -0.29336E-01  0.25635E-01  0.24029
  1.1708        0.89893       0.88344       1.1192
```

FIGURE 4-3G. RESULTS FROM INTEGRATING PRESSURE DISTRIBUTION

TABLE 4-2. MIRROR MODULE COEFFICIENTS FROM PRESSURE DATA

Conditions					No. 3			No. 4			No. 5			No. 6		
Run No.*	γ	θ	ϕ*	V (mph)	C_N	C_M IA	C_M OA	C_N	C_M IA	C_M OA	C_N	C_M IA	C_M OA	C_N	C_M IA	C_M OA
3-01G	0	20	0	30	0.437	0	0.045	0.438	-0.004	0.039	0.425	0.003	0.034	0.379	-0.004	0.045
3-01H	0	20	0	50	0.435	0	0.046	0.440	-0.003	0.036	0.432	0.002	0.032	0.398	-0.005	0.038
3-09	0	73	0	30	0.901	0.006	0.021	0.876	-0.006	0.023	0.903	-0.008	0.025	0.958	-0.024	0.021
3-10	0	73	0	50	0.950	0.009	0.021	0.912	0	0.022	0.954	-0.002	0.024	0.960	-0.014	0.020
3-06	0	55	0	30	0.826	0.002	0.042	0.786	0	0.040	0.754	0	0.037	0.851	-0.021	0.036
3-07	0	55	0	50	0.899	0.006	0.041	0.876	0	0.038	0.870	0.001	0.038	0.869	-0.014	0.036
3-03	0	30	0	30	0.685	0.003	0.066	0.594	0.001	0.040	0.576	-0.002	0.036	0.614	-0.015	0.060
3-04	0	30	0	50	0.678	0.004	0.066	0.608	0.001	0.046	0.589	-0.001	0.043	0.628	-0.013	0.059
3-89	0	25	0	30	0.540	0.001	0.058	0.516	-0.001	0.046	0.501	-0.003	0.043	0.463	-0.007	0.054
3-90	0	25	0	50	0.551	0.001	0.057	0.546	-0.001	0.047	0.526	-0.006	0.042	0.500	-0.008	0.053
3-01C	0	10	0	30	0.143	0.004	0.016	0.200	0.001	0.011	0.117	0.001	-0.010	0.116	-0.006	0.004
3-01D	0	10	0	50	0.189	0.003	0.021	0.217	0	0.009	0.205	0.001	-0.006	0.165	-0.006	0.007
3-01E	0	10	0	90	0.203	0.001	0.021	0.211	0	0.011	0.186	0	-0.006	0.157	-0.005	0.007
3-93	0	-10	0	30	-0.253	-0.015	-0.002	-0.264	0	0.022	-0.299	0.003	0.017	-0.213	0.012	-0.005
3-94	0	-10	0	50	-0.300	-0.010	-0.002	-0.318	-0.002	0.016	-0.337	0.003	0.020	-0.259	0.012	-0.004
3-95	0	-20	0	30	-0.615	-0.016	-0.053	-0.638	-0.004	-0.012	-0.634	0.008	-0.017	-0.644	0.021	-0.052
3-96	0	-20	0	50	-0.633	-0.018	-0.057	-0.649	-0.004	-0.016	-0.636	0.009	-0.013	-0.633	0.019	-0.052
3-48	-90	0	90	30	-0.801	0.004	0.006	-0.022	-0.006	-0.001	-0.198	0.008	0	-0.278	0.001	0.005
3-49	-90	0	90	50	-0.794	0.003	0.003	0.005	0.002	-0.007	-0.190	0.012	0.001	-0.269	0.004	0.002
3-99	-57	0	-90	50	0.684	0.006	0.035	0.621	0.022	0.034	0.737	0.007	0.034	0.554	0.008	0.014

Notes: * These runs are combined with the -180 run of the same 3-XY base.

C_m OA actually represents a moment about a module axis perpendicular to the module's inner axis.

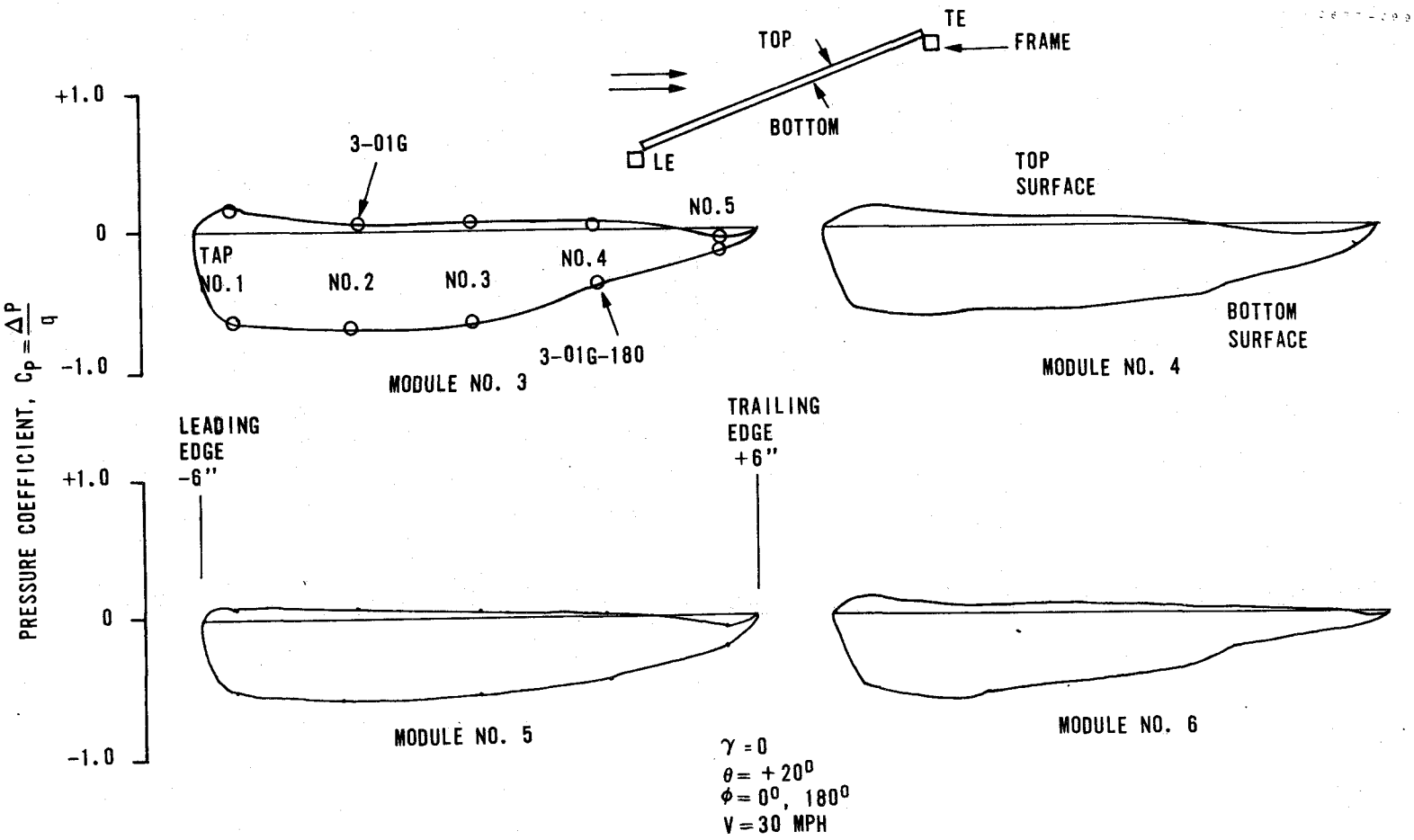

PRESSURE DISTRIBUTION ALONG INNER AXIS CENTER LINE OF HELIOSTAT MIRROR MODULES

FIGURE 4-4. PRESSURE DISTRIBUTION ALONG INNER AXIS CENTER LINE OF HELIOSTAT MIRROR MODULES

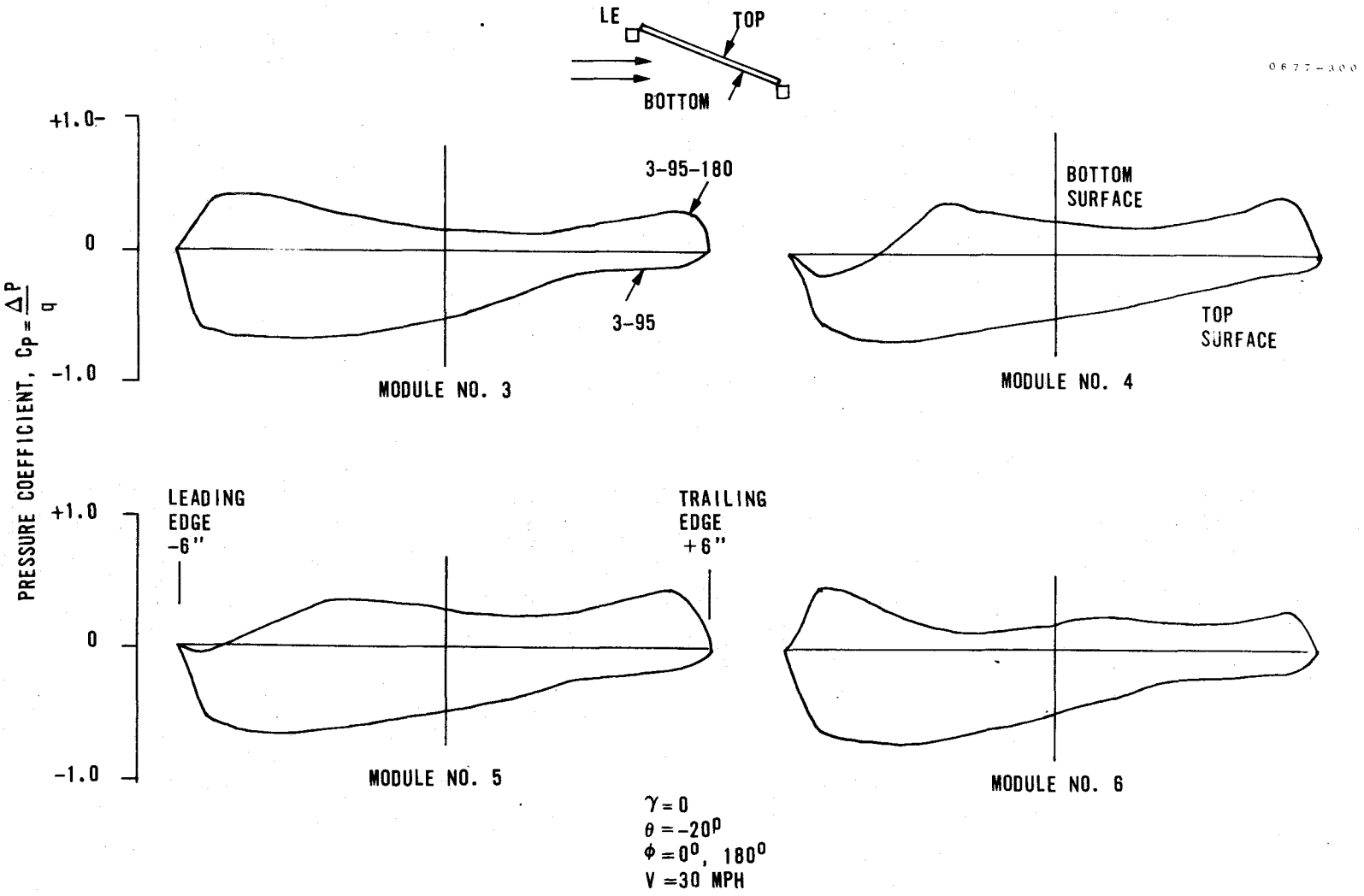

PRESSURE DISTRIBUTION ALONG INNER AXIS CENTER LINE OF HELIOSTAT MIRROR MODULES

FIGURE 4-5. PRESSURE DISTRIBUTION ALONG INNER AXIS CENTER LINE OF HELIOSTAT MIRROR MODULES

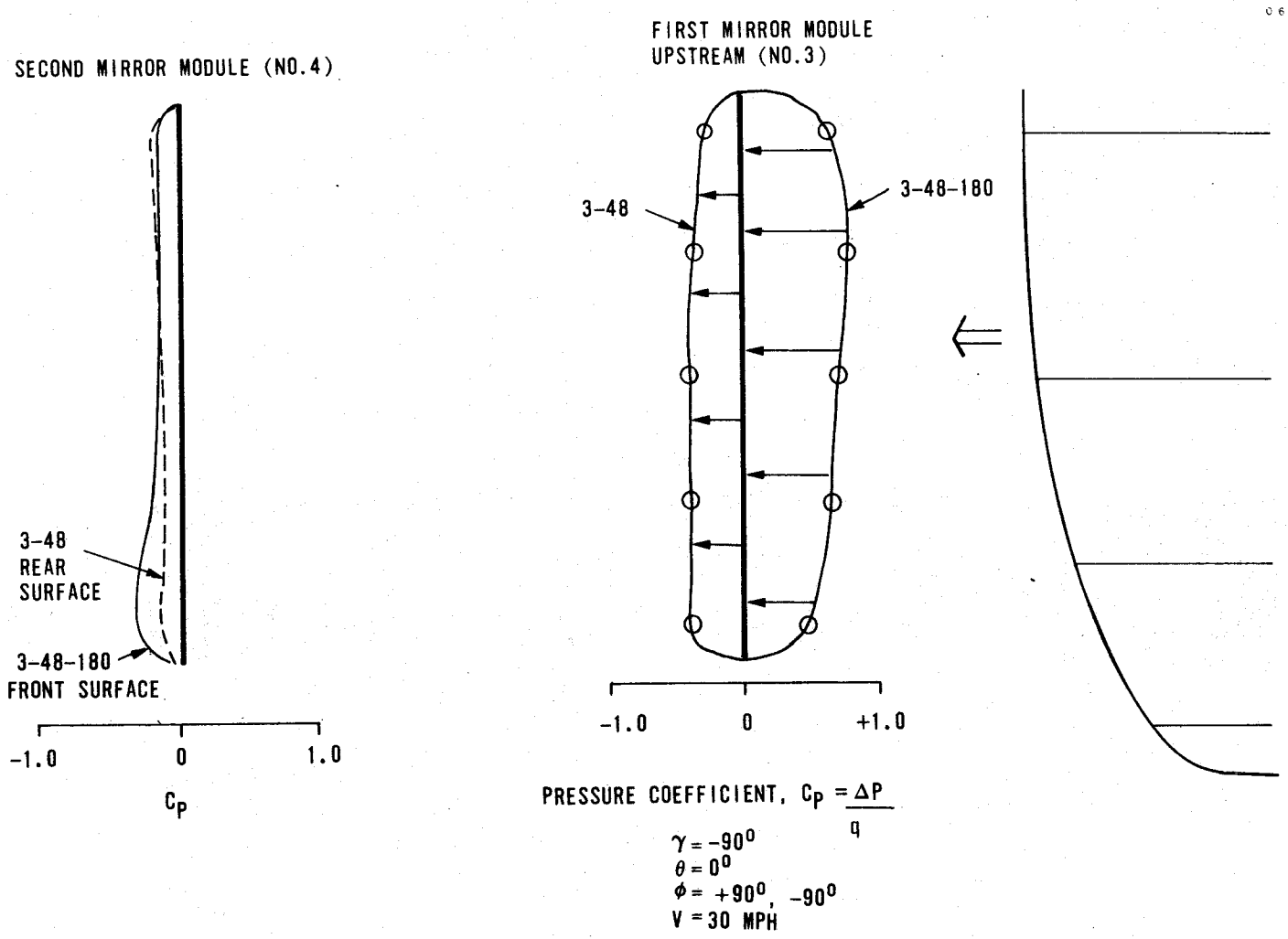

FIGURE 4-6. VERTICAL PRESSURE DISTRIBUTION ALONG MIRROR MODULE NORMAL TO SCALED WIND PROFILE

Now observe Figure 4-5 where θ = -20 deg. On modules 3 and 6, the positive pressures (this time on the bottom surface) are much larger than for θ = +20 deg. This is due primarily to wind force entrapment and the ground effects. However, note the significant negative pressures near the leading edge of modules 4 and 5 on the bottom surface. This phenomena is due to the stagnation and flow reversal caused by the frame near the leading edge for these two inboard modules. The outboard modules (3 and 6) extend beyond the frame ends, thus affording nearly normal pressure flow. But because the modules are positioned on top of the frame, positive pressures on the bottom side of the modules are significant.

Figure 4-6 shows the pressure distributions on the surfaces of the first two modules upstream normal to the wind vector. On module 3 the distribution caused only by the boundary layer profile is non-uniform, causing a net moment. Notice that negative pressures are experienced across the entire surface of both sides of the second and shadowed module.

Looking at the above cases, we can see why it is impossible to analytically predict what the axial aerodynamic moments might actually be. Wind tunnel tests or full scale instrumented heliostats are practically the only way to ascertain true environmental loads.

4.5 DATA AVAILABILITY

In addition to the information presented in this report, certain additional test data products can be made available to anyone with a need. This group includes the following:

1. Prints from 7 rolls of black and white 35mm photographs.
2. Some color slides.
3. Copies of the reduced pressure distribution data on paper tape.
4. Movies made of a portion of the test setup by Sandia Corp.
5. Copies of the computer printouts showing the integrated pressure distributions generated and used.

Section 5

CONCLUSIONS AND RECOMMENDATIONS

5.1 CONCLUSIONS

The wind tunnel tests were run to obtain a first look at the actual wind loading that Honeywell's low profile, tilt-tilt heliostat would experience within the wind environment specified by ERDA. This was successfully accomplished with regard to the present design. Good insight was obtained regarding the present SRE heliostat's response within the specified wind profiles while some useful comparisons between solid and vented modules were made.

A preliminary look at the test results shows that wind loads are in many cases less than those assumed for heliostat designs to date resulting in more than adequate design margins. Some unique combinations of gimbal angles and wind directions, however, result in higher than expected loads about the outer axis.

The wind moments which twist an individual mirror module are only 37 percent of the original design values. Bending stiffness and "g" sensitivity then become the design issue instead of torque as far as pointing accuracy is concerned.

High torques on all four mirror modules at 90 mph create stress problems on some inner drive components. Stress then takes over as a cost driver instead of pointing accuracy. Pressure relief vents appear attractive as a means to reduce these moments.

Actuator column loads under worst case conditions appear compatible with the capabilities of the smaller actuator (1 inch diameter screw) now being investigated.

Overturning moments loads on foundations due to worst case wind conditions are still less than seismic induced moments.

Field effects due to other heliostats and fences of course require further investigation but offer promise of yet further wind load reductions.

There are obviously several echelons or increments that may result in lower wind loading within a field of heliostats.

1. For a pilot plant, a wind profile power of 0.18→0.2 may be more applicable than 0.15.

2. Actual loads on a single, unprotected heliostat are in most cases lower than predicted results as shown by this test program.

3. The interference effects of fences and heliostat on heliostat has a net effect of reducing worse case loads as shown by this test program.

4. Changing mirror module configuration could have a positive effect in reducing loads.

Based upon results obtained so far, it is felt that a low profile within the boundary layer can best take advantage of these possible load reductions.

5.2 RECOMMENDATIONS

The largest unknown now regarding wind with respect to a field of heliostats is the field effects. It is not felt that small scale (<1/10) field models will give quantative data regarding induced moment loads. Since there are a few gaps in the envelope of cases run in the present tunnel test, it is recommended that additional testing be performed, emphasizing the following:

1. More runs with more heliostat orientations with one or two interference models upstream. Deeper down stream flows from the interference model should be explored.

2. Additional heliostat orientations using the vented mirror modules. Present testing consisted primarily of a comparison of the end-on wind vector case at $\theta = 0$ deg.

3. Obtain more pressure distribution data at worst case moment loading heliostat orientations.

4. Evaluate the influence of wind fences in more depth.

In all testing, it is recommended that direct hinge moment and drag loading instrumentation be used rather than relying solely on pressure distribution data.

Section 6

REFERENCES

6.1 Georgia Tech Wind Tunnel Test Plan - Internal Honeywell Document, March 1977.

6.2 Wind Tunnel Investigation of Wind Forces and Moments on a One-Tenth Scale Model of the Honeywell Heliostat - Georgia Institute of Technology Engineering Report, May 1977.

6.3 Hoerner, S. F. Dr. - Ing. Fluid Dynamic Drag, 1965.

6.4 Wind Forces on Structures, Paper No. 3269, American Society of Civil Engineers Transactions, 1961.

6.5 Model Simulation of Wind Effects on Structures, R. E. Whitbread of National Physical Laboratory - International Conference on Wind Effects on Buildings and Structures, Teddington, England, 1963.

Section 7

SYMBOL LIST

AR	Aspect Ratio = $\frac{\text{length (cord)}}{\text{width}}$
c	Length of mirror module side, ft
C_d	Non-Dimensional Drag Coefficient = $\frac{\text{drag (pounds)}}{qc^2}$
C_m	Non-Dimensional Moment Coefficient = $\frac{M}{qc^3}$
C_n	Non-Dimensional Normal Force Coefficient = $\frac{\text{force}}{qc^2}$
C_p	Pressure Coefficient = $\frac{P-P_{oo}}{q_{oo}}$
C_y	Side Force Coefficient = $\frac{\text{side force (pounds)}}{qc^2}$
ERDA	Energy Research and Development Agency
IAW	In accordance with
I/F	Interference
mph	Miles per hour
M/S	Meters per second
N/A	Not available
psf	Pounds per square foot
q	Dynamic pressure (psf) = $1/2\ \rho\ V^2$
Rn	Reynolds Number = $\frac{V\ (\text{length})}{V}$
Sp g	Specific gravity

SRE	Subsystem Research Experiment
V	Velocity
wrt	With respect to
ν	Kinematic viscosity

APPENDIX A

REDUCED PRESSURE COEFFICIENT DATA
(REFERENCE PARAGRAPH 4.1 FOR DATA DESCRIPTION)

LGL 3-01G

.151317	.108068	6.19861E-02	.102882
.169734	.123819	7.08261E-02	.123844
.127726	8.66371E-02	5.21247E-02	8.15423E-02
9.04827E-02	8.41509E-02	7.14286E-02	2.95435E-02
.100366	9.08746E-02	7.98277E-02	3.64484E-02
8.44693E-02	8.04156E-02	6.36493E-02	1.97801E-02
5.28498E-02	4.50055E-02	4.34979E-02	4.76913E-02
6.33308E-02	5.22717E-02	4.94059E-02	6.33676E-02
3.94245E-02	3.68158E-02	3.75996E-02	3.25416E-02
4.10254E-03	-1.00696E-03	1.01367E-02	5.54035E-03
8.45149E-03	7.16554E-03	2.02087E-02	1.50404E-02
-6.11377E-04	-1.08745E-02	3.78534E-03	-2.04429E-03
-7.30213E-02	-8.19212E-02	-8.73688E-02	-4.07379E-02
-6.94892E-02	-7.78050E-02	-8.05973E-02	-3.65812E-02
-7.84296E-02	-8.59126E-02	-9.40936E-02	-4.59502E-02
-1.96346E-03	-1.34831E-02	-1.55541E-02	-4.63826E-02
6.21027E-03	-5.32652E-03	-1.30055E-02	-3.83203E-02
-1.28218E-02	-1.96801E-02	-1.88228E-02	-5.46457E-02
3.80908E-02	3.87496E-02	3.71477E-02	2.45491E-02
4.49847E-02	4.68952E-02	4.13350E-02	3.51992E-02
3.18680E-02	3.06923E-02	3.38520E-02	1.63999E-02
3.72359E-02	4.51831E-02	3.13242E-02	5.93566E-02
5.16348E-02	5.14144E-02	3.54319E-02	6.31226E-02
2.12007E-02	4.04042E-02	2.68099E-02	5.03611E-02
-2.78551E-02	-1.03135E-02	-1.53483E-02	2.90267E-02
-2.12355E-02	2.94910E-04	-3.18327E-03	3.52849E-02
-3.51483E-02	-1.70960E-02	-2.58772E-02	2.04659E-02

LBL 3-01H

.215119	.131444	8.25660E-02	.194988
.240011	.200376	.1053	.272327
.195085	.104211	5.96689E-02	.150336
9.08607E-02	9.13898E-02	8.44137E-02	2.97742E-02
.128821	9.81665E-02	9.18884E-02	3.74089E-02
7.93895E-02	8.45654E-02	7.68280E-02	2.18107E-02
5.58959E-02	5.33445E-02	5.13906E-02	6.25545E-02
6.45936E-02	6.05860E-02	5.69355E-02	6.85968E-02
4.93876E-02	4.48422E-02	4.64955E-02	5.62962E-02
4.06262E-03	8.26993E-03	1.76033E-02	2.32620E-02
1.44524E-02	1.45229E-02	2.42487E-02	2.97200E-02
-9.58877E-03	3.32458E-03	7.04560E-03	8.61954E-03
-8.25406E-02	-8.74922E-02	-9.00898E-02	-2.87035E-02
-7.52666E-02	-8.27262E-02	-8.57110E-02	-2.14264E-02
-9.00669E-02	-8.99699E-02	-9.49342E-02	-3.51730E-02
1.01013E-02	-5.81088E-03	-1.22711E-02	-5.23889E-02
2.00471E-02	-1.93634E-04	-5.42687E-03	-3.99389E-02
-7.16393E-03	-1.06204E-02	-1.94689E-02	-6.57347E-02
4.05185E-02	5.05344E-02	4.22908E-02	3.25381E-02
4.70951E-02	5.83684E-02	4.82325E-02	3.74530E-02
3.43581E-02	4.39913E-02	3.58218E-02	2.70836E-02
4.61101E-02	4.71012E-02	3.61525E-02	6.84085E-02
5.71339E-02	5.38361E-02	4.64911E-02	8.42832E-02
3.20611E-02	3.93841E-02	3.19773E-02	5.72441E-02
-2.82428E-02	-1.69127E-02	-1.22617E-03	3.30218E-02
-2.00023E-02	-8.39840E-03	9.55861E-03	3.82246E-02
-3.62752E-02	-2.29474E-02	-1.06116E-02	2.48880E-02

LRL 3-09-180

-.594584	-.515578	-.529503	-.586967
-.573176	-.489774	-.505082	-.54611
-.614572	-.54758	-.549662	-.627554
-.613714	-.543208	-.579018	-.643561
-.584444	-.524678	-.543416	-.618246
-.638331	-.558602	-.614572	-.661601
-.643965	-.553899	-.56927	-.655306
-.61053	-.52431	-.540599	-.614204
-.675562	-.582117	-.592649	-.680216
-.608277	-.523514	-.541003	-.621859
-.583219	-.487447	-.519779	-.598405
-.629023	-.558357	-.573054	-.644455
-.49929	-.465096	-.505303	-.562901
-.470791	-.440785	-.469811	-.526025
-.544396	-.49602	-.550397	-.601467
-.621748	-.555761	-.566538	-.649635
-.61053	-.521983	-.545498	-.640781
-.64372	-.576483	-.589588	-.662336
-.630028	-.560476	-.571401	-.644259
-.606244	-.50643	-.540722	-.613469
-.656212	-.587996	-.593874	-.68683
-.611559	-.544249	-.585889	-.638184
-.574524	-.504838	-.55848	-.601345
-.6447	-.594241	-.626329	-.671766
-.614008	-.533643	-.565669	-.548719
-.587628	-.484262	-.531904	-.506675
-.640658	-.566318	-.605509	-.585913

LBL 3-10-180

-.579081	-.513337	-.563232	-.590249
-.543917	-.472274	-.530646	-.562302
-.612826	-.541139	-.594706	-.612341
-.648873	-.562703	-.582851	-.633274
-.630461	-.536378	-.527428	-.610225
-.673359	-.584213	-.607933	-.664409
-.649512	-.56459	-.58502	-.646615
-.627111	-.513893	-.527604	-.620806
-.666569	-.603259	-.610137	-.668024
-.606733	-.525819	-.556588	-.62197
-.566931	-.485677	-.525268	-.613267
-.624862	-.573897	-.590782	-.654798
-.51623	-.47816	-.518659	-.556755
-.488013	-.454066	-.498374	-.536687
-.542418	-.496258	-.545592	-.577821
-.637366	-.559088	-.578962	-.65165
-.605596	-.535937	-.53166	-.624377
-.658237	-.584346	-.612562	-.677239
-.632468	-.574836	-.608739	-.656169
-.597704	-.54471	-.565035	-.643908
-.647788	-.599909	-.654269	-.671287
-.649009	-.542749	-.61578	-.637948
-.621908	-.492907	-.5914	-.613796
-.679796	-.578261	-.6656	-.673668
-.61787	-.535359	-.584491	-.623615
-.599291	-.489909	-.552205	-.590959
-.631475	-.574426	-.623011	-.650213

LEL 3-09

.496414	.565598	.544716	.563638
.529677	.579277	.574746	.583074
.433782	.543516	.503345	.527595
.621101	.641224	.648694	.672564
.666477	.649821	.66562	.750737
.548537	.627041	.630838	.638799
.626784	.618958	.605156	.63145
.638799	.639411	.628266	.662435
.606466	.608916	.576828	.605731
.552885	.569884	.542475	.582009
.584421	.609895	.547068	.659251
.521839	.534208	.534575	.53776
.210942	.215043	.179734	.245224
.235378	.241441	.195943	.256492
.190836	.192183	.170873	.232574
.331301	.31018	.300371	.183942
.340422	.323925	.314691	.203952
.326264	.298831	.288347	.160989
.65074	.603062	.590361	.576375
.662313	.619448	.605609	.627409
.640146	.592872	.546823	.520981
.590214	.586981	.61101	.68497
.620918	.599485	.618591	.734693
.55662	.573032	.602425	.619693
.225015	.413917	.44985	.478423
.234129	.438436	.472972	.533473
.21675	.388467	.434394	.441865

LBL 3-10

.541942	.593009	.571146	.587115
.583059	.601928	.609423	.599459
.45829	.579708	.531079	.566438
.627896	.65956	.664242	.650447
.664886	.666341	.678509	.661535
.558061	.653335	.637331	.636273
.620137	.627777	.62287	.646682
.659419	.641387	.634465	.681022
.563396	.613435	.612245	.62481
.550151	.566645	.544711	.549561
.558899	.613744	.564013	.594566
.531079	.537825	.533857	.519969
.279046	.286594	.25769	.310035
.310639	.338724	.277794	.342691
.236043	.265008	.242391	.276604
.460389	.447943	.421468	.265749
.480466	.460979	.430911	.288022
.41795	.430074	.410366	.248916
.622738	.614348	.599548	.561645
.638036	.629792	.611011	.573095
.606249	.603472	.581692	.552109
.568109	.589623	.623404	.62667
.610129	.607439	.661623	.694425
.522262	.574462	.605632	.581516
.318849	.410344	.46168	.459979
.328627	.431969	.471604	.477556
.305658	.392467	.450178	.436334

LPL 3-06

.627592	.620906	.625008	.656153
.637819	.640391	.639901	.698687
.615039	.599363	.613814	.615774
.580404	.564483	.54779	.566626
.615162	.582339	.560662	.620673
.554661	.553314	.529187	.514245
.481141	.491098	.476047	.514478
.520736	.507877	.482158	.570949
.443334	.477994	.469788	.470768
.279911	.309073	.263473	.421253
.404634	.397408	.27174	.452275
.208778	.264698	.253382	.38859
4.72491E-02	6.12011E-02	4.95761E-02	5.64773E-02
6.34656E-02	9.16952E-02	5.67419E-02	8.84987E-02
3.16965E-02	3.18435E-02	4.17392E-02	3.38765E-02
.248806	.227074	.210552	.117074
.265678	.24133	.222641	.129588
.237485	.214742	.202397	.10153
.341599	.338444	.325027	.295642
.362626	.355314	.338842	.310625
.328603	.331702	.314103	.285126
.4571	.325768	.3274	.549443
.486077	.342798	.338352	.617488
.413329	.309669	.317226	.477137
.154869	.221674	.22506	.310947
.164039	.24547	.233345	.422147
.149783	.204797	.218036	.251434

LBL 3-07

.640338	.644381	.660287	.634844
.666297	.653599	.669956	.653511
.614493	.63614	.635567	.617668
.598313	.580065	.578267	.552369
.634421	.587379	.58491	.579929
.571067	.575476	.568466	.536502
.491325	.503317	.489284	.503524
.530859	.511945	.503304	.559384
.474647	.486065	.480598	.466049
.374876	.399243	.385479	.395293
.40997	.423284	.397889	.422931
.350892	.376904	.369894	.369056
4.29671E-02	7.05243E-02	5.54378E-02	6.06971E-02
5.34393E-02	8.48123E-02	6.26713E-02	8.71401E-02
3.27445E-02	5.90473E-02	4.72361E-02	4.58606E-02
.355499	.321446	.301235	.169214
.365353	.331185	.313814	.178332
.344587	.303497	.284892	.157125
.476362	.495483	.464789	.429496
.494751	.509961	.479981	.455689
.457496	.486638	.451544	.413408
.484258	.483063	.479126	.511085
.517412	.515957	.504097	.544085
.45948	.457981	.464595	.465741
.240297	.311909	.326882	.362677
.257866	.33696	.349745	.380122
.228107	.290491	.310419	.34009

LRL 3-06-180

-.632403	-.618932	-.568866	-.611375
-.611387	-.596568	-.544028	-.56791
-.65462	-.636249	-.583709	-.64225
-.642777	-.62154	-.597818	-.652256
-.607346	-.601345	-.562889	-.62143
-.669439	-.640046	-.623145	-.691606
-.660694	-.592086	-.608632	-.642581
-.64372	-.565216	-.590567	-.625472
-.684993	-.630493	-.626696	-.675195
-.619177	-.576802	-.580145	-.615907
-.592527	-.564848	-.550887	-.60061
-.645557	-.585178	-.607468	-.633922
-.586281	-.571437	-.579398	-.592331
-.563991	-.554438	-.554561	-.56938
-.606121	-.587628	-.601957	-.618736
-.630591	-.609881	-.578186	-.639923
-.618613	-.596201	-.55652	-.626329
-.648619	-.631595	-.62192	-.663438
-.650248	-.611522	-.602239	-.640621
-.629146	-.599018	-.577585	-.618368
-.672378	-.630493	-.644455	-.678624
-.648497	-.608044	-.609379	-.647945
-.621185	-.582852	-.577218	-.618246
-.685115	-.636371	-.628778	-.66552
-.682433	-.592331	-.581909	-.621589
-.669071	-.565216	-.543661	-.605141
-.698097	-.627921	-.609183	-.644822

LBL 3-07-180

-.616605	-.580338	-.561737	-.600433
-.597175	-.56261	-.544755	-.572618
-.628786	-.609784	-.588181	-.625039
-.647744	-.611257	-.601328	-.631365
-.621732	-.59065	-.587343	-.618778
-.696637	-.642145	-.623672	-.652814
-.65173	-.614277	-.601244	-.634341
-.617191	-.598674	-.588754	-.619307
-.677944	-.631343	-.629403	-.6559
-.633054	-.586091	-.581528	-.618738
-.607977	-.568562	-.563624	-.594221
-.655018	-.611592	-.597704	-.636016
-.591545	-.569219	-.585496	-.583547
-.57178	-.535011	-.563139	-.569973
-.610798	-.584654	-.612518	-.598674
-.631489	-.603749	-.585095	-.632256
-.612121	-.591796	-.572706	-.618602
-.647215	-.633944	-.600967	-.651227
-.648357	-.618139	-.608889	-.641483
-.622173	-.596426	-.592943	-.623848
-.674505	-.638662	-.624466	-.654577
-.648163	-.606773	-.60493	-.630651
-.629007	-.58342	-.577115	-.603303
-.669744	-.658281	-.627508	-.662205
-.636211	-.594772	-.601857	-.611332
-.626582	-.559788	-.582494	-.58774
-.643335	-.621776	-.632842	-.630682

L-L 3-03-180

-.716455	-.579435	-.574867	-.685912
-.703486	-.562276	-.557255	-.658661
-.726633	-.604284	-.599508	-.710834
-.726731	-.615935	-.611057	-.679922
-.709977	-.596201	-.587873	-.64225
-.74684	-.629268	-.634657	-.700791
-.63522	-.587714	-.592404	-.582582
-.624247	-.577218	-.575748	-.558235
-.667479	-.604284	-.605754	-.603182
-.49368	-.520869	-.530667	-.462475
-.465524	-.509981	-.51635	-.444459
-.530067	-.532761	-.547825	-.487447
-.391735	-.411527	-.407387	-.252153
-.364486	-.395471	-.385795	-.233968
-.415679	-.437846	-.421067	-.265137
-.64612	-.590188	-.603121	-.682053
-.629391	-.564113	-.589955	-.645312
-.671276	-.617633	-.613959	-.702261
-.710026	-.601724	-.605019	-.716786
-.679481	-.574524	-.58971	-.702628
-.725775	-.618491	-.617633	-.734594
-.724894	-.615478	-.600978	-.654485
-.706303	-.605754	-.579545	-.628778
-.753699	-.625227	-.622165	-.675562
-.672844	-.603292	-.583831	-.596764
-.661356	-.591425	-.565583	-.569625
-.681319	-.616899	-.599263	-.626207

LBL 3-04-180

-.691082	-.567733	-.566239	-.67783
-.663924	-.555115	-.552823	-.643467
-.700385	-.578879	-.584346	-.704705
-.708762	-.595279	-.594248	-.668104
-.688481	-.583728	-.57328	-.646157
-.723487	-.607183	-.610578	-.681868
-.617769	-.586797	-.580316	-.580748
-.606918	-.582935	-.566931	-.565167
-.629492	-.592105	-.594089	-.596426
-.482348	-.518139	-.513038	-.443577
-.46209	-.502562	-.502121	-.430214
-.50653	-.528354	-.526811	-.469144
-.372543	-.411468	-.396725	-.330522
-.35187	-.403541	-.383481	-.306415
-.387184	-.42219	-.411477	-.355176
-.626379	-.569796	-.581802	-.651209
-.60273	-.556173	-.571251	-.624642
-.639952	-.582185	-.590253	-.675916
-.6876	-.587952	-.592921	-.693864
-.670758	-.573985	-.585315	-.690413
-.706293	-.605949	-.613135	-.711319
-.694724	-.599723	-.59311	-.633129
-.663527	-.583993	-.565299	-.617367
-.716609	-.609608	-.621423	-.653872
-.67063	-.590782	-.564391	-.565855
-.65859	-.576233	-.55463	-.548678
-.686629	-.601584	-.582494	-.586638

LGL 3-03

.47514	.306466	.284146	.303314
.486077	.334041	.29354	.331433
.463175	.292805	.276945	.284844
.245906	.213733	.172428	.161384
.258881	.221796	.177964	.181479
.232157	.203781	.167529	.14426
.154023	.144769	.129244	.153216
.169109	.156666	.133837	.168472
.135148	.130445	.122337	.130567
6.16518E-02	7.25701E-02	6.85934E-02	5.79225E-02
7.48064E-02	7.88969E-02	7.47451E-02	6.96503E-02
5.03856E-02	6.69070E-02	6.49475E-02	4.41029E-02
-9.36871E-02	-9.34678E-02	-9.69766E-02	-8.19396E-02
-8.02666E-02	-8.63902E-02	-9.07502E-02	-7.42900E-02
-.105422	-9.91272E-02	-.103083	-8.80313E-02
6.07283E-02	5.47236E-02	4.55725E-02	-1.08267E-02
7.08261E-02	6.46780E-02	5.30800E-02	-3.91810E-03
4.94181E-02	4.47397E-02	3.67668E-02	-1.60795E-02
.13204	.139208	.123274	.108994
.141578	.145754	.135221	.132062
.12453	.130457	.116704	8.94907E-02
.137798	.135239	.127687	.182956
.146097	.148093	.138565	.197449
.127983	.121321	.117598	.161565
3.56732E-02	5.84773E-02	5.01995E-02	.10241
4.21556E-02	7.12057E-02	6.43106E-02	.119447
2.76182E-02	4.71279E-02	3.93877E-02	8.50450E-02

LAL 3-04

.455146	.407029	.390333	.422729
.480819	.431396	.408735	.45053
.438318	.386956	.375272	.399697
.300812	.297942	.257165	.186254
.330611	.312359	.274664	.206945
.289433	.278764	.245125	.168544
.190826	.196333	.187643	.199763
.219201	.206592	.205754	.227842
.163209	.186929	.167221	.181815
6.60467E-02	7.03709E-02	7.62540E-02	9.28266E-02
7.43326E-02	8.12500E-02	8.81365E-02	.132657
5.88621E-02	5.88754E-02	6.66348E-02	7.54083E-02
-9.30622E-02	-8.94660E-02	-9.07119E-02	-7.49972E-02
-8.26248E-02	-7.73607E-02	-8.21840E-02	-6.43636E-02
-9.99382E-02	-9.70195E-02	-9.68167E-02	-8.58873E-02
6.43264E-02	6.33869E-02	4.62455E-02	1.83838E-03
7.70307E-02	7.27366E-02	5.25267E-02	2.97862E-02
5.31836E-02	5.70766E-02	4.05083E-02	-1.55759E-02
.175678	.183389	.167627	.166847
.197686	.200111	.176039	.191955
.15664	.16753	.151482	.141518
.185888	.194371	.166983	.210225
.204167	.214748	.184901	.224668
.161181	.170087	.15567	.195041
2.96803E-02	5.46332E-02	5.54475E-02	8.94848E-02
4.07464E-02	6.77591E-02	6.17367E-02	9.58695E-02
1.92006E-02	3.95384E-02	4.45468E-02	8.22111E-02

L'L 3-89			
.267428	.232355	.198216	.229707
.294924	.273589	.209121	.253676
.247466	.206353	.187627	.21631
.162439	.155103	.126406	7.05064E-02
.172306	.16666	.133654	8.51552E-02
.142778	.148767	.119165	5.49783E-02
.104901	9.91573E-02	8.85391E-02	9.82290E-02
.109404	.106147	9.45365E-02	.118137
9.86148E-02	9.48672E-02	8.10524E-02	8.40774E-02
3.34087E-02	3.62182E-02	3.99707E-02	3.98041E-02
4.33803E-02	4.25475E-02	4.28781E-02	5.81503E-02
2.23642E-02	2.85858E-02	3.62647E-02	2.74713E-02
-9.75927E-02	-.100081	-.101642	-8.59628E-02
-9.78598E-02	-9.40324E-02	-9.65430E-02	-7.13997E-02
-.106402	-.106806	-.10808	-9.50734E-02
3.08123E-02	1.76674E-02	9.76193E-03	-3.45445E-02
4.30986E-02	2.91736E-02	1.63264E-02	-1.96067E-02
1.70612E-02	1.07172E-02	4.64264E-03	-4.72117E-02
9.12739E-02	9.25635E-02	7.72656E-02	5.84246E-02
.105069	9.88719E-02	8.93315E-02	7.02137E-02
7.66312E-02	7.85295E-02	6.97973E-02	4.96998E-02
9.55640E-02	9.09567E-02	7.98375E-02	.112306
.104702	.101603	8.71270E-02	.124934
7.97542E-02	8.39795E-02	6.71519E-02	.101015
9.59292E-03	1.34079E-02	1.14251E-02	6.18379E-02
1.87023E-02	2.43972E-02	2.30256E-02	7.91664E-02
-2.15451E-03	4.88758E-03	3.06276E-03	4.36375E-02

```
LBL 3-90
 .342511          .304551          .254617          .328142
 .360679          .322455          .27268           .372274
 .323645          .282555          .23979           .30482

 .219735          .210675          .185752          8.26132E-02
 .248608          .236836          .198392          8.75501E-02
 .190853          .198524          .170131          7.54656E-02

 .103277          .101006          8.95548E-02      9.62725E-02
 .133538          .113491          .102179          .117411
 8.73782E-02      9.59577E-02      7.62901E-02      8.29562E-02

 3.34785E-02      3.89785E-02      4.22697E-02      4.39057E-02
 3.98073E-02      5.00842E-02      4.81267E-02      5.70104E-02
 2.33625E-02      2.94687E-02      3.85993E-02      3.12102E-02

-9.41728E-02     -9.49681E-02     -9.69331E-02     -7.85965E-02
-8.70645E-02     -8.92953E-02     -9.23374E-02     -6.41961E-02
-9.87875E-02     -.100123         -.101799         -8.66897E-02

 3.76276E-02      2.23282E-02      1.04950E-02     -2.28015E-02
 5.31704E-02      3.02491E-02      2.60343E-02     -1.34376E-02
 2.28996E-02      1.51269E-02      1.57429E-03     -4.33249E-02

 9.44896E-02      9.33098E-02      8.53872E-02      7.56147E-02
 9.56227E-02      9.91365E-02      9.66852E-02      8.65891E-02
 7.54260E-02      8.76824E-02      7.66031E-02      5.84477E-02

 9.06597E-02      9.40148E-02      8.07703E-02      .114343
 9.97581E-02      .10429           8.99044E-02      .122988
 7.71542E-02      8.16732E-02      6.55855E-02      .104863

 8.04199E-03      1.93082E-02      2.49378E-02      6.42704E-02
 1.24861E-02      2.76479E-02      3.60775E-02      7.63500E-02
 1.56988E-03      1.08636E-02      1.85305E-02      5.35804E-02
```

LNL 3-89-180

-.637596	-.57799	-.549368	-.597757
-.618123	-.563991	-.537415	-.56889
-.651803	-.590567	-.558357	-.617144
-.654252	-.598601	-.590873	-.596899
-.647149	-.588363	-.578688	-.581382
-.663193	-.611143	-.599753	-.616041
-.582068	-.565498	-.55897	-.537464
-.561052	-.55701	-.550029	-.504348
-.601345	-.585301	-.568645	-.563501
-.421337	-.471317	-.458556	-.314275
-.392287	-.448501	-.443112	-.239626
-.433559	-.485732	-.468953	-.377467
-.215414	-.239024	-.223515	-.153229
-.189107	-.226644	-.214899	-.127198
-.233037	-.254335	-.231225	-.178758
-.612159	-.584211	-.628142	-.600487
-.569625	-.566685	-.525413	-.567298
-.65266	-.61249	-.701526	-.634657
-.614059	-.599153	-.587591	-.576042
-.598528	-.578565	-.571952	-.534843
-.629146	-.614082	-.603059	-.621553
-.624786	-.587371	-.595454	-.552356
-.602569	-.577708	-.582607	-.528107
-.65315	-.599263	-.608203	-.586648
-.611743	-.564028	-.556582	-.590457
-.595344	-.5466	-.51341	-.562521
-.620818	-.577953	-.619715	-.62045

LRL 3-90-180

-.607161	-.567315	-.532203	-.580523
-.581832	-.555865	-.523151	-.561552
-.625391	-.576542	-.546254	-.599556
-.642797	-.594847	-.574086	-.592114
-.630506	-.584301	-.558907	-.566049
-.655371	-.602907	-.586682	-.613399
-.593608	-.554242	-.549331	-.529403
-.57253	-.548017	-.538538	-.512967
-.606301	-.566446	-.561376	-.548502
-.409964	-.469245	-.451041	-.368152
-.379425	-.455477	-.435108	-.348343
-.430919	-.486206	-.474126	-.384892
-.280694	-.320845	-.309316	-.221484
-.256243	-.306371	-.290676	-.204925
-.307561	-.33807	-.336042	-.243634
-.605706	-.567156	-.632371	-.580166
-.583772	-.541051	-.545151	-.556482
-.646818	-.621159	-.671066	-.595897
-.611759	-.593926	-.583927	-.576727
-.599732	-.581039	-.575704	-.555248
-.636457	-.607492	-.603568	-.609696
-.624311	-.576485	-.578742	-.554952
-.601319	-.56843	-.562125	-.539155
-.65105	-.582229	-.590826	-.573412
-.581555	-.551756	-.529663	-.54844
-.5735	-.536157	-.507853	-.531219
-.58849	-.567151	-.554939	-.562434

LOL 3-01G-180

-.568755	-.55919	-.542301	-.526723
-.546478	-.542314	-.519289	-.511206
-.576973	-.585546	-.55897	-.555051
-.602472	-.585105	-.581186	-.568841
-.587996	-.570849	-.560684	-.550642
-.619715	-.602937	-.603304	-.596079
-.560991	-.557966	-.560439	-.482229
-.543538	-.551622	-.54513	-.465892
-.573544	-.566808	-.581627	-.504715
-.393254	-.427166	-.42904	-.24055
-.376733	-.411514	-.401349	-.229118
-.415679	-.44152	-.455604	-.253364
-.150053	-.195541	-.204129	-.124266
-.139322	-.196094	-.1973	-.105361
-.167858	-.210405	-.210527	-.136812
-.585644	-.596164	-.511316	-.56404
-.548437	-.578933	-.452542	-.551499
-.660496	-.617266	-.624125	-.581382
-.55216	-.548523	-.554634	-.451795
-.518677	-.537782	-.540477	-.418863
-.583709	-.574524	-.571339	-.470423
-.528842	-.549931	-.53412	-.501849
-.508512	-.544518	-.512308	-.464177
-.564236	-.565461	-.553704	-.528719
-.57325	-.504041	-.597646	-.528536
-.561174	-.486344	-.579422	-.479853
-.593139	-.541211	-.629023	-.559582

LBL 3-01H-180

-.55027	-.539706	-.522415	-.513721
-.520462	-.522137	-.489601	-.497316
-.56649	-.562478	-.538185	-.546298
-.577631	-.581996	-.558246	-.545949
-.559436	-.560758	-.541757	-.522887
-.592634	-.603303	-.572486	-.568077
-.534403	-.538274	-.528958	-.50016
-.520021	-.528971	-.508602	-.476374
-.55344	-.550354	-.542286	-.520109
-.369933	-.414448	-.412209	-.324469
-.344331	-.402747	-.389036	-.288824
-.398294	-.423821	-.427966	-.351164
-.189384	-.260127	-.260017	-.168314
-.170139	-.239446	-.232744	-.155017
-.203338	-.27983	-.273966	-.186011
-.539385	-.571177	-.513536	-.54867
-.485412	-.558642	-.459621	-.533336
-.582538	-.578394	-.62473	-.56455
-.549459	-.522971	-.537149	-.445751
-.533292	-.511997	-.52443	-.4251
-.576806	-.53748	-.545813	-.471084
-.504114	-.531043	-.523367	-.492815
-.469541	-.520286	-.504414	-.463545
-.529632	-.542594	-.548237	-.532498
-.545081	-.485862	-.570506	-.513783
-.537348	-.471304	-.558907	-.492378
-.555071	-.498683	-.581877	-.548326

LNL 3-01C-180

-.258287	-.294905	-.284633	-.264898
-.246007	-.285945	-.270403	-.243521
-.274285	-.310941	-.298596	-.276808
-.307447	-.33301	-.316013	-.307418
-.297433	-.323066	-.305393	-.285773
-.321216	-.347009	-.326862	-.324952
-.247022	-.29982	-.293032	-.238158
-.22793	-.289423	-.274322	-.223729
-.261083	-.311247	-.310696	-.252596
-.148852	-.2142	-.178558	-.129282
-.134423	-.194593	-.149806	-.116016
-.169462	-.238071	-.200717	-.145899
-5.41766E-02	-9.78596E-02	-.109897	-6.64262E-02
-3.18538E-02	-7.53188E-02	-8.65862E-02	-4.39417E-02
-9.10318E-02	-.11669	-.124062	-7.86623E-02
-.166375	-.286187	-.297264	-.28898
-.147956	-.272167	-.278352	-.266129
-.194373	-.303679	-.314064	-.311651
-.257437	-.321442	-.28755	-.256388
-.241035	-.312619	-.282601	-.235401
-.274334	-.331578	-.29333	-.275339
-.266125	-.294361	-.319812	-.239423
-.254788	-.284536	-.311137	-.215536
-.278903	-.302197	-.328001	-.262149
-.277187	-.316113	-.278432	-.13252
-.267831	-.296294	-.258683	-.111203
-.284892	-.327193	-.301841	-.157313

LPL 3-01D-180

-.353065	-.390244	-.381501	-.349956
-.331104	-.374222	-.364259	-.341377
-.375501	-.410022	-.394326	-.357822
-.410978	-.43722	-.412751	-.383886
-.396399	-.423557	-.391284	-.373429
-.425364	-.45336	-.424086	-.399397
-.329711	-.393013	-.381351	-.310154
-.308135	-.380086	-.369946	-.290896
-.35478	-.40019	-.402968	-.332251
-.162151	-.272445	-.28218	-.173662
-.131739	-.211009	-.261137	-.15656
-.194476	-.305048	-.311706	-.196548
-5.84585E-02	-9.75032E-02	-.155568	-6.54804E-02
-4.57982E-02	-7.32650E-02	-.138616	-5.45056E-02
-7.18938E-02	-.11111	-.180412	-7.31592E-02
-.262036	-.370396	-.403179	-.362685
-.223133	-.344243	-.374663	-.338555
-.318098	-.394679	-.421881	-.378763
-.32517	-.411419	-.370744	-.337193
-.294335	-.399705	-.360467	-.315321
-.360555	-.428406	-.382158	-.357072
-.356993	-.382198	-.407725	-.311617
-.342347	-.357733	-.385112	-.271409
-.366992	-.397589	-.41809	-.331766
-.348502	-.392735	-.380373	-.225218
-.339172	-.373341	-.362098	-.172476
-.354956	-.408302	-.408787	-.292087

LRL 3-01E-180

-.358223	-.393871	-.357205	-.324475
-.346477	-.373882	-.34419	-.315955
-.377937	-.40092	-.373474	-.338285
-.424053	-.427033	-.398607	-.370765
-.412024	-.421005	-.387667	-.361785
-.436518	-.442233	-.409983	-.382428
-.336367	-.380448	-.369211	-.295428
-.328106	-.371528	-.351675	-.286998
-.345293	-.392865	-.38104	-.306239
-.162155	-.247604	-.248426	-.170142
-.170953	-.212864	-.22522	-.154733
-.193487	-.267594	-.289515	-.185799
-8.12927E-02	-.111288	-.135463	-6.89956E-02
-6.10855E-02	-9.37164E-02	-.122374	-5.99153E-02
-9.92411E-02	-.136648	-.163292	-7.65845E-02
-.289749	-.359977	-.391119	-.350854
-.25962	-.32367	-.378332	-.340721
-.306157	-.385857	-.414746	-.360302
-.334697	-.402032	-.357005	-.31055
-.32514	-.393477	-.338707	-.285488
-.343374	-.418692	-.372467	-.325711
-.350231	-.361352	-.389471	-.29366
-.338761	-.347933	-.380468	-.28033
-.361159	-.371283	-.401152	-.317098
-.334058	-.377964	-.375598	-.20758
-.329617	-.365065	-.362316	-.18305
-.340816	-.398498	-.386578	-.234677

LEL 3-01C

-.125325	-.240915	-.555822	-.314963
-.104859	-.195965	-.529209	-.288823
-.158905	-.286986	-.569747	-.349703
-5.79681E-03	-2.03990E-02	-2.35319E-02	-3.14423E-02
4.25073E-03	-4.59169E-03	-1.50262E-02	-1.56876E-02
-1.24543E-02	-4.00226E-02	-3.20742E-02	-4.48725E-02
-7.91924E-03	-.10454	-1.53851E-02	-2.18636E-03
-1.88508E-03	-8.78721E-02	-1.07030E-02	3.68393E-04
-1.04581E-02	-.119004	-2.05129E-02	-4.32225E-03
-3.17240E-02	-3.60472E-02	-2.00916E-02	-1.80562E-02
-2.77020E-02	-2.90982E-02	-1.50385E-02	-1.32749E-02
-3.54544E-02	-4.18229E-02	-2.33665E-02	-2.42238E-02
-7.92464E-02	-8.23940E-02	-7.41994E-02	-6.48145E-02
-7.79029E-02	-7.74131E-02	-6.90360E-02	-5.58949E-02
-8.03891E-02	-8.63167E-02	-7.72906E-02	-7.22325E-02
-3.16370E-02	-4.77089E-02	-3.40730E-02	-3.26131E-02
-2.51546E-02	-4.37702E-02	-2.81184E-02	-2.75428E-02
-3.65077E-02	-5.42905E-02	-3.87489E-02	-3.72058E-02
-2.20781E-02	-1.31512E-02	-8.53281E-03	-1.39166E-02
-1.95822E-02	-7.39628E-03	-6.14707E-03	-9.71099E-03
-2.60609E-02	-1.62754E-02	-1.00172E-02	-1.71695E-02
-1.21653E-02	-1.38836E-02	-1.11978E-02	7.84159E-03
-8.32706E-03	-7.05336E-03	-7.78819E-03	1.65101E-02
-1.65694E-02	-1.94719E-02	-1.46711E-02	-1.60339E-03
-3.05862E-02	-5.15520E-02	-4.54273E-02	-1.17220E-02
-2.84613E-02	-4.85711E-02	-3.93735E-02	-7.50651E-03
-3.20987E-02	-5.48049E-02	-4.84364E-02	-1.49650E-02

COL 3-010

-.182788	-.352897	-.525109	-.340054
-.15127	-.29698	-.461296	-.264091
-.216696	-.412403	-.565035	-.394856
-4.29028E-03	-1.78138E-02	-1.62928E-02	-5.82786E-02
2.43401E-03	-1.22781E-02	-6.99199E-03	-4.23020E-02
-9.89298E-03	-2.28504E-02	-1.99362E-02	-7.40585E-02
-1.03052E-02	-1.89989E-02	-9.50280E-03	1.23261E-03
-6.56875E-03	-1.48485E-02	-6.70101E-03	8.26243E-03
-1.34685E-02	-2.39174E-02	-1.31334E-02	-3.63249E-03
-3.27715E-02	-3.33063E-02	-1.45425E-02	-1.39654E-02
-2.97193E-02	-2.96267E-02	-8.34108E-03	-1.12332E-02
-3.67249E-02	-3.66984E-02	-1.96055E-02	-1.80669E-02
-7.42979E-02	-7.84687E-02	-7.21689E-02	-5.56091E-02
-7.18497E-02	-7.23568E-02	-6.65063E-02	-5.02952E-02
-7.77223E-02	-8.28232E-02	-7.67743E-02	-6.24193E-02
-3.08444E-02	-4.35969E-02	-3.20123E-02	-2.47480E-02
-2.75370E-02	-3.78139E-02	-2.80528E-02	-1.90809E-02
-3.66543E-02	-4.86066E-02	-3.67690E-02	-2.96047E-02
-2.57902E-02	-7.84465E-03	-4.74130E-03	-3.12195E-03
2.75144E-03	-2.61847E-03	9.57060E-04	3.35985E-03
-4.14643E-02	-1.05543E-02	-8.83487E-03	-1.04749E-02
-1.74422E-02	-1.59242E-02	-9.86608E-03	8.29946E-03
-1.03559E-02	-1.03206E-02	-6.74951E-03	1.38704E-02
-2.24713E-02	-1.96452E-02	-1.35964E-02	1.89172E-03
-2.53101E-02	-4.82887E-02	-3.83006E-02	-8.48437E-03
-2.19422E-02	-4.58511E-02	-3.27305E-02	3.24963E-03
-2.89654E-02	-5.05685E-02	-4.32146E-02	-1.44913E-02

```
LBL 3-01E
-.178637        -.315066        -.550318        -.289125
-.150283        -.277024        -.489179        -.21828
-.221927        -.362982        -.581574        -.33921

 3.08875E-03    -1.40634E-02    -6.49845E-03    -7.87236E-02
 8.12517E-03    -1.08138E-02    -2.61156E-04    -6.41744E-02
-9.42894E-04    -1.87701E-02    -1.42130E-02    -8.60826E-02

-8.34578E-04    -1.04989E-02    -5.06092E-04     6.00852E-03
 5.60097E-03    -7.98616E-03     6.66645E-03     9.06545E-03
-3.83722E-03    -1.35435E-02    -3.39225E-03     3.76123E-03

-2.58922E-02    -2.57782E-02    -6.32060E-03    -1.01088E-02
-2.14359E-02    -2.24850E-02    -3.49605E-04    -5.76269E-03
-3.00658E-02    -2.90261E-02    -1.17323E-02    -1.48974E-02

-8.75372E-02    -9.26210E-02    -8.29447E-02    -6.22150E-02
-8.31706E-02    -8.81781E-02    -7.19579E-02    -5.98472E-02
-9.07636E-02    -9.73768E-02    -8.85455E-02    -6.52903E-02

-2.17780E-02    -4.99246E-02    -2.90647E-02    -1.15013E-02
-1.95798E-02    -4.58315E-02    -2.36008E-02    -7.17651E-03
-2.46472E-02    -5.54384E-02    -4.04973E-02    -1.72760E-02

-2.41775E-02    -3.23522E-03     2.16629E-03     4.63470E-03
-1.76489E-02     1.15267E-03     6.51948E-03     7.90201E-03
-2.61169E-02    -6.00354E-03    -1.68314E-03     1.89254E-04

-2.54382E-03    -6.43531E-03    -3.60929E-03     8.08408E-03
 2.31475E-03    -4.19004E-04     1.55137E-03     1.30715E-02
-7.83784E-03    -9.59049E-03    -9.85311E-03     3.55168E-03

-1.39797E-02    -5.82565E-02    -2.71973E-02    -1.04121E-02
-1.10628E-02    -5.25808E-02    -2.19339E-02    -6.96695E-03
-1.90586E-02    -6.24191E-02    -3.02617E-02    -1.62283E-02
```

LAL 3-91

4.58971E-02	-1.49025E-02	-8.24724E-02	-5.71392E-02
6.47025E-02	4.65488E-03	-6.58395E-02	-1.17195E-02
2.73978E-02	-4.63176E-02	-.104626	-.102409
5.14303E-02	3.66505E-02	3.18374E-02	-1.46111E-02
6.56823E-02	4.29149E-02	4.02328E-02	-7.09010E-03
3.86774E-02	2.97982E-02	2.66385E-02	-2.32196E-02
2.35216E-02	9.37247E-03	1.33014E-02	1.36663E-02
3.15006E-02	1.36810E-02	2.08701E-02	2.18253E-02
1.75633E-02	6.14903E-03	6.92060E-03	5.25499E-03
-1.67323E-02	-1.65534E-02	-5.61433E-03	-1.31108E-02
-8.48627E-03	-8.47403E-03	5.52100E-04	-6.93089E-03
-2.03292E-02	-2.62201E-02	-1.20134E-02	-1.65204E-02
-7.47934E-02	-8.78942E-02	-9.05322E-02	-6.52958E-02
-7.06894E-02	-8.09892E-02	-8.54472E-02	-5.74503E-02
-7.87602E-02	-9.48652E-02	-9.50489E-02	-7.57475E-02
-2.13494E-02	-3.02641E-02	-3.35733E-02	-4.06338E-02
-1.52712E-02	-2.26439E-02	-2.83144E-02	-3.63975E-02
-3.14741E-02	-3.37276E-02	-3.68506E-02	-4.29864E-02
3.51468E-03	1.00387E-02	1.03645E-02	-4.92726E-03
9.93339E-03	1.55181E-02	1.71959E-02	-1.60339E-03
-2.10553E-03	4.52017E-03	4.97331E-03	-8.22909E-03
1.33822E-02	1.03241E-02	8.31432E-03	2.37334E-02
1.88983E-02	1.75633E-02	1.53466E-02	2.84755E-02
6.99409E-03	1.81355E-03	2.09524E-03	1.67305E-02
-4.30036E-02	-3.83276E-02	-3.07981E-02	2.88395E-03
-3.78916E-02	-3.32989E-02	-2.30848E-02	1.13908E-02
-4.71014E-02	-4.11861E-02	-3.78549E-02	-3.36698E-03

LPL 3-92

1.62560E-02	-6.30731E-03	-8.33950E-02	-1.19902E-02
3.75677E-02	1.17498E-02	-6.22782E-02	1.67273E-02
-8.99799E-03	-3.94363E-02	-.111458	-3.79329E-02
4.46217E-02	4.12526E-02	4.46892E-02	-1.34712E-02
5.24606E-02	4.76065E-02	4.97844E-02	8.26684E-03
3.40980E-02	3.59144E-02	4.21528E-02	-2.59013E-02
1.82113E-02	1.52680E-02	2.15735E-02	2.33520E-02
2.31818E-02	1.91566E-02	3.00683E-02	3.00198E-02
8.92816E-03	1.16087E-02	1.74415E-02	1.28476E-02
-1.53176E-02	-1.59379E-02	-2.84905E-03	-3.69378E-03
-1.07306E-02	-1.39711E-02	5.73496E-04	1.51698E-03
-1.90104E-02	-1.91514E-02	-4.78319E-03	-9.58436E-03
-7.15054E-02	-8.73061E-02	-8.49447E-02	-5.53798E-02
-6.75953E-02	-8.02397E-02	-8.06541E-02	-5.28346E-02
-7.39263E-02	-9.26945E-02	-8.80300E-02	-6.07705E-02
-1.99662E-02	-2.46325E-02	-3.04106E-02	-3.41876E-02
-1.22429E-02	-2.04609E-02	-2.73606E-02	-2.99081E-02
-3.08700E-02	-2.75722E-02	-3.60063E-02	-4.00315E-02
-2.41787E-03	1.49955E-02	1.38581E-02	1.12692E-02
1.27449E-03	2.17357E-02	2.07525E-02	1.90375E-02
-5.92066E-03	6.23439E-03	7.65402E-03	8.51814E-03
1.20721E-02	1.40221E-02	1.07948E-02	2.82303E-02
2.10127E-02	1.80632E-02	1.75473E-02	3.90843E-02
6.71494E-03	7.18668E-03	5.59952E-03	2.06864E-02
-3.73337E-02	-4.17575E-02	-1.79113E-02	8.39787E-04
-3.22412E-02	-3.80564E-02	-1.22385E-02	1.10223E-02
-4.20243E-02	-4.54278E-02	-2.88067E-02	-6.84650E-03

LAL 3-93

-.512235	-.397149	-.456082	-.495224
-.475812	-.319637	-.437356	-.460136
-.563256	-.506675	-.480588	-.543416
-.456082	-.466749	-.448476	-.275297
-.436376	-.436499	-.411514	-.26886
-.485242	-.490753	-.477894	-.291774
-.187561	-.212793	-.217267	-.132552
-.170822	-.206963	-.205261	-.113089
-.211629	-.220116	-.229204	-.162433
-9.01268E-02	-.120921	-.121103	-6.76191E-02
-7.97390E-02	-.112673	-.115073	-5.81238E-02
-.100376	-.131656	-.126818	-7.55637E-02
-9.70415E-02	-.104305	-9.61548E-02	-8.64294E-02
-8.73945E-02	-9.99967E-02	-8.47491E-02	-7.86745E-02
-.102826	-.109207	-.107186	-9.31384E-02
-.150427	-.17589	-.195479	-.136709
-.11571	-.159163	-.185702	-.110701
-.170699	-.202615	-.208078	-.15577
-.17622	-.231403	-.218805	-.119284
-.168544	-.218292	-.201697	-.111999
-.185004	-.249118	-.234311	-.137522
-.181528	-.214223	-.227994	-.123463
-.165078	-.20095	-.205824	-.107602
-.214189	-.231604	-.240716	-.13146
-.155207	-.173204	-.186012	-.130289
-.130676	-.159787	-.172365	-.119776
-.188127	-.186902	-.195549	-.14051

LBL 3-94

-.519832	-.490809	-.481365	-.541647
-.483164	-.442603	-.465661	-.512703
-.567857	-.517993	-.499653	-.581832
-.473936	-.493996	-.452337	-.377564
-.460547	-.4732	-.434358	-.361349
-.486294	-.513364	-.47439	-.392475
-.260784	-.281889	-.309277	-.173605
-.240724	-.266472	-.29557	-.160616
-.280712	-.296672	-.320171	-.188039
-.129999	-.156706	-.172079	-.100301
-.119509	-.141438	-.156252	-9.40524E-02
-.153915	-.175474	-.180544	-.107632
-.131553	-.136046	-.135767	-.120776
-.126126	-.127859	-.128961	-.10999
-.138616	-.145053	-.145318	-.130469
-.214298	-.243145	-.256225	-.172084
-.192801	-.23054	-.240283	-.144833
-.238608	-.265678	-.267	-.198356
-.247981	-.300472	-.295098	-.163888
-.231466	-.288824	-.278111	-.142276
-.258095	-.309766	-.318627	-.177458
-.264007	-.276744	-.312081	-.157667
-.24747	-.255273	-.29094	-.150476
-.284592	-.293762	-.331589	-.170007
-.243793	-.248325	-.260118	-.188237
-.202632	-.230893	-.251658	-.175827
-.28199	-.257478	-.27357	-.209157

L/L 3-93-180

-.487153	-.285162	-.266145	-.284971
-.445194	-.270428	-.201501	-.249522
-.516227	-.309606	-.311309	-.333194
.19734	-.271246	-.155346	.146926
.21615	-.194214	-4.95264E-02	.156556
.175282	-.304034	-.206865	.12584
.135327	.258337	.296064	.138904
.145595	.270822	.307061	.151939
.123697	.237975	.281513	.129
.1122	.234989	.254739	.117278
.120696	.251508	.272855	.132319
.107837	.222568	.239346	.10622
.263303	.331023	.375167	.209045
.274667	.343778	.383936	.21457
.25212	.316197	.367892	.198135
-1.18702E-02	.172003	.195692	.129778
-7.99639E-03	.192146	.207051	.153825
-1.52589E-02	.156482	.181124	.108119
4.18347E-02	.257957	.285464	.157743
4.64666E-02	.275365	.29921	.166182
3.48440E-02	.231116	.247099	.141896
.163142	.24085	.261941	6.91151E-02
.180438	.280301	.280374	7.90439E-02
.147911	.214521	.24645	5.94975E-02
.170537	.180352	.147824	-9.56647E-03
.178895	.205201	.178025	-4.79989E-03
.165202	.156936	.127432	-1.54304E-02

LEL 3-94-180

-.419668	-.26126	-.276193	-.380064
-.339481	-.250203	-.265105	-.338687
-.466234	-.284107	-.283137	-.43039
.199741	-.220607	-.143285	.157707
.219069	-.164452	-.105431	.177009
.151923	-.264884	-.182219	.143793
.138554	.227816	.280179	.138534
.150292	.241377	.300852	.144604
.127701	.209678	.254031	.134773
.120408	.220784	.254494	.12364
.128883	.232824	.262892	.130254
.114647	.211089	.248872	.117318
.274655	.323579	.376388	.219955
.285862	.337225	.389028	.231722
.26276	.312667	.36597	.207253
-5.78707E-03	.139704	.199979	.134443
2.72499E-03	.154348	.218363	.161975
-1.43150E-02	.120762	.180933	.118107
4.79372E-02	.243	.283525	.162341
5.34129E-02	.257866	.296399	.17432
4.31051E-02	.223742	.270872	.148175
.160538	.235831	.256319	7.95134E-02
.170837	.264479	.266111	8.93710E-02
.150909	.215895	.245522	7.13787E-02
.143033	.174919	.153801	3.70065E-03
.155759	.196496	.17141	8.76503E-03
.131598	.156067	.138035	-3.25334E-03

LPL 3-95

-.609549	-.531408	-.541686	-.620841
-.571601	-.511697	-.519306	-.564234
-.645033	-.58223	-.575708	-.694913
-.65304	-.594452	-.608981	-.654815
-.642255	-.570394	-.586819	-.618341
-.684768	-.612303	-.627037	-.711579
-.534113	-.471298	-.472905	-.475755
-.497687	-.456624	-.45602	-.443097
-.551553	-.491165	-.501915	-.496359
-.206738	-.238733	-.239766	-.221301
-.178057	-.209761	-.22057	-.195835
-.255583	-.263373	-.257358	-.246959
-.136874	-.139157	-.143513	-.166517
-.106378	-.12633	-.127284	-.140762
-.155207	-.158407	-.16162	-.184011
-.905628	-.87378	-.718922	-.570949
-.852402	-.778368	-.674018	-.51061
-.937911	-.908442	-.758561	-.635491
-.414655	-.499088	-.4541	-.503702
-.387058	-.461817	-.425102	-.441406
-.432107	-.549258	-.470876	-.553485
-.552157	-.477119	-.532845	-.373181
-.508074	-.456624	-.486938	-.332347
-.586457	-.512905	-.568944	-.399015
-.626929	-.850543	-.729684	-.947851
-.602761	-.800953	-.645516	-.902403
-.667134	-.930423	-.85977	-.984409

LBL 3-96

-.588751	-.549147	-.52963	-.635858
-.560673	-.52263	-.500892	-.61528
-.611628	-.591063	-.544891	-.678148
-.64971	-.608394	-.601955	-.679192
-.630019	-.588455	-.578803	-.652192
-.668279	-.629628	-.624541	-.696756
-.511157	-.477262	-.491183	-.490261
-.446719	-.450197	-.473327	-.460328
-.540991	-.494457	-.512457	-.510233
-.208303	-.244376	-.256985	-.224294
-.165509	-.218681	-.235159	-.173552
-.247115	-.280984	-.267854	-.265072
-.1213	-.149827	-.150318	-.159426
-.110784	-.139727	-.14064	-.152118
-.133205	-.158509	-.160074	-.170422
-.937899	-.84557	-.725677	-.578999
-.867013	-.721408	-.703756	-.507413
-.99388	-.929881	-.752538	-.637062
-.425194	-.522187	-.473697	-.505113
-.383808	-.471023	-.453545	-.484501
-.474545	-.559586	-.496066	-.523935
-.559229	-.464623	-.516291	-.368034
-.454502	-.444372	-.489544	-.346504
-.592585	-.482631	-.539152	-.413459
-.622706	-.860031	-.792311	-.964937
-.600281	-.823579	-.672018	-.887752
-.677974	-.907229	-.842579	-1.02849

LRL 3-95-180

.368798	-.156916	-1.00296E-02	.473087
.420683	-6.14494E-02	5.76465E-02	.512109
.319643	-.208191	-5.81402E-02	.439886
.281508	.371684	.344288	.176161
.292263	.394233	.36724	.202528
.27364	.351286	.330851	.163143
.195037	.254956	.272633	.218907
.198144	.263905	.279823	.22969
.189496	.247818	.266707	.210656
.173316	.252216	.287206	.207574
.178687	.26312	.297553	.219315
.166899	.245379	.281768	.198047
.312009	.427603	.435756	.31757
.342928	.44991	.441456	.350259
.293374	.404378	.428896	.287324
1.46108E-02	8.52761E-02	.149771	.12393
2.43610E-02	9.25020E-02	.156658	.134362
9.54843E-04	7.86854E-02	.1415	.110546
.139835	.233962	.26296	.249887
.145256	.248724	.26928	.267746
.13551	.222311	.259582	.233953
.210535	.24478	.238387	.180872
.216658	.253954	.246949	.192781
.203578	.239965	.227431	.171259
.114272	.126788	8.19983E-02	5.58493E-02
.120775	.135462	9.09682E-02	6.64268E-02
.108444	.115026	7.03640E-02	4.13540E-02

LBL 3-96-180

.407847	-.141605	-4.98998E-02	.430972
.445476	-8.78585E-02	7.07835E-03	.45878
.356131	-.171596	-.134031	.396912
.286641	.393482	.359113	.159422
.303523	.413086	.366478	.174961
.276133	.381869	.349696	.149397
.201187	.258872	.27595	.221764
.21083	.264133	.280263	.231699
.195613	.253872	.270046	.213221
.176626	.25442	.290419	.203591
.181265	.263307	.300393	.210873
.172918	.244351	.28435	.196091
.303954	.411494	.44015	.302106
.321218	.418564	.453128	.313871
.292524	.386869	.428172	.285915
2.76626E-02	8.78772E-02	.155805	.130988
4.49035E-02	9.63935E-02	.163309	.139962
1.55173E-02	8.39417E-02	.143701	.124049
.137248	.235721	.266302	.237164
.145092	.245872	.271524	.250742
.128493	.230003	.262524	.228786
.210304	.246016	.242386	.185135
.218047	.250698	.245872	.190178
.200221	.243177	.239699	.179265
.123422	.134055	8.20017E-02	6.60165E-02
.127641	.143353	8.68633E-02	7.48680E-02
.11791	.127867	7.56332E-02	5.79162E-02

LPL 3-48-180

.410924	-5.89530E-02	.23802	.113001
.453775	-1.56154E-02	.315186	.163723
.36259	-.109095	.189907	5.25498E-02
.62879	-9.58690E-02	9.62376E-02	9.22303E-02
.690977	-6.74036E-02	.146875	.138288
.611386	-.112549	3.88177E-02	4.68130E-02
.684419	-.153155	.130193	.103523
.71013	-.120327	.177926	.131138
.657884	-.177441	7.77917E-02	7.04365E-02
.685614	-.120927	.152014	.118913
.769963	-7.53385E-02	.217685	.135063
.655107	-.164253	9.59199E-02	.104048
.492689	-6.35823E-02	.204976	.160844
.51694	-4.66118E-03	.299763	.249871
.464524	-.119047	.133227	5.23324E-02
.620988	-.140872	.135518	.1207
.655348	-.112404	.162104	.21312
.551723	-.192731	9.73934E-02	2.13537E-02
.752052	-.125391	.164473	.129498
.840254	-8.75730E-02	.205752	.211586
.670083	-.166294	.122188	7.84318E-02
.63972	-.177563	5.95004E-02	.107638
.650396	-.12331	.110038	.130039
.630831	-.230039	1.83343E-02	8.45067E-02
.452785	-.232133	-2.15708E-02	1.56036E-02
.459452	-.139711	9.26414E-03	4.33830E-02
.447978	-.285112	-4.16786E-02	-1.36347E-02

LTL 3-49-180

.435355	-4.68882E-02	.1969	.154033
.457085	-2.16383E-02	.22909	.212395
.415129	-8.54585E-02	.15457	9.30067E-02
.649341	-.107576	8.92820E-02	8.25134E-02
.670732	-9.31757E-02	.125023	.116293
.631863	-.131901	5.72945E-02	5.51380E-02
.689049	-.134334	.118735	.120695
.717513	-.111927	.165657	.143092
.670688	-.157074	7.71027E-02	9.61327E-02
.67601	-.169226	.136037	.134942
.712644	-.136857	.180048	.173874
.63595	-.185943	.103376	.110289
.484132	-.113005	.188787	.164896
.502301	-8.69280E-02	.239481	.215047
.470215	-.13277	.143484	.128354
.608124	-.137705	.159528	.130221
.626776	-.121423	.21896	.180265
.574125	-.14964	7.38419E-02	6.93768E-02
.725726	-.110481	.171944	.155994
.769121	-9.72365E-02	.233829	.182918
.657384	-.12777	.132136	.110593
.637859	-.184513	6.33704E-02	9.53436E-02
.646645	-.152031	9.24675E-02	.113715
.628776	-.210203	3.70515E-02	7.71201E-02
.446368	-.235042	-1.78528E-02	2.74605E-02
.450302	-.203725	-2.02578E-03	8.41808E-02
.442737	-.260115	-04.23465E-02	7.26331E-04

L'L 3-42			
-.355306	-.118599	-8.51635E-02	-.170226
-.344666	-9.41189E-02	-5.92392E-02	-.137586
-.37134	-.150581	-.106921	-.205835
-.371454	-.12371	-.104905	-.161691
-.358555	-9.87808E-02	-7.47588E-02	-.132284
-.38271	-.147779	-.143697	-.186439
-.375222	-.122653	-7.71163E-02	-.137616
-.35626	-.100556	-5.29348E-02	-.122875
-.394184	-.152924	-.103274	-.151946
-.357794	-.124676	-6.52743E-02	-.162903
-.346719	-.100061	-5.05555E-02	-.141656
-.381502	-.142296	-7.75728E-02	-.20842
-.361647	-.135133	-9.72929E-02	-.19033
-.3437	-.10982	-6.15581E-02	-.15133
-.384763	-.161644	-.155581	-.246875
-.360487	-.132853	-.144656	-.232976
-.349014	-.105725	-.114288	-.187683
-.383435	-.166777	-.197816	-.270015
-.385452	-.10631	-.114524	-.194673
-.368821	-9.49885E-02	-8.87565E-02	-.156427
-.404329	-.124059	-.144965	-.276827
-.325419	-.128633	-5.36305E-02	-.146644
-.310342	-.112875	-4.33936E-02	-.119482
-.340584	-.149253	-6.41185E-02	-.17935
-.229622	-.150122	-8.32202E-02	-.168496
-.218541	-.117561	-5.95895E-02	-.140074
-.244966	-.187695	-.12796	-.227019

LRL 3-49

-.352926	-.11227	-9.49678E-02	-.186982
-.335505	-8.97453E-02	-7.20067E-02	-.162987
-.367895	-.144031	-.115197	-.207899
-.379025	-.106827	-7.21862E-02	-.148687
-.372199	-9.93668E-02	-5.99331E-02	-.130423
-.385764	-.128336	-8.73802E-02	-.167639
-.375795	-.111187	-7.09941E-02	-.147022
-.358373	-.101915	-4.75812E-02	-.129857
-.388764	-.124901	-9.22583E-02	-.160509
-.365404	-.122255	-7.44070E-02	-.157018
-.357374	-9.55496E-02	-5.45201E-02	-.125118
-.374373	-.137379	-9.34670E-02	-.172117
-.352056	-.131533	-7.73704E-02	-.166817
-.334852	-.102397	-6.04939E-02	-.127988
-.364373	-.161596	-.104571	-.213073
-.353504	-.120381	-.126453	-.224268
-.343678	-.101758	-9.71234E-02	-.184682
-.359852	-.144422	-.172422	-.249681
-.380443	-.100389	-9.27370E-02	-.185386
-.366939	-8.36064E-02	-6.82285E-02	-.168987
-.393373	-.122032	-.129814	-.210681
-.323774	-.127006	-6.75576E-02	-.150735
-.308157	-9.13279E-02	-5.47158E-02	-.124944
-.333418	-.157161	-8.46498E-02	-.166639
-.221625	-.155848	-7.20832E-02	-.168074
-.212899	-.136162	-5.46332E-02	-.143683
-.229638	-.191465	-9.32105E-02	-.227594

LPL 3-97

.613294	.583856	.557691	.520222
.664471	.600646	.597299	.556908
.559517	.562473	.505344	.494866
.577577	.436811	.439259	.309567
.604907	.461041	.455867	.345261
.543126	.420173	.422216	.28248
.498418	.338618	.368704	.31714
.52404	.358652	.38226	.335044
.480084	.321697	.353739	.296915
.425051	.26925	.30821	.252738
.456302	.301089	.318175	.269046
.405869	.237829	.28935	.234612
.260803	.206334	.292358	.251707
.298915	.233047	.304306	.27248
.231438	.18657	.279785	.23709
.423798	.447772	.399734	.362135
.456954	.462128	.430564	.400956
.391347	.434564	.36513	.324305
.542148	.467498	.452372	.410094
.575299	.498431	.484171	.428216
.513866	.444955	.418694	.393782
.452085	.26395	.374474	.266985
.465345	.26922	.382608	.282872
.427738	.254568	.365	.252046
.265045	.164927	.313101	.159444
.294437	.174657	.331523	.172613
.276959	.146353	.297654	.137223

LBL 3-99

5.37009	5.42313	5.29157	4.68363
5.93234	5.6393	5.47931	5.38322
4.9641	5.21236	5.06367	4.32542
5.31601	4.21308	4.15599	2.4899
5.5467	4.45498	4.27847	3.02067
5.15758	4.03934	4.0563	2.01026
4.89171	3.3278	3.52614	2.87011
5.01801	3.50979	3.62414	3.0698
4.69281	3.19371	3.36066	2.69677
4.34638	2.7229	2.89859	2.23295
4.74107	2.93981	3.08763	2.45243
3.96022	2.50547	2.76938	2.01287
2.51038	2.1283	2.71429	2.35986
2.76938	2.34069	2.86807	2.51243
2.25852	1.98026	2.60851	2.08635
3.68035	4.10756	3.49188	2.96872
3.89239	4.43238	3.82196	3.29893
3.47458	3.71761	3.03067	2.53329
5.02149	4.57255	4.18664	3.57301
5.42235	4.79019	4.28716	3.835
4.63498	4.32934	3.99456	3.35501
4.66185	2.66329	3.51975	2.36173
5.12193	2.71242	3.6537	2.60416
4.40064	2.59851	3.39414	2.21548
2.75625	1.31395	2.7969	1.35666
2.83546	1.38028	2.92894	1.4268
2.62329	1.20354	2.62981	1.2132

L RL 3-99R

.567691	.566665	.541674	.466606
.616341	.585821	.567778	.501692
.526126	.543691	.52917	.440737
.531896	.430972	.425603	.283502
.548169	.445302	.461041	.311132
.510735	.414651	.415825	.242525
.514188	.343031	.355252	.288058
.541604	.365087	.367522	.306697
.492127	.32461	.344783	.272133
.456902	.27492	.298171	.235516
.466301	.315349	.327349	.247872
.412781	.25709	.28648	.226134
.255211	.220077	.287041	.231203
.274524	.233177	.322218	.255655
.221525	.206395	.261481	.2007
.373778	.427646	.361809	.303962
.397217	.440042	.382869	.32687
.335566	.417738	.328436	.271741
.508827	.448841	.411386	.378978
.550604	.485519	.427781	.408521
.484258	.428738	.382043	.330783
.450289	.269011	.356857	.256724
.473737	.281002	.368348	.277872
.430259	.252351	.348174	.238394
.290554	.137789	.288211	.139172
.301306	.149875	.298828	.162092
.283176	.122528	.273089	.109958

LFL 3-99-180

-.394681	-.334565	-.458906	-.303597
-.37833	-.324374	-.433198	-.289462
-.411111	-.344896	-.476936	-.31494
-.405259	-.378386	-.485901	-.34297
-.386416	-.373721	-.468588	-.312896
-.422068	-.387069	-.509718	-.35733
-.364778	-.360195	-.459506	-.375225
-.350722	-.3522	-.441458	-.341765
-.379938	-.367939	-.483457	-.408068
-.312127	-.324235	-.422881	-.34467
-.294245	-.311592	-.411155	-.307505
-.333374	-.337026	-.438937	-.381677
-.162304	-.225586	-.250124	-.303075
-.152509	-.204508	-.22142	-.281419
-.177378	-.252767	-.270984	-.337461
-.399764	-.388425	-.474575	-.395577
-.377547	-.367286	-.456197	-.373982
-.417676	-.402286	-.498544	-.426154
-.406881	-.376164	-.493088	-.392947
-.390068	-.360678	-.47024	-.379895
-.431894	-.385895	-.516022	-.40572
-.392751	-.37483	-.48511	-.357791
-.374982	-.357678	-.45798	-.323287
-.413894	-.386982	-.510892	-.387808
-.394894	-.368091	-.494401	-.325218
-.384329	-.3532	-.483805	-.312505
-.404329	-.395851	-.517978	-.341591

END